

NAVAL POSTGRADUATE SCHOOL

Monterey, California



A TEST FACILITY TO MEASURE HEAT TRANSFER PERFORMANCE
OF ADVANCED CONDENSER TUBES

by

A.C. Beck

and

P.J. Marto

20 January 1977

Approved for public release; distribution unlimited.

NAVAL POSTGRADUATE SCHOOL
Monterey, California

Rear Admiral Isham Linder
Superintendent

J.R. Borsting
Provost

A TEST FACILITY TO MEASURE HEAT TRANSFER PERFORMANCE
OF ADVANCED CONDENSER TUBES

An experimental test facility has been designed and constructed to measure the heat transfer characteristics of enhanced condenser tubes under simulated marine conditions. Design details, including instrumentation selection and data reduction, are provided in this report.

The work reported herein has been supported by the Naval Sea Systems Command, Energy Conversion and Explosive Devices Division, Code 0331, Washington, D.C., work request N0002476, WR62221.

REPORT DOCUMENTATION PAGE		READ INSTRUCTIONS BEFORE COMPLETING FORM
1. REPORT NUMBER NPS-69MX77011	2. GOVT ACCESSION NO.	3. RECIPIENT'S CATALOG NUMBER
4. TITLE (and Subtitle) A TEST FACILITY TO MEASURE HEAT TRANSFER PERFORMANCE OF ADVANCED CONDENSER TUBES		5. TYPE OF REPORT & PERIOD COVERED INTERIM
		6. PERFORMING ORG. REPORT NUMBER
7. AUTHOR(s) A.C. Beck and P.J. Marto		8. CONTRACT OR GRANT NUMBER(s)
9. PERFORMING ORGANIZATION NAME AND ADDRESS Naval Postgraduate School Monterey, California 93940		10. PROGRAM ELEMENT, PROJECT, TASK AREA & WORK UNIT NUMBERS N0002476WR62221
11. CONTROLLING OFFICE NAME AND ADDRESS Naval Sea Systems Command Code 0331 Washington, D.C. 20360		12. REPORT DATE 20 January 1977
		13. NUMBER OF PAGES 140
14. MONITORING AGENCY NAME & ADDRESS (if different from Controlling Office)		15. SECURITY CLASS. (of this report) UNCLASSIFIED
		15a. DECLASSIFICATION/DOWNGRADING SCHEDULE
16. DISTRIBUTION STATEMENT (of this Report) Approved for public release; distribution unlimited.		
17. DISTRIBUTION STATEMENT (of the abstract entered in Block 20, if different from Report)		
18. SUPPLEMENTARY NOTES		
19. KEY WORDS (Continue on reverse side if necessary and identify by block number) Heat Transfer, Condensation, Condensers, Enhanced Tubes.		
20. ABSTRACT (Continue on reverse side if necessary and identify by block number) An experimental test facility capable of investigating plain and enhanced condenser tube heat transfer characteristics was designed and built. The completed facility, including a stainless steel test condenser, has the capability of testing tubes under simulated marine conditions utilizing variable steam flowrate and orientation, cooling water flowrate and temperature, vacuum pressure, non-condensable gas concentration, and condensate inundation effects.		

The test condenser has the capability of being tested with a wide variety of tubing configurations and has glass windows on both sides to view the condensation process over nearly its entire length. Initial tests will be performed using 5/8 inch tubes.

Data will be automatically gathered and processed to yield the overall, internal and external heat transfer coefficients of corrugated or internally finned tubes operating with filmwise or dropwise condensation.

ABSTRACT

An experimental test facility capable of investigating plain and enhanced condenser tube heat transfer characteristics was designed and built. The completed facility, including a stainless steel test condenser, has the capability of testing tubes under simulated marine conditions utilizing variable steam flowrate and orientation, cooling water flowrate and temperature, vacuum pressure, non-condensable gas concentration, and condensate inundation effects.

The test condenser has the capability of being tested with a wide variety of tubing configurations and has glass windows on both sides to view the condensation process over nearly its entire length. Initial tests will be performed using 5/8 inch tubes.

Data will be automatically gathered and processed to yield the overall, internal and external heat transfer coefficients of corrugated or internally finned tubes operating with filmwise or dropwise condensation.

TABLE OF CONTENTS

I.	INTRODUCTION -----	13
	A. BACKGROUND INFORMATION -----	13
	B. CONDENSER HEAT TRANSFER -----	16
	C. DROPWISE CONDENSATION ENHANCEMENT METHODS --	19
	D. GEOMETRIC TUBE ENHANCEMENT METHODS -----	24
II.	DESIGN PROPOSAL -----	30
	A. EXPERIMENTATION AREAS -----	30
	B. OBJECTIVES OF THIS DESIGN -----	31
	C. CAPABILITIES OF THE TEST FACILITY -----	32
III.	DESIGN DESCRIPTION -----	33
	A. DISCUSSION -----	33
	1. Brief System Overview -----	34
	B. DESCRIPTION OF COMPONENTS -----	35
	1. Major Components -----	35
	a. Boiler -----	35
	b. Test Condenser -----	36
	(1) Tube length -----	38
	(2) Distance between tube supports -	39
	(3) Tube spacing -----	39
	(4) Pressure and temperature in a marine condenser -----	40
	(5) Vapor velocity -----	40
	(6) Creative design synthesis -----	40
	(7) Detailed design -----	43
	c. Secondary Condenser -----	44

2.	Auxiliary Systems and Components -----	45
a.	Desuperheater -----	45
b.	Condensate Collection System -----	45
c.	Cooling Water System -----	47
d.	Boiler Feed System -----	49
e.	Vacuum System -----	50
C.	UNCERTAINTY ANALYSIS -----	51
IV.	MEASUREMENT AND CONTROL -----	52
A.	OPERATIONAL MEASUREMENTS -----	52
B.	CONTROL -----	54
C.	TEST MEASUREMENTS -----	54
D.	DATA REDUCTION -----	58
V.	CONCLUSIONS AND RECOMMENDATIONS -----	63
A.	CONCLUSIONS -----	63
B.	RECOMMENDATIONS -----	63
APPENDIX A.	Calculation of Steam Flow Velocity -----	103
APPENDIX B.	Detailed Test Condenser Design Calculations and Considerations -----	105
APPENDIX C.	Secondary Condenser Design Calculations -	120
APPENDIX D.	Test Condenser Hot Well Calculations ----	123
APPENDIX E.	Calculation of Cooling Water Requirements -----	125
APPENDIX F.	Details of Uncertainty Analysis -----	127
APPENDIX G.	Calculation of Pressure Head of the Annubar, Primary Flow Sensor -----	134
APPENDIX H.	Properties of Water as a Function of Temperature -----	135
BIBLIOGRAPHY	-----	136
INITIAL DISTRIBUTION LIST	-----	140

LIST OF FIGURES

1. Comparison of Various Tube Enhancement Results -----	65
2. Withers and Young's Corrugated Tube -----	66
3. Spiral Indented (Rope) Tube -----	67
4. Catchpole and Drew's Test Tube (Kydena) -----	68
5. Turbotec Spirally Grooved Tube -----	69
6. Steam Side Coefficient versus Groove Depth -----	70
7. h_o versus h_i with Contours of Overall Heat Transfer Coefficient, U_o -----	71
8. Design Flow Diagram -----	72
9. Schematic of the Main Steam System -----	73
10. Schematic of the Condensate Collection System -----	74
11. Schematic of the Cooling Water System -----	75
12. Schematic of the Boiler Feed Water System -----	76
13. Schematic of the Vacuum System -----	77
14. Photograph of Fulton Boiler -----	78
15. Artist's Conception of the Test Condenser Body -----	79
16. Photograph of Test Condenser -----	80
17. Artist's Conception of the Test Condenser and the Dynamic Test Frame -----	81
18. Test Condenser with Initial Tube Configuration -----	82
19. Test Condenser Maximum Tube Configuration -----	83
20. Thermal Entrance Region Nusselt Numbers for Turbulent Flow -----	84
21. Thermal Entrance Lengths Based on $Nu/Nu_{\infty} = 1.05$ -----	85
22. Photograph of Marman Flexmaster Couplings -----	86
23. Photograph of Tube Sheet and Drilled Out Swagelok Fittings -----	87

24.	Photograph of Disassembled Secondary Condenser (Heliflow) -----	88
25.	Photograph of Condensate Pump and Associated Piping -----	89
26.	Photograph of Test Condenser Hot Well Solenoid Control Valve -----	90
27.	Photograph of Cooling Water Heater, Pump, and Associated Piping -----	91
28.	Photograph of Feed System (Fulton Return System) -----	92
29.	Photograph of Graham Air Operated Air Ejector ----	93
30.	Photograph of Control and Operational Section of Instrument Panel -----	94
31.	Photograph of Test Section of Instrument Panel ---	95
32.	Photograph of the Annubar, Primary Flow Sensor ---	96
33.	Schematic of the First Phase of Data Collection and Reduction -----	97
34.	Schematic of the Second Phase of Data Collection and Reduction -----	98
35.	Schematic of the Third Phase of Data Collection and Reduction -----	99
36.	Photograph of Test Condenser Window Frame -----	100
37.	Photograph of Overpressure Relief Valve Located Between the Secondary and Test Condensers -----	101
38.	Photograph of Test Condenser Flow Straightener ---	102

NOMENCLATURE

A	area [ft ²]
A _t	tensile stress area of screw thread [in ²]
a	length of plate being analyzed [in]
b	width of plate being analyzed [in]
D	diameter [in]
d	diameter [ft]
E	Young's Modulus of Elasticity [psi]
F	force [lbf]
F _a	expansion factor for Annubar equations
F _m	manometer correction factor for Annubar equations
F _v	velocity distribution factor used in the Annubar equations
F ₁	fouling factor
F ₂	wall material conduction factor
F ₃	inlet cooling water factor
f _s	factor of safety
G	cooling water flow rate [GPM]
GPM	gallons per minute
h	enthalpy [Btu/lbm]
\bar{h}	average heat transfer coefficient [Btu/hr-ft ² -°F]
h _{fg}	change in enthalpy between liquid and vapor [Btu/lbm]
h _n	pressure head developed by the Annubar [in. H ₂ O]
K _g	geometric constant used in the Annubar equations

k	tube constant when used in conjunction with the Design Data Sheet
L	effective tube length [ft]
\dot{m}	mass flow rate [lbm/hr]
N	grouped constant, conversion factors for Annubar equations
n	number of threads per inch
Q	flow rate [GPM]
q	load [psi]
S	constant for Annubar equations = $K_g F_v$
S_m	yield strength [psi]
S_w	working strength [psi]
T	temperature [°F]
T_w	wall temperature [°F]
T_{sat}	saturated steam temperature [°F]
t	thickness of material being analyzed [in]
U	overall heat transfer coefficient [Btu/hr-ft ² -°F]
U_c	corrected overall heat transfer coefficient [Btu/hr-ft ² -°F]
UTS	ultimate tensile strength [psi]
V	velocity [ft/sec]
V_a	gas adiabatic correction factor used in Annubar equations
v_g	specific volume of saturated vapor [ft ³ /lbm]
W	steam condensed [lbm/hr]
W_n	steam flow rate [lbm/hr]
y	deflection of plate being analyzed [in]

α	coefficient of linear expansion in Equation (28)
α	} constants used in conjunction with stress and strain equations
β_1	
β_2	
γ_f	specific weight of steam including compressibility [lbf/ft ³]
μ	dynamic viscosity [lbm/ft-hr]
ν	Poisson's ratio
ρ	density [lbm/ft ³]
σ	stress [psi]
σ_b	stress due to bending [psi]

ACKNOWLEDGEMENT

The authors would like to express their appreciation to Mr. James C. Selby for his fabrication achievements and to Mr. Thomas Christian for his advice on instrumentation. We would also like to thank the many people who offered their creative ideas to us during the design of this facility.

I. INTRODUCTION

A. BACKGROUND INFORMATION

Marine steam condenser design has become more important in recent years. Improvements in turbine machinery and boiler design have brought about an increase in the horsepower to weight ratio of marine propulsion systems. However, there has been no similar improvement, in practice, in the steam plant condenser. Consequently, increased power output has necessitated increased condenser size. This trend cannot continue, or the condenser will become the controlling factor in the marine steam propulsion installation [1].

The question then raised is, "Why do we need steam propulsion plants in the marine context?" The alternatives are diesel engines, gas turbine engines, or nuclear power plants. Since nuclear power plants utilize steam to transfer thermal energy to the turbine, as do conventional steam propulsion plants, they will be considered as conventional steam power plants for the purpose of condenser discussion. Diesel engines have proven to be reliable in many applications, but they have a low horsepower to weight ratio which makes them undesirable where very high horsepower is required. Furthermore, they are difficult to apply to a reversing application. The gas turbine is a formidable competitor of steam propulsion. When a gas turbine is used in conjunction with a controllable pitch propeller, it can be

quite efficient. The initial cost of a gas turbine is low when compared with the steam propulsion plant, and the horsepower to weight ratio is extremely attractive. However, the marine environment is very corrosive, and sulfidation or "hot corrosion" takes a heavy toll on the gas turbine engine. Since the use of the gas turbine is relatively recent in the U.S. Maritime community, the experience level of the operating personnel is limited. In contrast, steam propulsion systems have been used successfully for many years. A wealth of experience has been gained, and reliability of steam propulsion has been well documented. This has importance to the commercial shipping industry in quest of a crew and a reliable ship. It also has importance to the Navy, which has decided to make extensive use of Nuclear Power, with its associated steam propulsion plants. Consequently the steam propulsion plant has a permanent place in both military and commercial applications for the foreseeable future.

Of specific interest to the U.S. Navy is increased efficiency, not only engine efficiency, but also combat efficiency. By increasing engine efficiency, cruising radius is expanded, and logistics problems are reduced. If smaller condensers are produced, there could possibly be a manufacturing cost savings as well as a weight and space savings, resulting in increased combat effectiveness. It may be within the state-of-the-art to reduce weight, size, and cost of condensers.

However, large Marine condensers, utilizing advanced tube designs have not been built. The reason for this has been apparent lack of confidence that they will work as expected, plus the fact that those presently in use with standard tubes have been very reliable.

Practical marine steam condenser design is based almost exclusively upon two documents. The Heat Exchange Institute Standards for Steam Surface Condensers (HEI) [2] and the Standards of Tubular Exchange Manufacturers Association (TEMA) [3]. The U.S. Navy amplifies the HEI information in the Design Data Sheet (DDS) [4]. These standards have proven to be reliable. However, it is evident that the resulting condensers are significantly overdesigned. This is due in large measure to the use of average values for heat transfer coefficients rather than local values which vary throughout the condenser.

Obvious in the overdesign of naval condensers is increased weight with a greater resultant displacement and wetted hull area. The machinery spaces are more crowded and less available for maintenance. A less obvious problem, more detrimental to plant operation, is overdesign for full power operation and then operation at reduced power. The problem then is inefficient operation due to cooling of the condensate below the saturation temperature. It is also possible that the assumed fouling factors are overly generous, which increases the design size of the condenser [5].

B. CONDENSER HEAT TRANSFER

With the advent of heat transfer enhancement concepts, much data is needed to refine the existing condenser design methods. Computer aided design has become a reality. Oakridge National Laboratory has developed the ORCON 1 computer program, which Lt. Harry T. Search, USN, used extensively in his feasibility study of enhanced condensation methods. He showed that the configuration of tubes, baffles, tube sheets, steam inlet, air ejector placement, and condensate affect overall heat transfer [6].

The Westinghouse Corporation has also developed a radial flow design program to synthesize its condenser designs. Their program has been used to design large station condensers [7]. The increased use of the computer in condenser design and data reduction and the reality of tube enhancement have necessitated comprehensive experimentation to investigate the myriad of possible condenser configurations. Experimental data must be obtained to verify the existing computer codes and lend credence to computer design assumptions.

To aid in understanding tube enhancement techniques it is useful to think of heat flow as an electric current controlled by a potential (temperature difference) across a resistance or series of resistances [8]. In equation form this is expressed as:

$$\begin{array}{l} \text{Rate of Heat Flow} \\ \text{Per Unit Area} \end{array} = \frac{\text{Thermal Potential Difference}}{\text{Thermal Resistance}} \quad (1)$$

The thermal resistances pertinent to the condenser problem are as follows:

1. Internal Convective Film Resistance - R_i
2. Solids Fouling Resistance - R_f
3. Tube Wall Resistance - R_w
4. Condensate Film Resistance - R_o
5. Non-Condensable Gas Film Resistance - R_g

The sum of these resistances is the reciprocal of the overall heat transfer coefficient, U_o [9]. The condenser heat duty is then defined as a function of the overall heat transfer coefficient, as given below:

$$Q = U_o A \text{ LMTD} \quad (2)$$

where Q is the heat transfer rate,

A is heat transfer surface area, and

LMTD is the log mean temperature difference between the outside and the inside fluids.

The approach to enhanced heat transfer is to reduce any or all of these resistances or to increase U_o . Those resistances with the greatest relative magnitudes offer the greatest opportunity to reduce the overall resistance to heat transfer. The solids fouling resistance (R_f) is a function of the cleanliness of the system. In a controlled experiment it can be measured or reduced to zero, but in practical condensers it can never be eliminated. The tube wall resistance (R_w) is dependent upon the tube wall thickness and the thermal conductivity, which is fixed for a particular material. In controlled test conditions the non-condensable gas film resistance can be reduced essentially to zero, if care is taken during construction and operation of the equipment. The two remaining resistances are the convective film resistance, R_i (internal, cooling water), and the condensate film resistance, R_o (external, condensate). With conventional condenser designs, these last two resistances form the greatest portion of the overall resistance, with the convective resistance being the larger of the two. See Figure 1.

A great deal of research has been done in the area of heat transfer augmentation. A recent and very informative

compilation of the augmentation methods was presented by Bergles [10,11]. He categorized augmentation techniques into three areas:

Passive Techniques, consisting of

- Treated surfaces,
- Rough surfaces,
- Extended surfaces,
- Enhanced tubes,
- Displaced Enhancement devices,
- Swirl flow devices,
- Coiled tubes,
- Surface tension devices,
- Additives for liquids (liquid, solid, gas), and
- Additives for gases (liquid, solid).

Active Techniques, consisting of

- Mechanical aids,
- Surface vibration,
- Fluid vibration,
- Electric fields,
- Injection, and
- Suction.

Compound Techniques, consisting of

- any combination of the above categories or subcategories.


Bergles' recommendations indicate that much fundamental work remains to be done in each of these areas. For condensing applications in particular, the two most promising techniques include treated surfaces and enhanced surfaces. Treated surfaces will be considered under the heading of dropwise condensation, and enhanced surfaces, under the heading of geometric enhancement.

C. DROPWISE CONDENSATION ENHANCEMENT METHODS

There are two modes of condensation. One is dropwise and the other is filmwise. If dropwise condensation could be induced and maintained, there would be a large increase,

on the order of two hundred percent, in the heat transfer coefficient. The dropwise condensation mode can be induced by promoters, or non-wetting agents. The non-wetting agents cause the drops, formed at small pits or scratches called nucleation sites, to remain discrete. Because the drops remain discrete, no continuous film develops. This is important because discrete drops are many times smaller than a film of condensate, giving much higher heat transfer coefficients.

The dropwise condensation mechanism is presently considered to involve four phases:

- | | | |
|--|---|--------------------|
| 1. Nucleation of small drops |  | Decreasing |
| 2. Condensation on these small drops and coalescence | | rate of |
| 3. Coalescence of larger drops | | growth of |
| 4. Departure of large drops. | | condensation drops |

The theory is that heat is transferred through the numerous small drops (nucleation phase) which then coalesce. Further, the condensation, coalescence, and departure phases serve to impede heat transfer by progressively insulating that portion of the surface covered by drops [12]. Therefore, to increase heat transfer or decrease the resistance, the coalescence and departure phases should be accelerated.

There are four accepted methods of promoting dropwise condensation. They are:

1. Plating the surface with noble metals,
2. Chemically attaching promoters to the surface,
3. Injecting promoters into the steam, and
4. Physically attaching permanent promoters to the surface.

Considerable experimentation using noble metals has been conducted by Erb, at the Franklin Institute. He found that gold promoted dropwise condensation throughout the tests, which were as long as 150 days [13]. As late as 1973, Erb wrote that more engineering study was needed in the heat transfer area of dropwise condensation under varying operating conditions [14].

The second method of promoting dropwise condensation involves applying a thin coating of a promoter, such as oils, montan wax, or Benzyl mercaptan, to a test surface [15]. Many chemical non-wetting agents have been tried in this fashion, but each of them promoted dropwise condensation for only a short period of time (about 100 hours on the average) [16].

The third and more practical method of using chemical promoters is to inject the promoter into the steam flow. This is done periodically as the dropwise condensation mode begins to revert to the filmwise mode due to removal of the promoter by the steam. Boiler manufacturers look askance, with justification, at any additives in the steam cycle. Research is needed to allay their fears. Among the substances used in steam injection have been montan wax, filming amines,

Xanthates, Selenium compounds, Disulphides, and a host of others. Limited tests were actually conducted on a marine condenser of the S.S. Normannia (British Transport Commission). However, no heat transfer data was collected, except to note the effective length of time and the overall usefulness of the various compounds tried [16,17].

Condensation data on tubes was found to be scarce within the dropwise condensation literature. Watson at The Admiralty Materials Laboratory, London, conducted large scale experimentation injecting montan wax into a condenser containing 45 tubes. The results showed that montan wax performed well at low steam temperatures in a vacuum environment. Further tests examining the effect of condensate flooding, or inundation, on tubes deep within the condenser were conducted using a condenser with 33 tubes, arranged in a close packed hexagonal array, 11 tubes deep. The top, center tube was configured to be used as an inlet to supply condensate to simulate flooding conditions in the bottom portions of a tube bank [17].

The final method of dropwise promotion involves the physical attachment of permanent promoters to the condensing surface. This method presently holds the greatest attraction for dropwise researchers with teflon receiving the most attention. In the late 1950's and early 1960's, there were several researchers who investigated some of the emerging teflon coatings on tubes. E. F. Coxé of the Westinghouse

Corporation performed a series of tests culminating in the use of a 12 square foot heat exchanger. This experiment was unique in that a vertical baffle was installed in the heat exchanger separating four rows of tubes. On one side of the baffle, the tubes were coated with teflon; and on the other side, the tubes were uncoated. The condensate from each side was collected separately to allow for individual calculations of the heat transfer. This was one of the most promising designs of condensers encountered for comparative heat transfer analysis, with the capability of investigating simulated conditions found in a marine condenser. However, after 40 hours of operation the uncoated tubes started to exhibit dropwise condensation. The contamination causing this phenomenon was never isolated. After approximately 100 hours of operation one of the teflon coated tubes was deliberately damaged by removing a small section of the teflon coating. Further testing showed no continued degradation of the teflon bond. Mr. Coxe recommended that extended tests be conducted to determine the endurance of the teflon tube coating [18]. During the same time frame, the Naval Engineering Experiment Station at Annapolis, Maryland, was tasked with examining condensation on teflon coated tubes. A single tube calorimeter was used to test each of six 60-inch long tubes, with 117 ft/sec steam velocity. The results indicated an average increase of ten percent in overall heat transfer coefficient in the teflon coated tube over the bare tube [19]. It was noted that the parameters of operation

in this experiment, as would be expected, closely resembled those which can be found on a Navy ship. However, the geometry and flow conditions were not similar to those found in a marine condenser, and the teflon coating may have been too thick.

D. GEOMETRIC TUBE ENHANCEMENT METHODS

The other major thermal resistance, R_i , is due to convection of the cooling fluid within the tube. At a cooling water velocity of 10 feet per second (near that found in marine condensers) it has been established that the ratio of convective film resistance (R_i) to condensate film resistance (R_o) for a plain tube is approximately 2.5:1. See Figure 1. This indicates that tube enhancement efforts which concentrate on reducing the convective film resistance could be more beneficial than efforts dedicated to the reduction of the condensate film resistance.

There are many methods being used to try to reduce the convective film resistance. Most of these employ changes in the tube shape to increase the turbulent mixing in the cooling water. Some of the methods include:

1. Swirling the flow with twisted tapes inside the tubes,
2. Roughening the inner surface of the tubes,
3. Increasing the cooling water velocity within the tube, and
4. Corrugating the tube.

Unfortunately any of these methods increases the work required to pump cooling fluid through a tube. If no increase in

work input is desired, then the cooling water velocity must be decreased.

In the late 1960's at the University of Michigan, Briggs and Young [20] constructed a steam condensing system to test heat transfer in copper and titanium tubes. The system consisted of a reboiler and a condenser 18 inches in diameter and 6 feet long. Tubes could be changed by changing the tube sheet. In the early 1970's, Withers and Young tested a proprietary tube shape called "corrugated tube" in the same facility. Corrugated and plain tubes were tested in these experiments [21]. By 1975, more experimentation had been done at the facility by Withers and Young to test additional tubes (Figure 2). This work tended to verify their previously obtained results [22]. Withers and Young reported as a result of these experiments that they had witnessed a decrease in both the convective film and the condensate film resistances, with an overall significant increase in heat transfer [21,22].

* In the late 1960's, Oak Ridge National Laboratory developed the "roped tube" (Figure 3) in an effort to optimize heat transfer without increasing the required pumping power significantly. Since the need for a multiple condenser test was also recognized, a test apparatus was built by Eissenberg in approximately 1970 [9]. His design had many noteworthy features. It incorporated an Inconel condenser, 3 feet in diameter and 8 feet long, which accommodated 163 one-inch diameter tubes 7-1/2 feet long.

These were arranged in an equilateral triangular pitch with a center line spacing to diameter ratio of 1.33. Five of the tubes were instrumented. The remainder of the tubes provided a simulated condenser steam flow. Steam was generated in a stainless steel tubed heat exchanger and flowed horizontally across the tubes. The vacuum in the test section was controlled by a direct contact barometric condenser downstream of the test condenser. Nitrogen could be metered into the steam flow before entering the test section to simulate non-condensable gas effects. Cooling water temperature was controlled. Fouling was prevented by a chromate-type corrosion inhibitor. The maximum steam velocity in the test section was approximately 75 feet per second. Condensate, heated to within 1° to 2° F of the steam temperature, could be pumped to three tubes in the top of the tube bundle to provide spray (inundation simulation) for deep flooding effects.

Based on his experimental results, Eissenberg concluded that the roped tube was 1.9 times as effective as the plain tube and that the convective film resistance was reduced. However, the condensate film resistance did not appear to change from that of a smooth tube [9,23].

There appears, therefore, to be some uncertainty attached to condensate side enhancement based on the previous two works cited here. Further research by both of the above investigators tended to verify each initial contention [22,24,25]. It was stated by Eissenberg that additional

development of tube geometry would probably be needed after such parameters as fouling were quantified. At Oakridge this indicated that there was doubt that the tube geometry had been optimized [9].

Experimentation with the primary emphasis on marine condensers has been very sparse. Two of the very few to do research in this area were Catchpole and Drew of the British Ministry of Defense. They performed a multitube evaluation on a condenser which had two tube banks arranged in five rows with a triangular pitch. The tubes, called Kydensa (Figure 4), were manufactured by Imperial Metal Industries Ltd. The system had the capability of simulating deep inundation by pumping condensate through a perforated tube at the top of the condenser. The results showed an overall increase in heat transfer for the Kydensa over the plain tube under similar conditions.

Within the open literature, this author can find no indication that the optimum tube geometry has been found. Experimentation by Taborek, under the auspices of Heat Transfer Research Incorporated (HTRI), indicated that overall heat transfer coefficients for steam had been doubled by the use of a Turbotec spirally grooved tube over that of a plain tube [26], see Figure 5. The geometries of the various tubes are quite different, as can be seen in Figures 2, 3, 4, and 5.

Several explanations for the improvement in the spirally grooved, corrugated, or roped tubes have been suggested. The convective film heat transfer coefficient has been shown to increase with both groove depth and groove frequency [27]. Increasing these parameters increases the turbulence and therefore the mixing. In conjunction with the increased turbulence there is also a reduction in the thickness of the laminar-sub-layer. These factors serve to increase the convective film heat transfer coefficient. The hypothesis put forth to explain the improvement, if any, in the condensate film heat transfer coefficient appears logical and well founded. Improvement was noted with increased groove frequency and groove depth. The heat transfer over the convex portions of the tube is evidently increased by a thinner condensate film, while the thicker condensate film in the concave portions of the tube promote more rapid drainage, or departure, of the condensate. The increases in condensate film heat transfer coefficient were shown to be limited as groove depth was increased, see Figure 6. This was apparently due to the increased thickness of the condensate film in the concave portions of the tube, offsetting the increase in heat transfer due to film thinning on the convex portions of the tube [27]. Tube number three (III) of Figure 2 yielded the best results for Withers and Young. The trend of data presented by Withers and Young shows that as both the groove height and groove frequency

were increased beyond those of tube number III the overall heat transfer coefficients decreased [22]. This supported the work of Catchpole and Drew [27], that there are limitations in shellside improvement with increased groove depth and groove frequency. The graphic presentation of Figure 7 indicates that the convection film heat transfer coefficient increased more than the condensate film heat transfer coefficient.

E. SUMMATION

In summation of the literature reviewed, it is evident that only the first steps have been taken in the determination of an optimum tube geometry for enhanced heat transfer. It is further evident that more experimental research on marine condenser heat transfer enhancement possibilities is justified. Once an optimum corrugation geometry has been developed, or a new permanent type of dropwise promoter has been developed, the Navy's interest in new and innovative condenser designs requires the testing of such tubes in a variety of steam flow conditions to provide the data base for realistic application. Furthermore, there is no evidence that dropwise promotion of geometrically enhanced tubes or combined techniques has been investigated. The tube geometry optimization process will have to be reinvestigated if the shellside coefficient is altered by promoting dropwise condensation.

II. DESIGN PROPOSAL

A. EXPERIMENTATION AREAS

Based on the foregoing review, it was ascertained that there are approximately ten areas where clarification or additional experimentation is needed. They are:

1. An experimental condenser should be built which has the flexibility of being changed to accommodate various tube spacing to diameter, S/D, ratios. It is believed that varying this parameter can affect the heat transfer [6].
2. Data is needed which shows the results of steam velocity changes.
3. It is necessary to compare the various tube geometries and/or materials under very nearly identical test conditions.
4. Data should be obtained with the condenser slowly oscillating to simulate ship roll.
5. More data is required on the condensation heat transfer coefficients, for a variety of corrugated tubes.
6. Extended tests are needed on promoter coatings for possible dropwise condensation applications.
7. There should be experimental research conducted in combined enhancement; for example, apply various promoter coatings on corrugated tubes or internally finned tubes.

8. Data is needed with different orientation of steam flow. In cramped spaces it could be desirable to position the condenser other than suspended below the turbine as is traditionally done. Computer aided design codes could investigate many possibilities if the data were available to use them with confidence.
9. More data is needed on non-condensable gas concentration and inundation effects on the steam condensation process.
10. Lastly, more data is needed on the fouling factors, both biological and mechanical. This is a serious unknown quantity in the area of corrugated tubes in the ocean cooling water marine system, especially with titanium tubes.

B. OBJECTIVES OF THIS DESIGN

These ten areas, for additional research, define this design problem. After consideration of the problem and several iterations on the initial design synthesis, the following list of objectives was decided upon.

To design a test condenser with the following features:

1. Variable steam flowrates,
2. Variable cooling water flowrates,
3. Variable cooling water temperatures (heating only, initially),
4. Variable vacuum pressures (controlled by controlling air ejectors),
5. Variable non-condensable gas concentrations,
6. Variable steam flow orientation (tilt condenser),

7. variable inundation effects (using condensate spray),
8. variable periodic motion (capability to simulate ship's roll),
9. Adequate visibility to observe the modes of condensation, and
10. Relatively easy exchange of a variety of test tubes.

C. CAPABILITIES OF THE TEST FACILITY

When the objectives are completed, the test facility will have the capability of:

1. Testing single tubes in both the dropwise and filmwise modes to ascertain the outside and inside heat transfer coefficients under varying steam velocity conditions and varying cooling water flow-rates,
2. Performing #1 in a variety of steam flow orientations (0-180 degrees) relative to gravitational force,
3. Performing #1 and/or #2 while studying the effects of inundation and/or non-condensable gas concentration,
4. Performing #1 and any combination of #2 and/or #3 while oscillating the tubes to simulate ship's roll,
5. Testing multiple tubes (up to nine 5/8" tubes in vertical rows) in any of the operations mentioned above.

III. DESIGN DESCRIPTION

A. DISCUSSION

In any design effort there are design phases or processes which are undertaken. In this project, the areas of creative design synthesis, preliminary design and development, detailed design, and prototype building were performed. See Figure 8.

The basic system and the test condenser were conceptualized in the creative design synthesis phase of design. In the preliminary design the basic dimensions, general layout and capabilities were agreed upon. The actual components to be used were chosen in the detailed design phase, and the prototype was built as materials, time, manpower, and money became available.

The myriad of variables in the condensation process complicated the process of deciding upon a rational design. Often the optimum component, from the standpoint of meeting the test objective, was found to be impractical or prohibitively expensive. Initially, funding was not to play an important part in the design alternatives. It was desired to engineer the system to meet the design objectives in the best way known to the designer. However funding quickly became the lead designer. Even in light of this, care was taken to insure that all components were chosen to allow for expanding the research and the facility's

capabilities. Due to time constraints, the "off-the-shelf" or readily available item was often used even when a more appropriate component could possibly have been built.

1. Brief System Overview

To understand the test facility it is perhaps best to follow an element of fluid through the entire cycle, beginning at the boiler. The five systems comprising the overall test facility are schematically represented in Figures 9 through 13, and photographs of the various components are included in Figures 14 through 38.

The boiler generates steam, which exits through a throttling valve. The throttling valve maintains a positive boiler pressure. The steam is then filtered prior to entering the stainless steel piping enroute to the test section. While enroute, the flow rate is measured by an Ellison Annubar, primary flow element. From there, the steam passes through a 3 foot long section of corrugated tubing. The corrugated sections, both upstream and downstream of the test condenser, are installed to allow for dynamic tests. Next, the steam passes an inline, direct contact desuperheater, which may be necessary to reduce the steam temperature to saturation. The steam then enters the test condenser where the installed back pressure screen and flow straightener insure that the steam is evenly distributed across the test section. Here the quality, temperature and pressure are recorded. The remaining steam proceeds to the secondary condenser. The condensate meanwhile flows down to an

expanded section of pipe where it is stopped by a solenoid valve and collected, and the volume is measured. At the conclusion of the volume measurement, the condensate is released as the solenoid valve is opened. The condensate flows to the secondary condenser hot well where it mixes with the condensate from the secondary condenser. The condensate is then pumped to the feed tank. Here it is periodically pumped into the boiler to replenish the water supply and complete the cycle.

B. DESCRIPTION OF COMPONENTS

1. Major Components

a. Boiler

The steam generator, or boiler (See Figures 9 and 14.), available for this project, is a Fulton Electric Boiler, Model 4.2, which has the following capabilities:

Power Rating: 4.2 HP (42KW),

Steam Production: 141 lbm/hr (at saturated conditions), and

Maximum Pressure: 150 psi.

It has three electric heating elements installed in a 20 gallon capacity tank. Its overall dimensions are approximately 30 inches high, 30 inches deep, and 27 inches wide.

The ability to produce only approximately 140 lbm/hr of steam placed a constraint on the test condenser size in order to achieve a desired steam velocity of 100 ft/sec. It was decided to accept temporarily the reduction in vapor velocity and maximize the efforts to meet the other

objectives. Of present concern is whether or not the boiler exit conditions will fluctuate too much to permit stable conditions in the test condenser. Fluctuations will possibly be caused by intermittent injection of feed water into the boiler. The recovery time of the boiler is unknown. Tests will be conducted after system activation. In the event that boiler fluctuations are too large, a provision has been made to supply house steam, which is available at up to 80 psi. to the system. The complete details of the boiler operation are found in the manufacturer's instruction book [28].

The boiler is constructed of carbon steel. Although it would have been desirable to have a stainless steel boiler to minimize system contamination, the severe increase in cost was not justifiable for initial tests. With a filter installed (Johnson, Type S, Steam Separator), the effect of contamination on filmwise condensation at the test section is considered minimal. When dropwise condensation tests are undertaken, it may be necessary to have a completely stainless steel system.

b. Test Condenser

The test condenser is a completely unique design (See Figures 15, 16 and 17), although many features were dictated by the decision to use the available boiler with 140 lbm/hr steam supply. The test condenser consists of a stainless steel rectangular box approximately 35 inches high, 3 inches

wide, and 3 feet long. The diverging entrance region, also of stainless steel, contains steam baffles which are to be used for condensate collection when the condenser is tilted more than 90° from the vertical. The bottom of the main section is slanted to facilitate condensate collection while in the upright position. The heart of the test condenser is the tubed section (See Figures 18 and 19.), which is preceded by a flow straightener also of stainless steel. The tubed section, in the initial configuration, has constant flow area between all tubes and the condenser walls for consistent flow simulation. There are windows on both sides to allow viewing of the condensing process. Tubes with 5/8 inch outside diameter may be changed without changing the tube sheet. If other diameter tubes are to be tested, the tube sheets must be modified.

There were numerous decisions to be made as the design proceeded. The following parameters were among those first considered:

- 1) The length of tube within the condenser to establish a fully developed temperature profile and hydrodynamic entrance length in the cooling water.
- 2) The length of tube between the tube supports in a Naval Condenser.
- 3) The tube spacing (pitch) in a Naval condenser.
- 4) The pressure/temperature in a Marine Condenser.

- 5) The cross sectional flow area to determine vapor velocity.
- 6) The creative design synthesis.
- 7) The detailed design.

An examination of each of these parameters was conducted and is outlined below.

(1) Tube Length. In order for the data to reflect accurately the heat transfer characteristics, the tube length to be tested was selected to insure fully developed temperature and hydrodynamic profiles. As defined by Sparrow [29], the thermal entrance length is the tube length required to obtain a local Nusselt number (Nu) within five percent of the fully developed flow Nusselt number (Nu_{∞}). It was determined by examination of a plot of the ratio Nu/Nu_{∞} versus x/D (distance/Diameter), parametric in Reynolds Number, that the effect of Reynolds Number is small; see Figure 20 [29].

Using the parameters in a marine condenser and those anticipated in this test facility, Reynolds numbers of approximately 40,000 and a Prandtl number of approximately 7 were calculated. To be within five percent of a fully developed Nusselt number required that $Nu/Nu_{\infty} \leq 1.05$. Analytical results for entrance length, expressed as a ratio, x/D , ranged from 2 to 4 for $Pr = 10$. Experimental results by Hartman indicated that $x/D = 3$ for $Pr = 7-8$. This is displayed in tabular form in Figure 21 [29]. The developed thermal profile was, therefore, not a design

constraint as the tube length required by an entry length of $x/D = 5$ is 2.64 inches for a 5/8 inch tube size. Hydrodynamic entrance length for fully developed flow is considered to require approximately 50 diameters of length [30]. Due to the length of the piping leading to the test condenser, this was not a serious constraint.

(2) Distance between tube supports. The next possible constraint was the distance between tube supports in a Naval condenser. According to the Military Specification which governs the construction of Naval condensers, the tube support plates are not to be over three feet apart [31]. Also, an examination of the working plans of three different ships revealed a maximum of three feet between tube support sheets. Thus, the working length of the test condenser tubes for this design was set at three feet.

(3) Tube spacing. The initial test configuration depicted in Figure 18 clearly shows the consistent flow area between tubes. The window frame forms part of the geometry to make the flow area consistent. Only the central tube is to be instrumented in this configuration.

Tube spacing (pitch) was desired to conform, as nearly as practicable, to that used in an actual marine condenser. Various researchers have used values of S/D (Spacing/Diameter) from 0.875 to 1.33. However, upon examination of the condensers used in seven different ships, an average value of 1.5 for S/D with equilateral triangular pitch was decided upon. Within those condensers examined,

the S/D ratio changed depending upon what area of the condenser was considered. No attempt to duplicate this is expected to be undertaken in this research. But, by merely changing the easily removable tube sheet of the final design, the pitch and number of tubes can be changed.

(4) Pressure and temperature in a marine condenser. Pressures and temperatures in a naval condenser vary with each group of operators. Vacuum pressures vary from approximately 25 to 28 inches of Mercury in a variety of shipboard main condensers, with saturation temperatures from approximately 133 °F to 101 °F. Therefore, in the design calculations, 2.0 psia and 127.07 °F were selected as operating conditions.

(5) Vapor velocity. Having decided upon a reasonable facsimile of the naval condenser, steam flow calculations yielded a maximum steam velocity in the test condenser of approximately 43 ft/sec. The desired vapor velocity was 100 ft/sec; therefore, it was considered pertinent to examine the possibility of increasing the system capability. Should this be desired a steam supply of 324 lbm/hr would be required (See Appendix A.).

(6) Creative design synthesis. During the creative design synthesis phase of the test condenser design, each of the thesis objectives was considered. Notable among these were:

- Design objective #6 - Variable steam flow orientation (tilt condenser)
- Design objective #7 - Variable condensate inundation (recycle condensate)
- Design objective #8 - Variable periodic motion (simulate ship's roll)
- Design objective #9 - Adequate visibility to observe the condensation process
- Design objective #10 - Relatively easy change of a variety of tubes.

Design objective number six requires consideration of a multitude of problems. The first problem is that of inventing a method of rotating the condenser about the centerline of the tube being tested to a new position and then re-establishing the vacuum tight integrity of the system. This is accomplished with the use of Marman Flexmaster pipe joints (See Figure 22,). By loosening one end of the Flexmaster pipe joint at the ends of the main steam piping and, of course, the restraining mechanism at either end of the test condenser, the test condenser may be rotated as desired (See Figure 17,). Alternate condensate collection has to be provided after rotating the test condenser past the 90° position. This is done by having the baffles in the steam vapor entrance region serve as condensate collection vanes as well as steam baffles. Framing for the test condenser will be designed to support adequately the test condenser during testing in conjunction with design objectives number eight and number six. This has been deferred until a later stage of testing.

Design objective number seven encompasses two unknowns. The first is the question of true flow characterization of the condensate. The second is how to best supply the condensate to simulate deep tube inundation or flooding. It was decided that observation with the aid of high speed photography is going to be necessary to characterize the inundation. To accomplish this an inundation system will be installed in the "dummy tubes" above the "test tube" in a later stage of the testing. Then, with the use of high speed photography the condensation process can be analyzed, and the effect of condensate inundation on the heat transfer process can be realistically characterized. Another consideration in the inundation studies is how many tubes deep the tube bank should be made. It was concluded, as a result of the literature search, that most of the previous researchers used vertical rows of tubes less than nine deep in their test condensers. This means that the test condenser has to be at least 13.62 inches deep to accommodate a vertical row of nine tubes, each with a 5/8 inch diameter (Figure 19).

Design objective eight necessitates considering the effect a rocking motion will have upon the various connections of the test condenser. In preparation for this, flexible/corrugated tubing was selected for all connections. The most promising method of rocking the condenser is considered to be a hydraulic system, yet to be designed but schematically shown in Figure 17.

Design objective number nine is incorporated to allow three advantages. They are:

1. Operator/Researcher visibility,
2. Camera Access, and
3. Lighting ease for photography.

The choice is whether to use glass on one or both sides. Advantage three, lighting ease, makes the option for glass on both sides most attractive.

Design objective number ten requires that a complete redesign of the test condenser not be necessary to change the number of tubes, tube size, or type pitch. The only logical choice is to redesign the tube sheet for major changes using a type of through sealing device, for quick changes of small numbers of key tubes. (Figure 23).

The choice of construction material is dictated by a requirement that a clean system must be obtained to minimize the unpredictable variables such as corrosion, fouling, and outgassing of the metal in a vacuum environment. This is desirable for filmwise condensation tests and may be a necessity for dropwise condensation tests. Therefore, due to availability, ease of manufacture, and cost, stainless steel type 304 was chosen over other acceptable metals such as titanium and stainless steel type 316.

(7) Detailed design. The detailed design of the test condenser involved careful consideration of the following areas:

1. Stresses on the test condenser,
2. Stress on the glass,
3. Thermal stress,
4. Fastener (bolt/stud) selection,
5. Tube sheets,
6. Pipe size,
7. Test condenser overpressure,
8. Steam velocity in the entrance region,
9. Flexible connectors for dynamic testing, and
10. Flow straightener and backpressure screen.

Each of these is considered in Appendix B.

c. Secondary Condenser

The concept of using a secondary condenser has several advantages. It is believed that conditions will be more stable in the test condenser if only a controlled amount of the steam generated is drawn through the test condenser. This approach allows a high steam generation rate, thereby minimizing fluctuations in the boiler. It also provides a method of operation and/or warm-up while bypassing the test condenser. Therefore, the secondary condenser was designed to accommodate the maximum amount of steam the boiler could generate. A model 9-14S Heliflow heat exchanger made by Graham Manufacturing Co., Inc., was available (See Figure 26.). Utilizing the Design Data Sheet procedure outlined in Appendix C [4], it is deemed feasible to use the Heliflow for the presently installed boiler capability. By installing the heat exchanger with

the openings facing downward and the condensing, steam side being the inside of the tubes, the Heliflow becomes a condenser.

2. Auxiliary Systems and Components

a. Desuperheater

The steam is expected to flash in passing through the throttle valves and perhaps upon expansion when entering the test section. To reduce superheat, an inline desuperheater is to be installed at the entrance to the test condenser, which spray mixes condensate, at the saturation temperature from the secondary condenser hot well, with the entering steam. This will lower the temperature of the steam to the saturation temperature desired for the test.

b. Condensate Collection System

The condensate collection system, Figure 10, utilizes stainless steel tube or pipe to connect the two condensers with their respective hot wells. The hot wells are connected by stainless steel tubing and a solenoid operated valve. The condensate is pumped to the feed system from the secondary condenser hot well.

The condensate collection system is designed to perform two functions. First, it provides a means of measuring the condensate obtained from the test condenser. Second, it provides for the return of the condensate to the feed system. To accomplish this, two hot wells are required, one for each condenser. The one for the test condenser will be sized according to the amount of condensate expected to

condense in the test section. The other one provides a drain for the test condenser hot well, collects condensate from the secondary condenser, and provides a positive head for the condensate pump. The computation for the minimum size of the secondary condenser hot well is relatively straightforward. It is believed that it should hold at least two minutes of condensate or 9 lbm, at full power operation of 170 lbm/hr. The value of 170 lbm/hr. was arbitrarily selected to allow approximately a twenty percent greater capacity than would be actually needed. Since 9 lbm of water occupies about one gallon, a tank which holds two gallons has been constructed for this hot well. To preclude the possibility of cavitation at the condensate pump inlet, it was decided to position the pump as far as possible below the test condenser hot well.

The condensate pump selected, once again because of availability, was a Teel, model 1P700, stainless steel centrifugal pump made by the Dayton Electric Manufacturing Company (Figure 25). Its output for a head of 4.5 feet is approximately 19.6 GPM. Since 140 lbm steam/hr. equals 16.78 gallons of condensate/hr., the pump is quite adequate. A recirculation line between the pump discharge and the secondary condenser hot well provides for pump cooling.

The hot well for condensate collection from the test condenser is designed for measurement of the condensate from the initial configuration test condenser. To accomplish this, the expected amount of condensate is determined, in

Appendix D, to be approximately 0.60 gal/hr. It is desired to determine the condensation rate in a short period of time - less than one minute. This means a container with a volume of at least 0.010 gal. Since two methods of measurement are desired, this hot well is to be made of glass and graduated to provide a visual backup reading. Therefore, a cylinder with a capacity of 5 cubic inches, graduated in inches, and rated for vacuum application is suggested for this application.

A solenoid valve is positioned between the test condenser hot well and the secondary condenser hot well (See Figure 26.). To take a measurement, the solenoid valve is closed, and the rate of condensate collection is measured electronically (Additional information is presented in the section on Measurement and Control.). The condensate pump is run constantly when the system is on but only delivers condensate to the feed system when the float valve in the feed tank opens, indicating a need in the feed system for more water.

c. Cooling Water System

The cooling water system (See Figure 11.) consists of two pipe branches from a 1-1/2 inch main line. One branch goes to the secondary condenser, and the other goes to the test condenser. The flow is controlled in each branch by throttling valves. The cooling water to the test condenser is temperature regulated by controlled heating. The piping throughout the cooling water system is galvanized

iron. The pipe to the secondary condenser is 1-1/2 inch diameter which is reduced to 1-1/4 inch diameter to conform with the secondary condenser fittings. The pipe to the test condenser is 3/4 inch diameter. The maximum flow to the secondary condenser is calculated in Appendix E to be 34.43 GPM. For the test condenser with a maximum cooling water velocity of 26 feet per second, the necessary flowrate would be approximately 18 GPM. Therefore, the total flow for the system is conceivably 52 GPM. However, on the basis of condensing calculations (Appendix C), it is determined that approximately 27 GPM is the most required by the secondary condenser. The total would then be nearly 45 GPM at maximum capacity. For the early experimentation, only 33.19 GPM are computed to be needed. Plans to cool and recycle the cooling water are not completed due to the excessive cost of such a venture. However, for long term operation of this facility, a small cooling tower or large reservoir could be used to cool the cooling water.

To control the temperature and the flowrate of the cooling water to the test condenser requires three steps (See Figure 27.). The first step is to heat the cooling water to a predetermined temperature and to maintain that temperature. The second is to provide a pump in the system to boost the line pressure to allow for higher cooling water velocity. The third is the regulation of the water pressure to reduce the line fluctuations to an acceptable level. For temperature control, two alternatives are available:

1. Electrically heat the water, or
2. Steam heat the water.

Commercial heat exchanger units are available, such as the Leslie Constantemp, Johnson Cor-Tube Steam water heater, Bell and Gossett "SU" heat exchangers, or Watlow electric heaters, to name a few. The choice was, once again, controlled by what was most readily available. House steam was available; therefore, steam heating was chosen. A Bell and Gossett Type Su 42-2 heat exchanger was available which far exceeds the necessary heating capability. The resultant unit consists of a Powers model 11A self-actuating temperature regulating valve with a range from 55 °F to 115 °F. This valve is installed in the steam inlet line to the Bell and Gossett heat exchanger. The temperature sensing bulb (temperature regulating valve actuator) is installed in a locally manufactured surge tank (See Figure 27). The cooling water is routed through the heat exchanger and then through the surge tank to a booster pump which supplies water to the test section as well as circulation in the surge tank for mixing. A backpressure regulator and a filter are installed in the line to the test condenser to minimize contamination and pressure fluctuations.

d. Boiler Feed System

The feed system is a Fulton return system (See Figures 12 and 28.) rated for a six to ten horsepower boiler and having a 30 gal. capacity. The feed pump is a Burks pump, model 5CT5M serial number 17888. The condensate is

returned to the feed system via a float operated valve. The Burks pump is intermittently operated when the boiler liquid level sensors indicate the boiler needs water. This system is constructed of galvanized iron pipe with carbon steel tanks. It may be necessary to replace it with a stainless steel system when dropwise studies are undertaken. The low level sensor turns on the feed pump, and the high level sensor switches the feed pump off. As the water level decreases in the feed tank, the float valve opens allowing the condensate to enter from the secondary condenser hot well via the condensate pump.

e. Vacuum System

The system vacuum pressure in the test and secondary condensers is maintained by a two stage air operated air ejector (See Figures 13 and 29.). Vacuum is controlled by bleeding air, by means of a Model 16 Fairchild vacuum regulator, into the suction of the air ejector to provide a false load.

Non-condensable gases have been proven to be very detrimental to the condensing process. Also, naval/marine condensers operate in a vacuum for increased plant efficiency. Non-condensable gases collect at the point of lowest pressure. Therefore, the maintenance of a vacuum and the removal of non-condensables are interrelated. To accomplish these ends a two stage non-condensing air operated air ejector was procured from the Graham Manufacturing Company. The motive air required is 43 SCFM at 100 psig.

The volume to be evacuated was estimated to be less than 4 ft.³ . The calculated time for the Graham air ejector to evacuate this volume to 25.5 inches of Mercury vacuum is approximately 45 seconds.

C. UNCERTAINTY ANALYSIS

In the design of an experiment, two questions which must be answered are:

1. What is the desired accuracy of the quantities to be measured?
2. Can the needed quantities be measured to the desired accuracy?

In some applications these questions are academic and, the best measurement devices are, by definition, those readily available. However, in this situation, the critical measurements most affecting the results must be known to determine where to place the monetary emphasis. For example, the range of cost for the steam flow measurement is from \$50. to \$2,000. Therefore, an uncertainty analysis is determined prudent in order to make rational purchase decisions. To analyze the problem, the "Second Order Equation" described by Kline and McClintock [32] is used. The details of the uncertainty analysis are in Appendix F.

IV. MEASUREMENT AND CONTROL

A. OPERATIONAL MEASUREMENT

The area of operational measurement encompasses those measurements enabling the operator to run the system safely. These measurements (See Figure 30.), designated to be used only by the operator, are independent of those needed for test measurement.

Generally, all temperature measurement for operations only is to be accomplished by the use of locally manufactured copper-constantan thermocouples. This type of thermocouple was chosen because it has the desired temperature range between -300 and +700 °F and is resistant to corrosion in most atmospheres. [33]. There are no temperatures in this system which are expected to approach these limits. The following temperatures are planned to be measured:

1. Steam at the boiler exit,
2. Steam at the test condenser inlet,
3. Steam at the secondary condenser inlet,
4. Condensate at the secondary condenser hot well,
5. Condensate pump casing,
6. Feed pump casing,
7. Cooling water pump casing,
8. Feed water at the boiler inlet,
9. Cooling water at the secondary condenser inlet, and
10. Cooling water at the secondary condenser outlet.

All but one of these thermocouples are to be connected to the display unit, a Newport digital pyrometer model 267. The boiler temperature is to be displayed for constant monitoring on an Omega, Series "S", indicating pyrometer.

There are three pressures to be monitored continuously.

They are:

1. Boiler pressure,
2. Secondary condenser pressure, and
3. Test condenser pressure.

The boiler pressure is registered on an Ashcroft 0-100 psig pressure gauge. The condenser pressures are indicated on two Wallace and Tiernan 0-30 psia absolute pressure gauges. These gauges are all locally available.

The cooling water flowrates in both condensers are designed to be monitored continuously with the use of rotameters. Recall that the calculated flowrates for the initial configuration of the test condenser are approximately 27 GPM for the secondary condenser and 10 GPM for the test condenser. The flowrate monitoring for the secondary condenser is not considered critical, and therefore an available Fisher & Porter Rotameter, model 10A2735P, with a capacity of 86 GPM is used. The test condenser cooling water flowrate is monitored with an available Fisher & Porter Rotameter, model 10A3565A (11 GPM capacity). In addition, the operator has an installed boiler water low level alarm.

B. CONTROL

The entire electrical power to the control panel is wired through a key operated circuit breaker and a master switch. The master switch permits rapid shutdown of the system for any safety problem. The boiler controls consist of:

1. An ON/OFF switch,
2. Two Honeywell Pressuretrols,
3. Heating element thermostats,
4. A steam throttling valve, and
5. A feed water flow valve.

The Pressuretrols are for high limit pressure control, operating pressure and operating pressure differential.

The steam flow is designed to be controlled by two valves: one to control steam flow through the test condenser and one to control the flow through the bypass directly to the secondary condenser. Steam temperature is regulated by controlling a valve in the condensate line to the desuperheater.

Cooling water flow controls and the vacuum pressure controls have been described earlier. Additionally there are ON/OFF switches to control all pumps.

C. TEST MEASUREMENTS(See Figure 3L)

For test data collection, the following quantities are to be measured:

1. Vapor temperature in the test condenser,
2. Cooling water flow rate to the test condenser,
3. Temperature of the cooling water into the test condenser,

4. Temperature of the cooling water out of the test condenser,
5. Temperature of the "test tube" wall,
6. Steam flowrate,
7. Steam quality,
8. Vacuum pressure in the test condenser,
9. Cooling water pressure drop, and
10. Condensation rate in the test condenser.

For the data collection temperature measurements, copper-constantan thermocouples with grounded junctions, in 1/16 inch diameter type 304 stainless steel sheaths, are to be used. This choice was made because they are easily obtainable, and they operate in the desired temperature range. The grounded junction offers a faster response than other types of shielded junctions. Copper-constantan extension wire and an Omega 28 pole thermocouple selector switch are also being used to insure proper readings on a Newport model 267 digital pyrometer.

The cooling water flowrate can be measured by using:

1. A rotameter, and
2. A turbine flowmeter.

The rotameter was discussed in the section on operational measurements. The turbine flowmeter is available locally and is encased in plexiglass for observation.

The pickup for the turbine flowmeter is an Electroproducts magnetic type pickup, model 3010 HTB. The display chosen is a Fluke digital frequency counter, model 1950A, calibrated to read mass flowrate directly.

There are several choices to consider for the steam flowrate measurement. These are listed below:

1. An ITT Barton, series 7000, precision turbine flowmeter,
2. An Eastech V/C, 3000 series Vortex cell flow transmitter,
3. A venturi meter,
4. A pitot-static tube,
5. A hot wire anemometer,
6. An Ellison Annubar, or
7. An orifice plate.

Saturated steam flowrate is inherently difficult to measure. Pitot static tubes and hot wire anemometry are noted as being inaccurate with change of phase. The venturi meter is difficult to calibrate and would have to be manufactured locally, incurring a time delay. The Barton turbine flowmeter and the Eastech Vortex shedding meter are simply too expensive to consider. The resultant choice is the Ellison Annubar (See Figure 32.).

The Annubar, a primary flow element, is named after a method of self-averaging the annular segments within the pipe. Calculations for the pressure head developed in the Annubar are found in Appendix G. The output of the Annubar is sensed by a Celesco KP15 pressure transducer. This signal is then fed to a Celesco Carrier demodulator, model CD10, and from there to a Hewlett-Packard, model 3430A, digital voltmeter for readout. The HP 3430A was chosen because it has

an analog output which is compatible with an Autodata-Nine data acquisition system manufactured by Vidar Autodata, Inc. To improve the accuracy of the Annubar, it is to be positioned with 7 diameters upstream to a tee and 23 diameters downstream to the control valve. These values include the manufacturer's recommended distances and a twenty-five percent increase for laboratory work.

Steam quality measurement poses a unique problem. The only method readily available at an acceptable cost is the throttling calorimeter. The use of the calorimeter is not difficult in a positive gage pressure application. The principal of the calorimeter is based on the fact that enthalpy is constant in a throttling process. By knowing the temperature before and after throttling, the enthalpies can be found and the quality calculated as follows [34]:

$$x = \frac{h_2 - h_f}{h_{fg}} \times 100 \quad , \quad (3)$$

where: x = steam quality (expressed as a percentage),
 h_2 = enthalpy of superheated steam at
 calorimeter pressure and temperature,
 h_f = enthalpy of saturated liquid in mixture
 prior to throttling, and
 h_{fg} = enthalpy of vaporization corresponding
 to pressure or temperature of steam
 entering calorimeter.

The problem is to throttle from the vacuum in the test condenser to a lower pressure in one of two ways as follows:

1. Throttle to the secondary condenser if sufficient vacuum differential exists between the test and secondary condensers, or
2. Throttle to a lower pressure provided by a mechanical vacuum pump through a cold trap [35].

Tests will have to be made, after the system is activated, to determine the best course of action.

Vacuum in the test condenser will be measured in two ways using:

1. A standard mercury manometer, and
2. An absolute pressure transducer.

The pressure transducer is a Celesco model PLC absolute pressure transducer with a range from 0 to 15 psia. The output from this transducer will go to a strain gage amplifier and then to a Hewlett-Packard model 3430A digital voltmeter. The cooling water pressure drop across the test condenser is to be measured directly with a differential pressure manometer with static taps.

The condensation rate is to be measured with the use of a locally manufactured liquid level monitor. This monitor operates on the principal of variable capacitance of a wire immersed in a liquid.

D. DATA REDUCTION

The data collection and reduction are schematically represented in Figures 33, 34 and 35. During the measurements, the heat transfer rate across the test condenser tube will be determined by two independent methods. The heat

transfer rate in each of these cases is given by

$$Q = \dot{m}_c C_p (T_{co} - T_{ci}) , \quad \text{and} \quad (4)$$

$$Q = \dot{m}_{cond} (h_i - h_o) . \quad (5)$$

In addition, the heat transfer rate is related to the overall heat transfer coefficient by:

$$Q = U_o A_s \text{LMTD} . \quad (6)$$

In the above equations,

- Q = heat transfer rate,
- \dot{m}_c = mass flow rate of the cooling water = $\rho V A_f$,
- \dot{m}_{cond} = mass flow rate of condensate,
- \dot{m}_s = mass flow rate of the steam,
- C_p = specific heat of water at constant pressure,
- T_{co} = temperature of the cooling water at tube exit,
- T_{ci} = temperature of the cooling water at tube entrance,
- h_i = steam vapor enthalpy prior to condensing,
- h_o = condensate enthalpy,
- U_o = overall heat transfer coefficient,
- A_s = area of the steam condensing surface, and
- LMTD = log mean temperature difference,

$$= \frac{(T_s - T_{ci}) - (T_s - T_{co})}{\ln \frac{(T_s - T_{ci})}{(T_s - T_{co})}}$$

where T_s = saturation temperature of the steam.

Equations (4), (5), and (6) may be combined to show:

$$U_o = \frac{Q}{A_s (\text{LMTD})} = \frac{\dot{m}_c C_p (T_{co} - T_{ci})}{A_s (\text{LMTD})} = \frac{\dot{m}_{\text{cond.}} (h_i - h_o)}{A_s (\text{LMTD})} \quad (8)$$

By substituting symbols for \dot{m} and LMTD, Equation (8) becomes:

$$U_o = \frac{\rho V A_f C_p}{A_s} \ln \frac{(T_s - T_{ci})}{(T_s - T_{co})} \quad (9)$$

where

V = cooling water velocity and

A_f = cooling water flow area.

The density ρ and specific heat C_p are functions of temperature only (See Appendix H.). The procedure outlined in Figure 33 is used to solve for the overall heat transfer coefficient U_o .

An empirical equation often used to obtain the Nusselt number for turbulent flow in a tube is the Sieder-Tate relationship expressed as [8]:

$$Nu = \frac{h_i d_i}{k} = C_i Re^{0.8} Pr^{1/3} (\mu/\mu_w)^{0.14} \quad , \quad (10)$$

where,

Nu = Nusselt number,

h_i = convective, or internal, heat transfer coefficient,

d_i = tube inside diameter,

k = thermal conductivity of the fluid,

C_i = empirical coefficient,

Re = Reynolds number = Ud_i/ν , (11)

Pr = Prandtl number = $C_p\mu/k$, (12)

μ = dynamic viscosity of the fluid,

μ_w = dynamic viscosity evaluated at the wall temperature, and

ν = kinematic viscosity of the fluid.

(All properties other than μ_w are evaluated at the bulk or average temperature.)

Figure 34 depicts the procedure to obtain the Sieder-Tate parameter, which is written [9]:

$$Re^{0.8} Pr^{1/3} (\mu/\mu_w)^{0.14} . \quad (13)$$

The expressions for the temperature dependent quantities ρ , μ , μ_w , k , and C_p are found in Appendix G.

The computation of the coefficient, C_i , may cause confusion. The Wilson Plot technique is used to arrive at this value. The technique developed by Lt. E.E. Wilson, USN, in 1915 [36], has been modified by many researchers since that time [37]. The procedure as adopted for this study is as follows (See Figure 35). First,

$$\frac{1}{U_o} \quad \text{vs.} \quad Re^{-0.8} Pr^{-0.33} (\mu/\mu_w)^{-0.14}$$

is plotted. The values for this plot are obtained by varying only the cooling water velocity and collecting data while holding all other parameters nearly constant. The slope of

the plot is $\frac{d_o}{C_i k}$, and this expression is solved to obtain C_i . The convection heat transfer coefficient, h_i , is calculated as follows using the Sieder-Tate relationship:

$$h_i = \frac{k}{d_i} C_i Re^{0.8} Pr^{1/3} (\mu/\mu_w)^{0.14} \quad (14)$$

Lastly, as noted in Figure 35, the condensation heat transfer coefficient, h_o , is calculated as follows [9]:

$$h_o = \frac{1}{\frac{1}{U_o} - R_w - \frac{d_o}{d_i h_i}} \quad (15)$$

This approach to the heat transfer data reduction has been used extensively by many researchers. It is considered appropriate to utilize the Autodata-Nine automatic data acquisition system to collect the data and provide a paper tape record of all data for later use. In addition, the Hewlett-Packard model 9830A computer, which is compatible with the Auto-data-Nine, is considered an excellent method for rapid automatic data reduction, although a programmable hand calculator, such as the SR52 or the HP65 can also be used.

V. CONCLUSIONS AND RECOMMENDATIONS

A. CONCLUSIONS

A test condenser apparatus having overall dimensions of 35 inches in height, 3 feet in length and 3 inches in width was designed and constructed of stainless steel. It has the following features:

1. Visibility for 29 $1/4$ inches by 2 $1/2$ inches is provided on each side in the initial configuration. Visibility height (See Figures 18 and 19.) can be expanded to 4 inches with maximum tube configuration.
2. Three of the $5/8$ inch tubes in the initial configuration may be changed without removing the tube sheet.
3. The maximum configuration of $5/8$ inch tubes provides for nine tubes in a vertical row.
4. Other diameter tubes may be tested by simply redesigning the tube sheet.
5. Baffles in the entrance section can also serve as condensate collection vanes when the condenser is tilted to experiment with various steam flow directions.

B. RECOMMENDATIONS

It is recommended that:

1. Experimentation be conducted as outlined in the objectives (page 31).

2. A frame such as depicted in Figure 17 be designed and built to enable the tests involving condenser motion to be conducted.
3. The house steam be connected to the steam line exiting the boiler since it is considered possible that an increase in boiler output might be desirable to investigate condensation at higher vapor velocity in the test condenser. Further an automatic control valve be installed at that point to insure a constant flow rate.
4. A high/low water level control circuit be built and installed to control the condensate pump as a function of the secondary condenser hot well water level.
5. The combined effects of internal enhancement and dropwise enhancement be investigated since no literature was found which described experiments in this area. For example, a corrugated tube, or an internally finned tube should be coated with teflon promoter and tested in the dropwise mode of condensation.
6. Feasible topics for future thesis work in this area include:
 - a. Tests on the effects of fouling in enhanced tubes,
 - b. Tests on the effects of tube vibration on condensation heat transfer.

Tube Data: 5/8" OD
 18 gage (.049" Wall Thickness)
 90-10 Cu-Ni
 Cooling Water Velocity: 10 ft/sec.

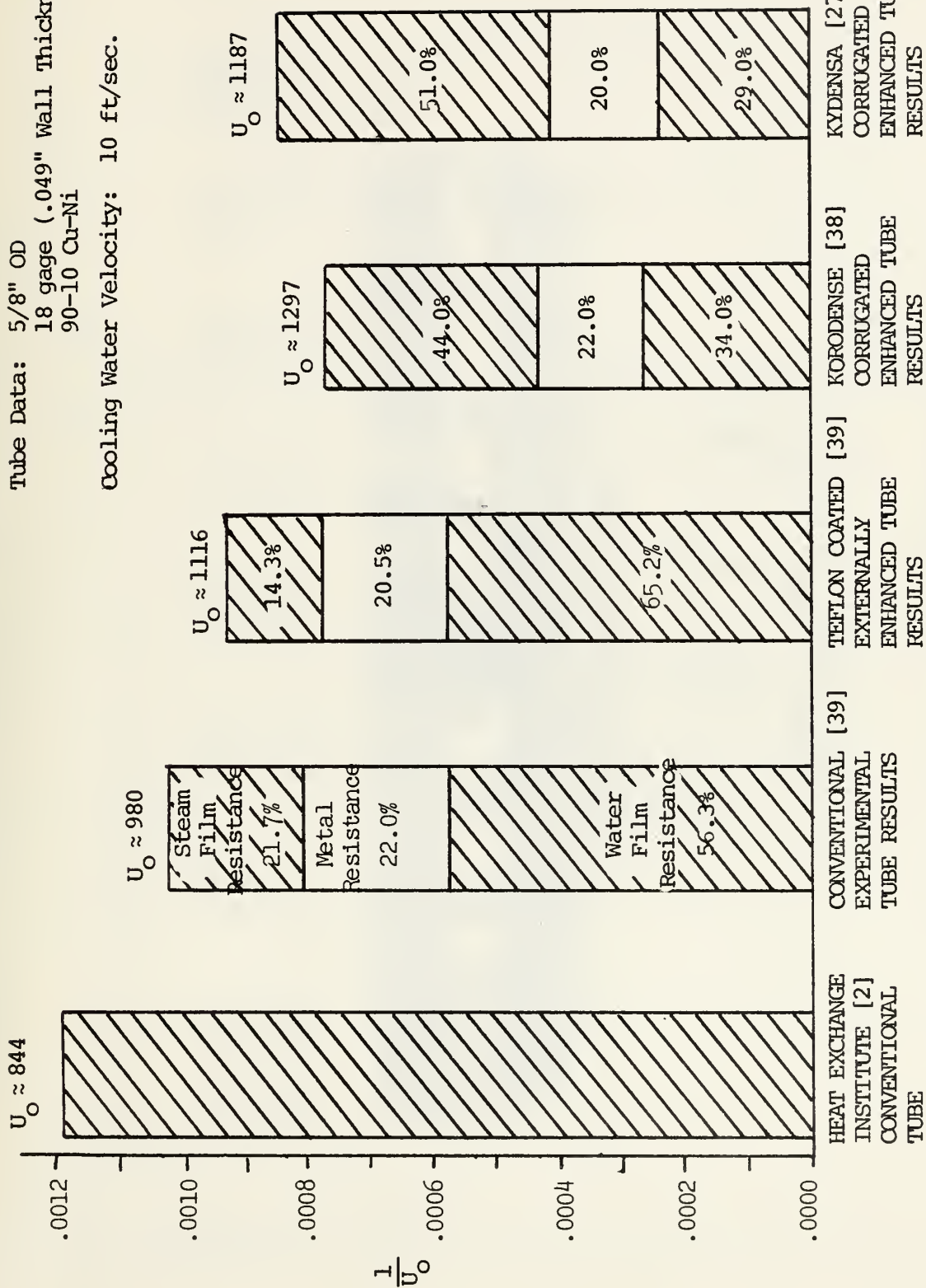
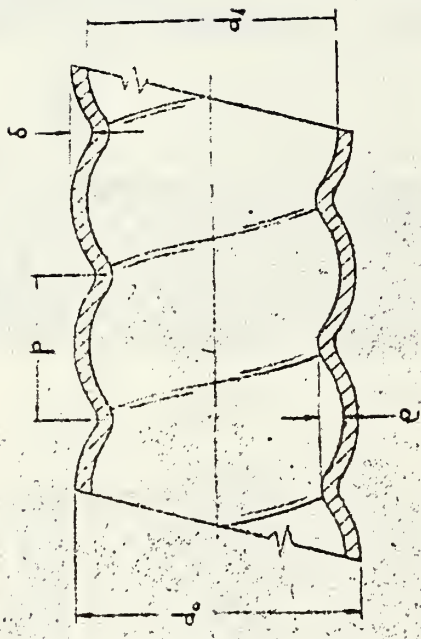


FIGURE 1. Comparison of Various Tube Enhancement Results.



Tube No.	Tube Material	Tube Interior			Tube Exterior			Bank Layout Pitch
		Inside Diameter d_i , in	Inside Surface A_i^* , ft ² /ft	Ridge Height e , in	Outside Diameter d_o , in	Outside Surface A_o^* , ft ² /ft p. in	Groove Pitch s , in	
I	DHP copper	0.530	0.139	0.0294	0.613	0.160	0.0272	0.875
II	90-10 CuNi	0.822	0.215	0.0290	0.936	0.245	0.0310	1.250
III	90-10 CuNi	0.855	0.224	0.0313	0.937	0.245	0.0302	1.250
IV	90-10 CuNi	0.863	0.226	0.0408	0.943	0.247	0.0388	1.250

FIGURE 2. Withers and Young's Corrugated Tube. [22]



FIGURE 3. Spiral Indented (Rope) Tube. [21]

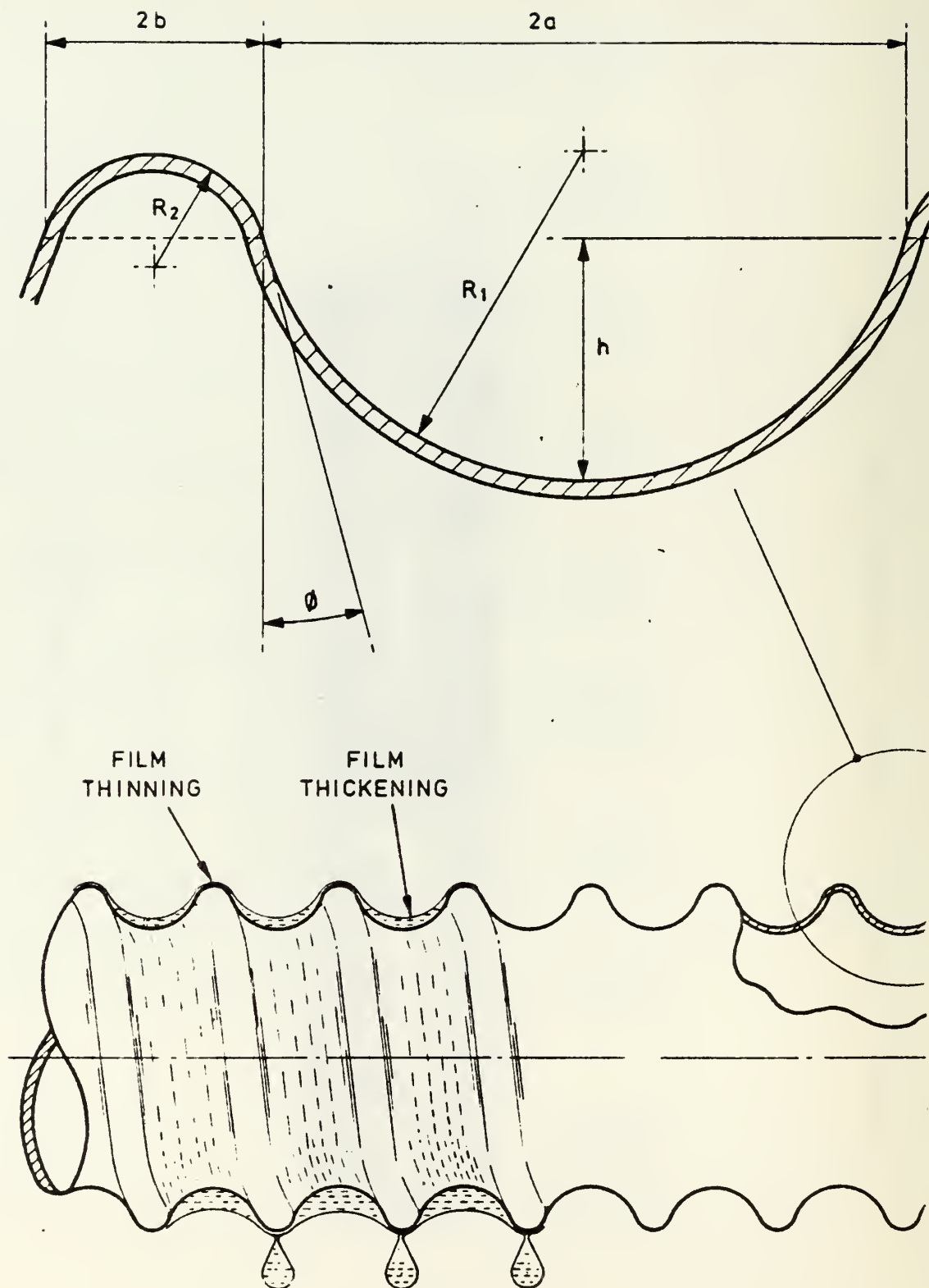


FIGURE 4. Catchpole and Drew's Test Tube (Kydensa). [27]

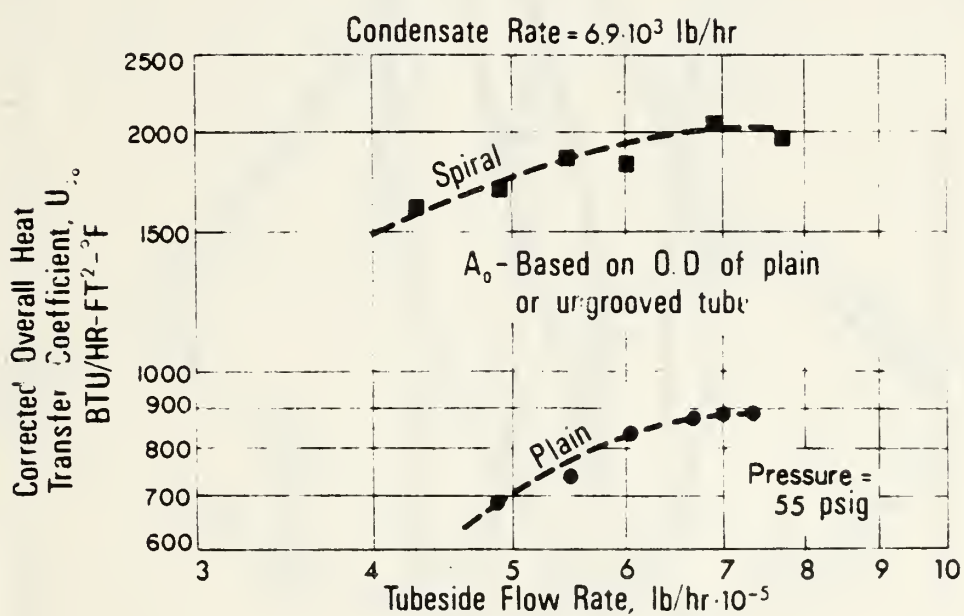
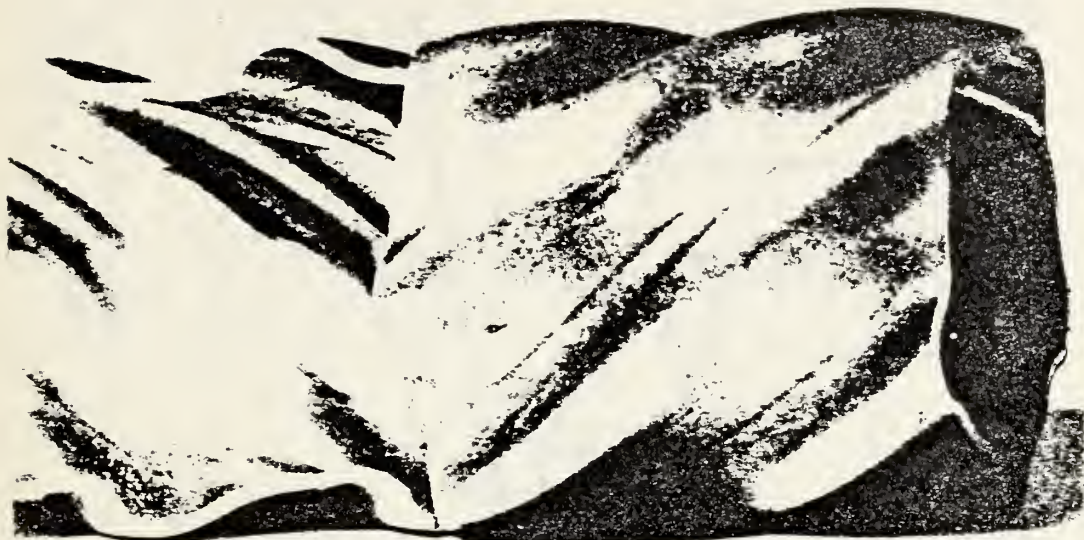


FIGURE 5. Turbotec Spirally Grooved Tube . [26]

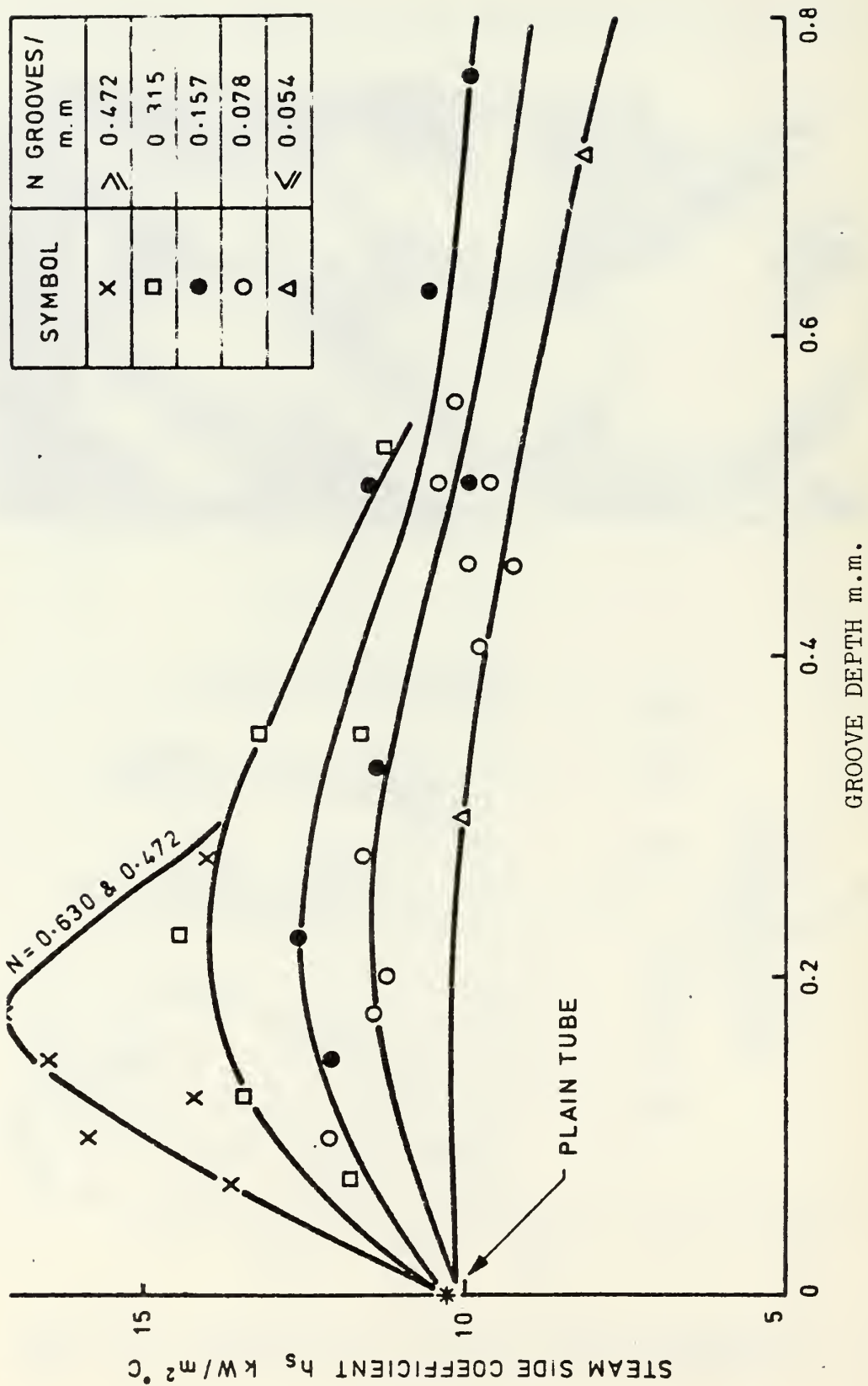
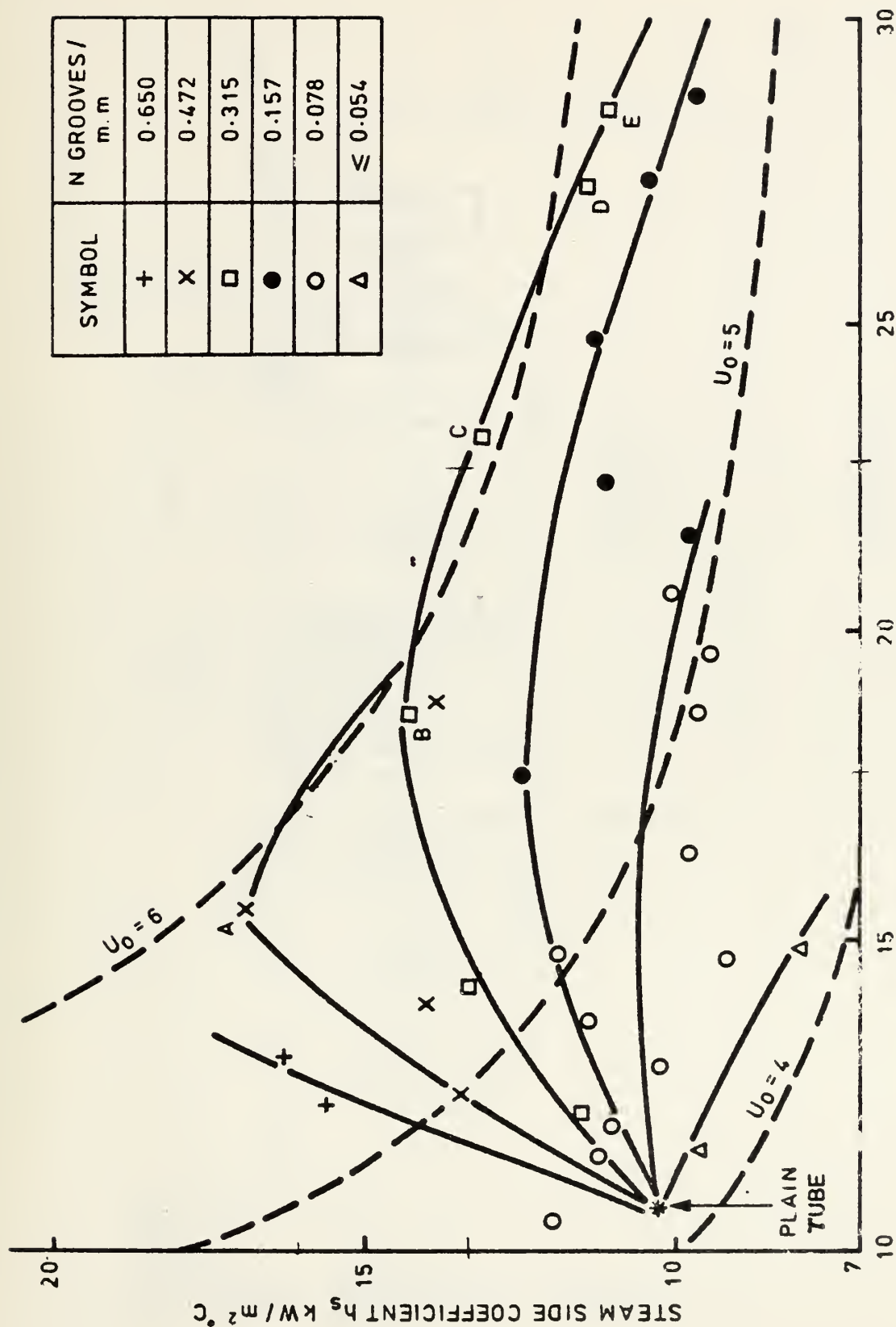


FIGURE 6. Steam Side Coefficient versus Groove Depth. [27]



WATER SIDE COEFFICIENT h_i kW/m² °C

FIGURE 7. h_o versus h_i with Contours of Overall Heat Transfer Coefficient, U_o . [27]

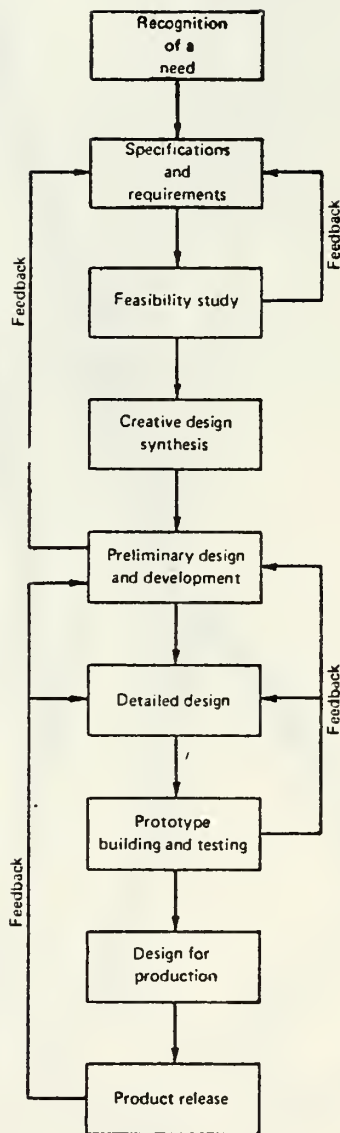


FIGURE 8. Design Flow Diagram. [40]

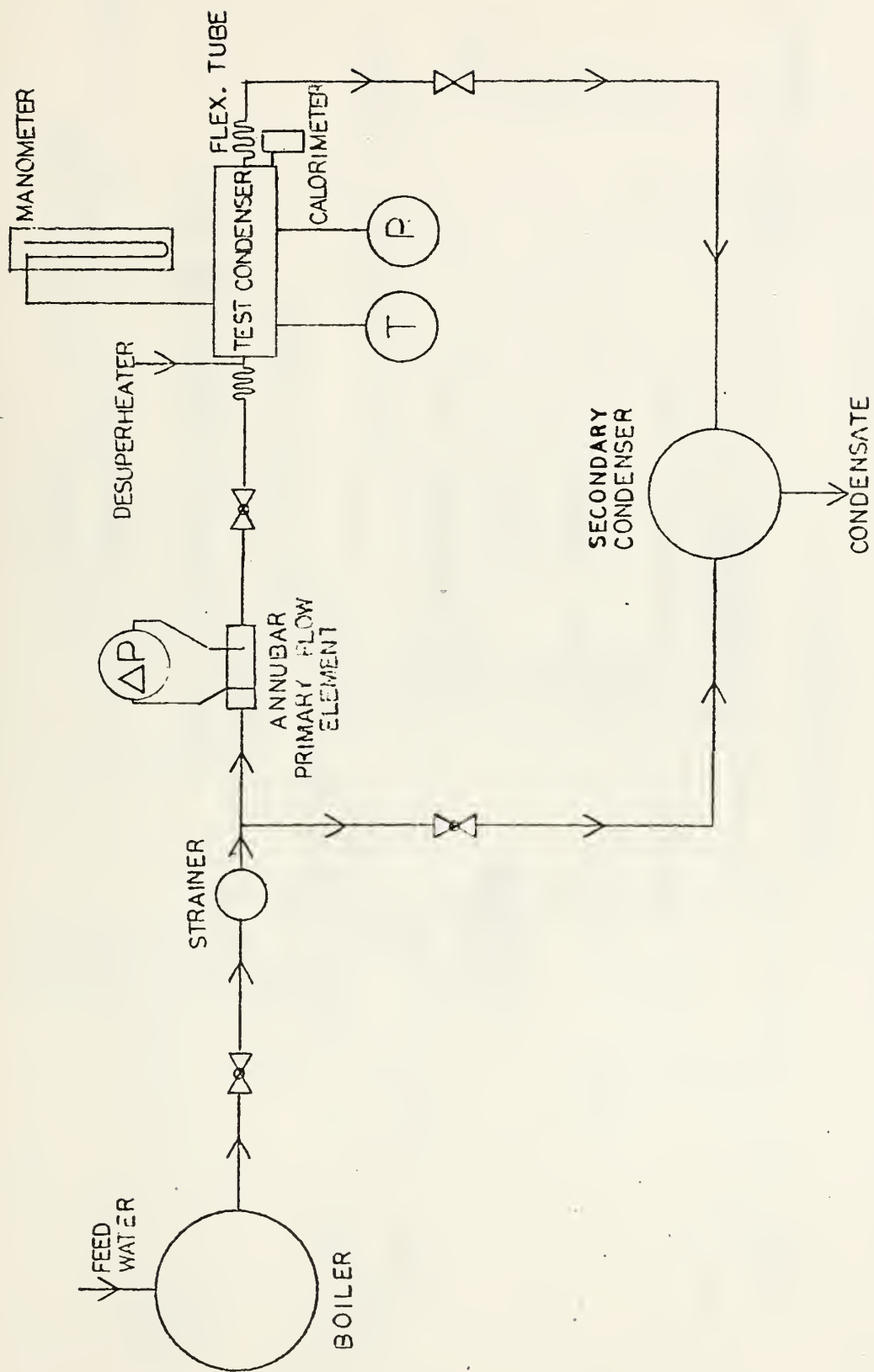


FIGURE 9. Schematic of the Main Steam System

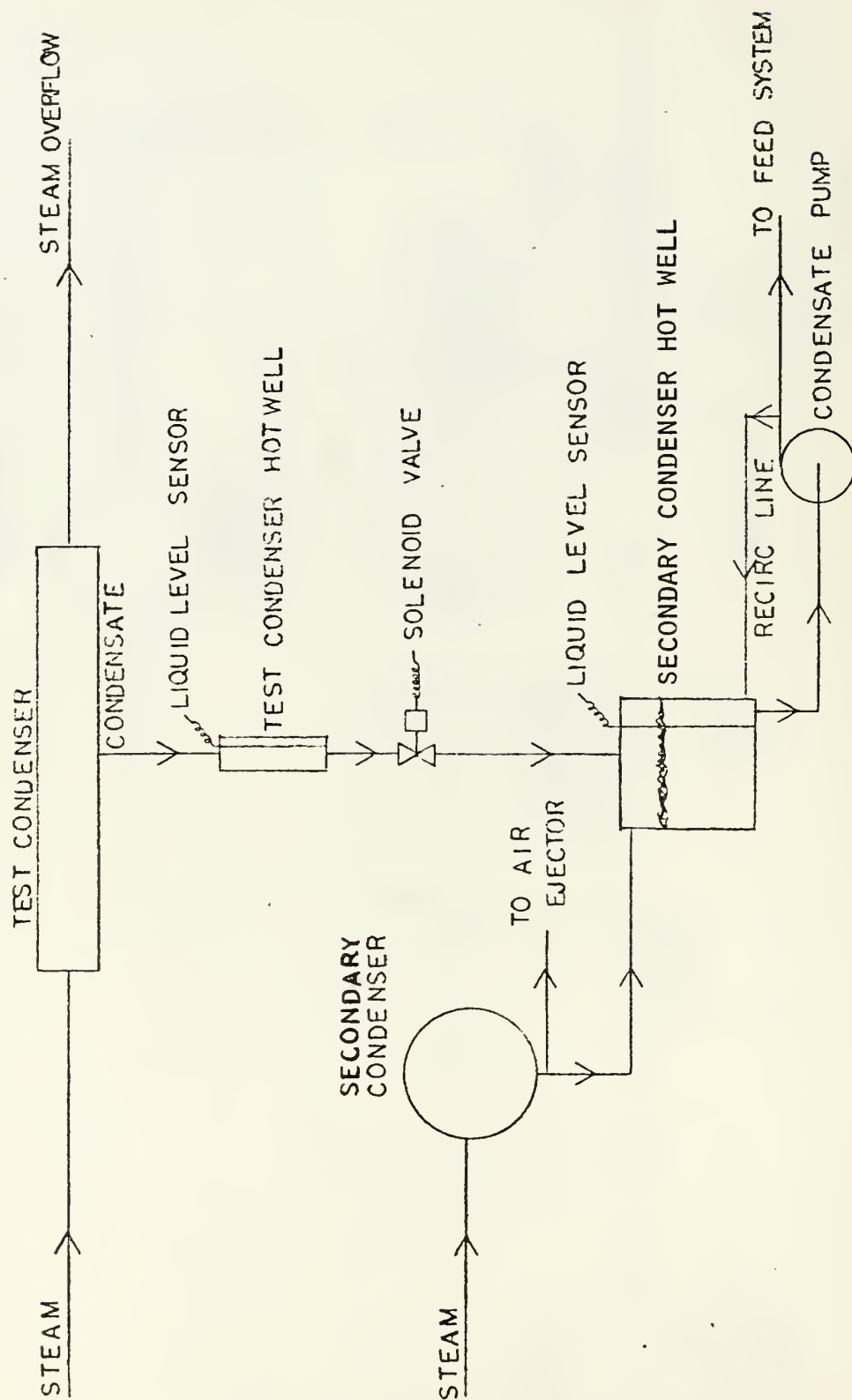


FIGURE 10. Schematic of the Condensate Collection System.

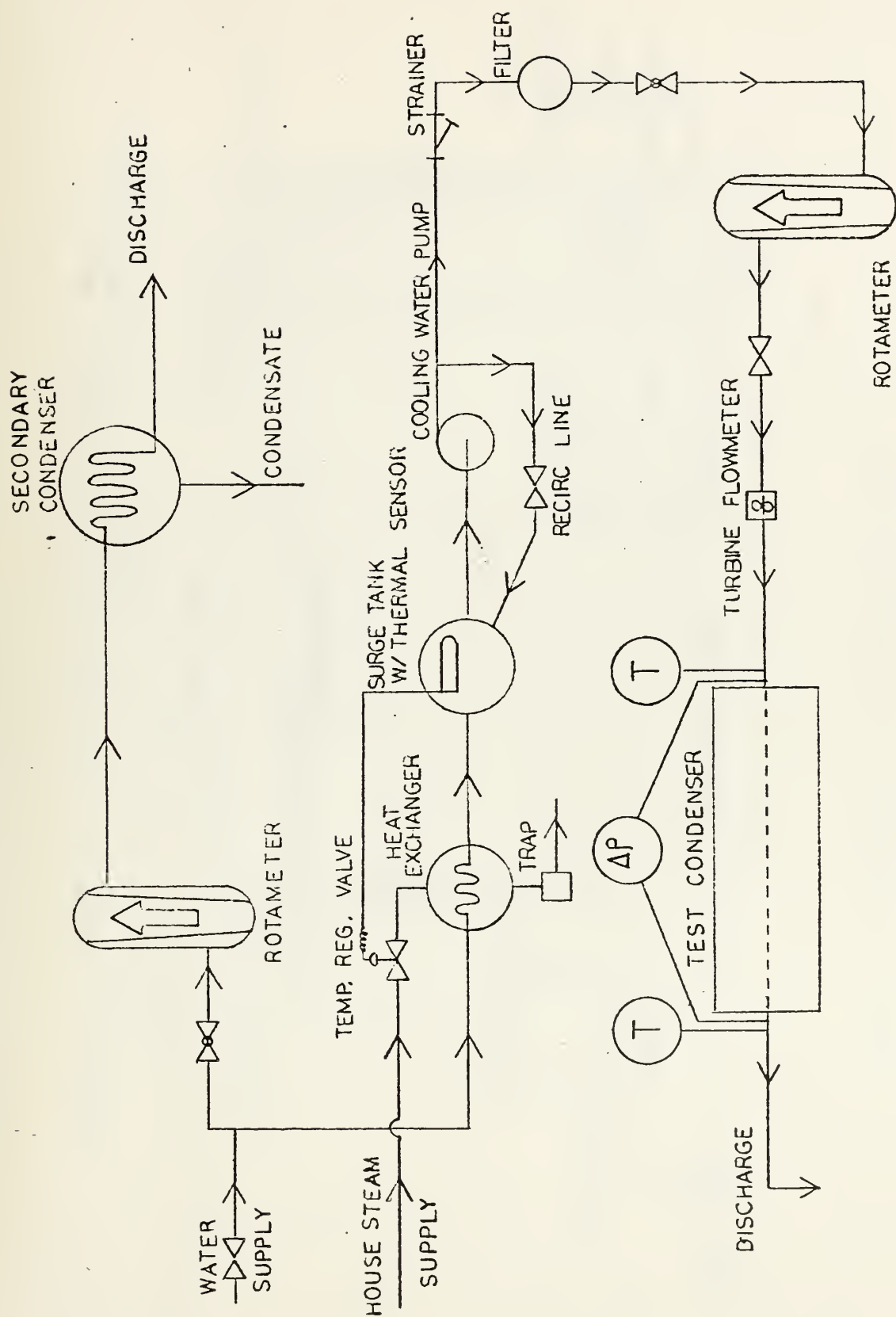


FIGURE 11. Schematic of the Cooling Water System.

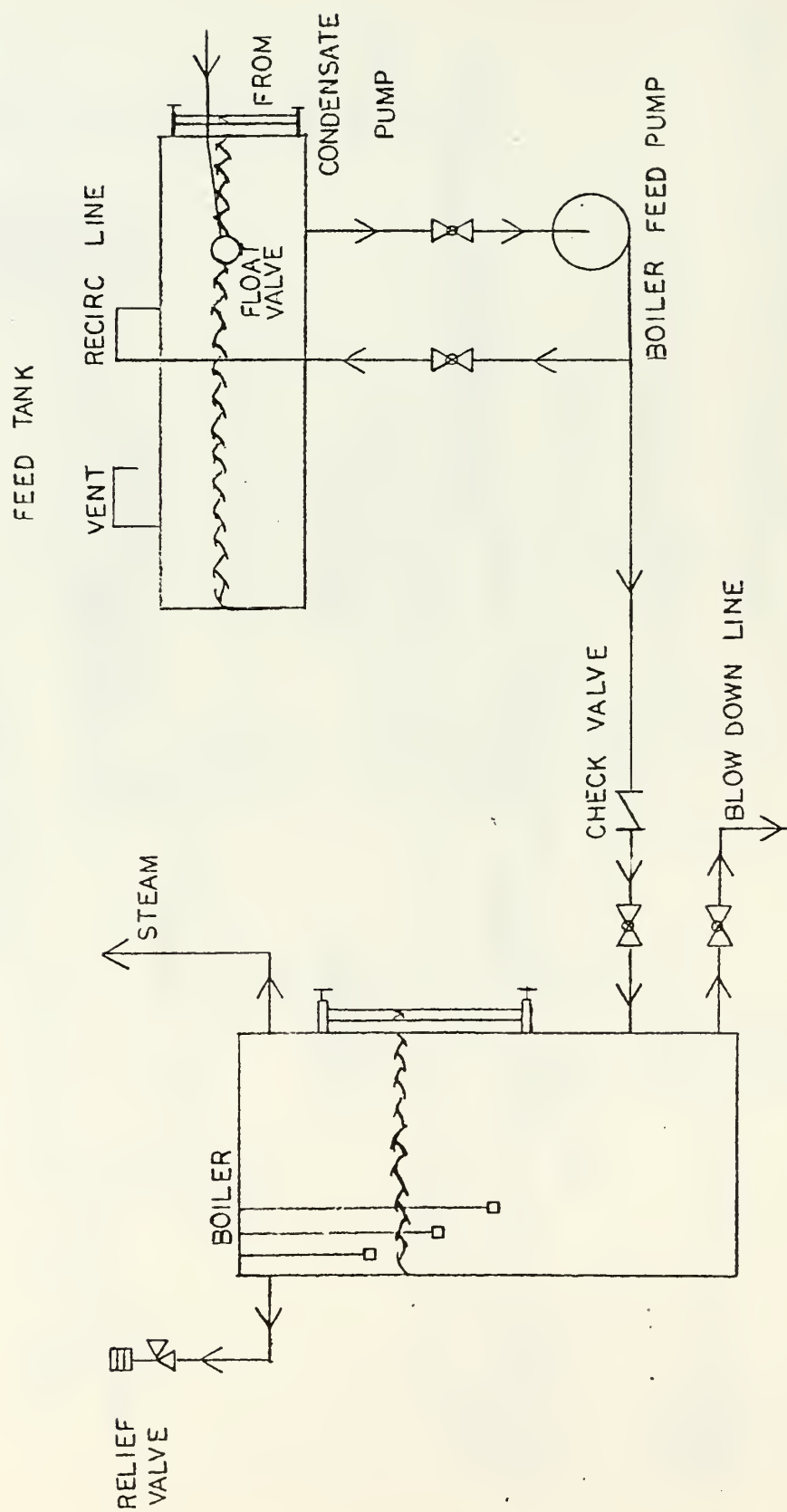


FIGURE 12. Schematic of the Boiler Feed Water System.

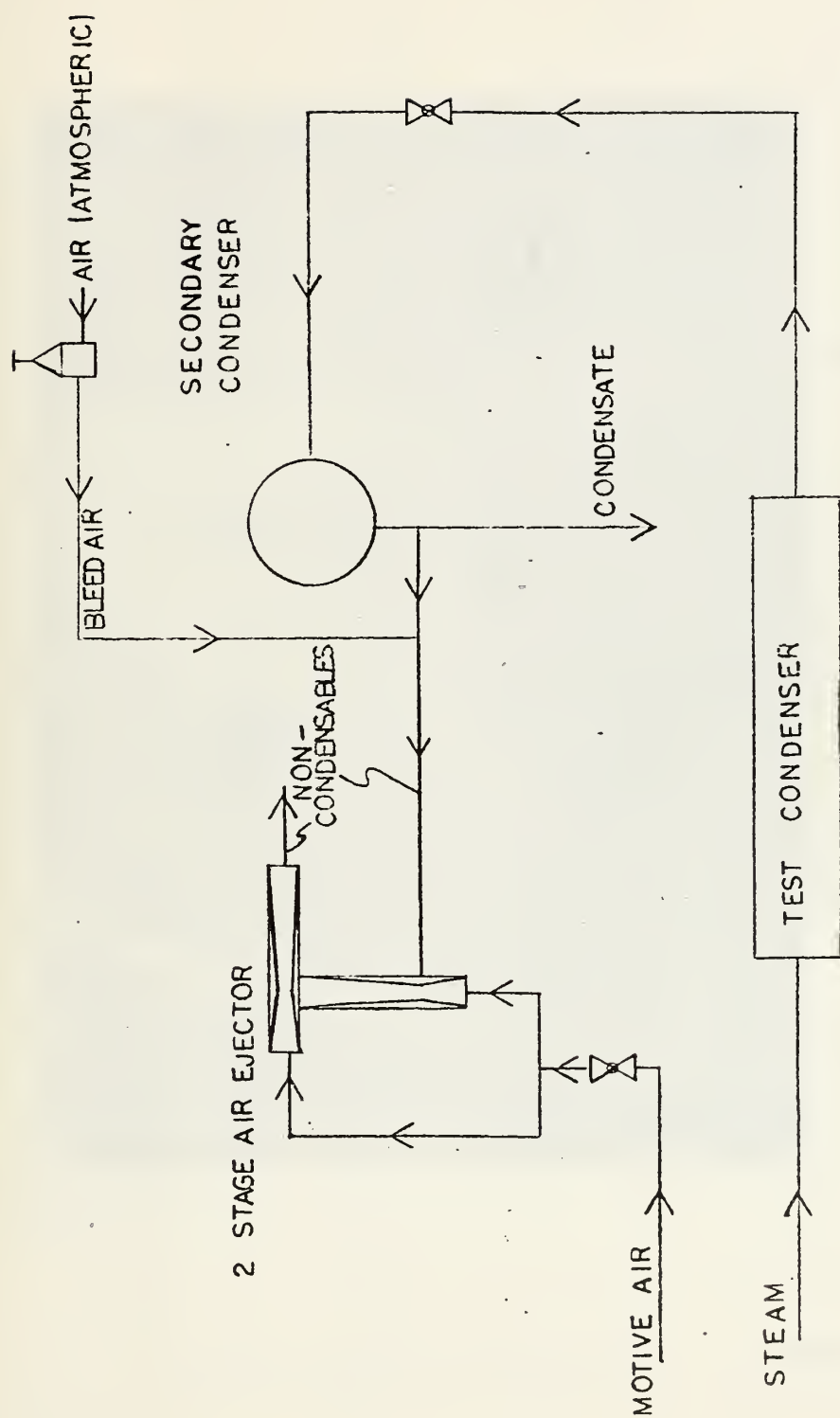


FIGURE 13. Schematic of the Vacuum System.

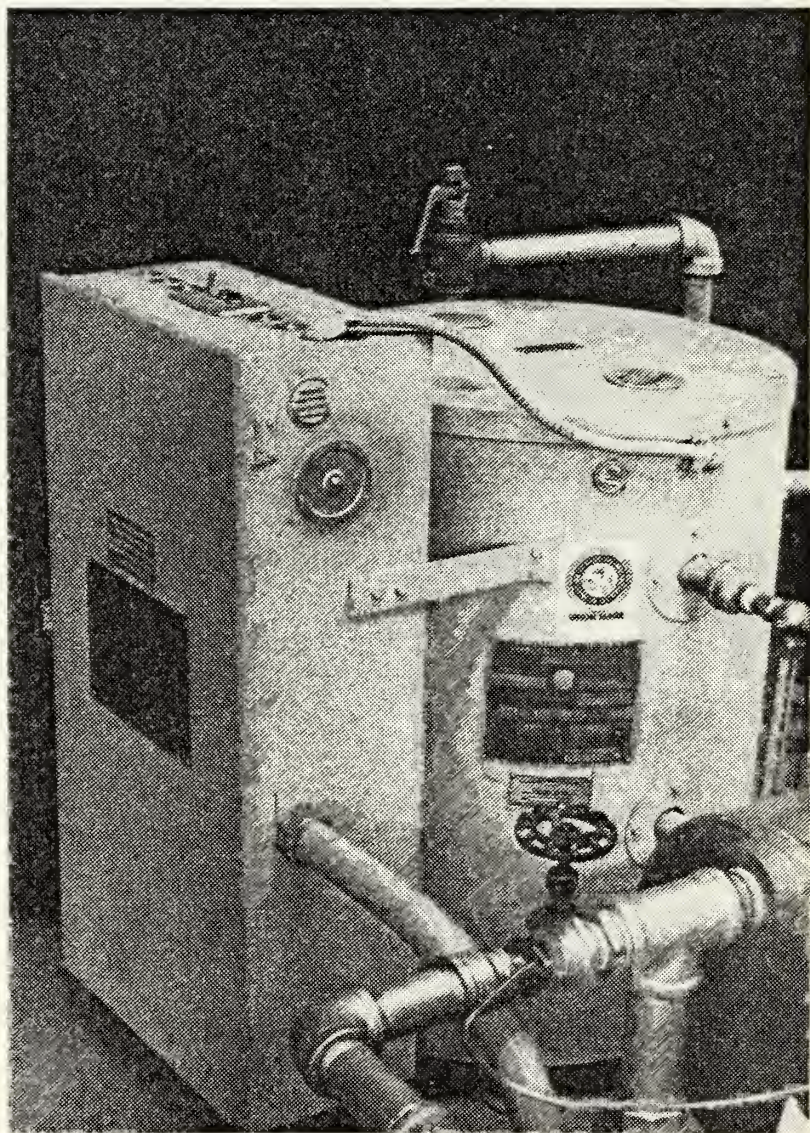


FIGURE 14. Photograph of Fulton Boiler.

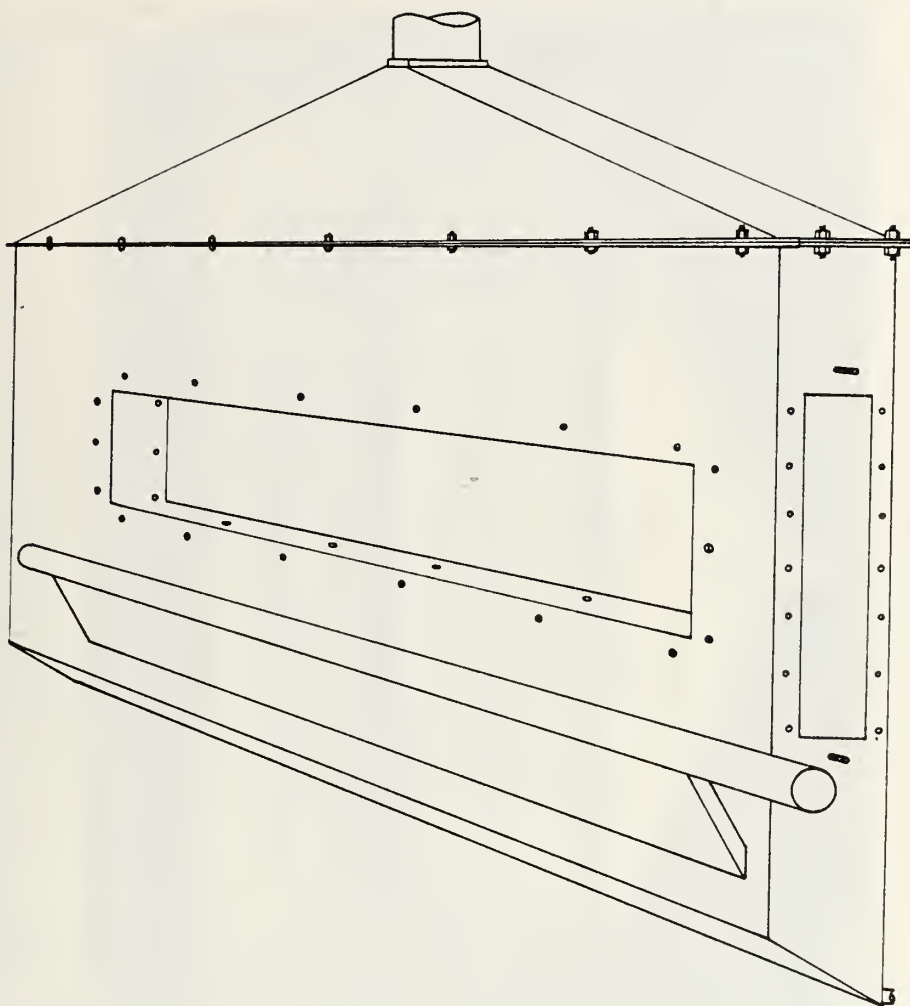


FIGURE 15. Artist's Conception of Test Condenser Body.

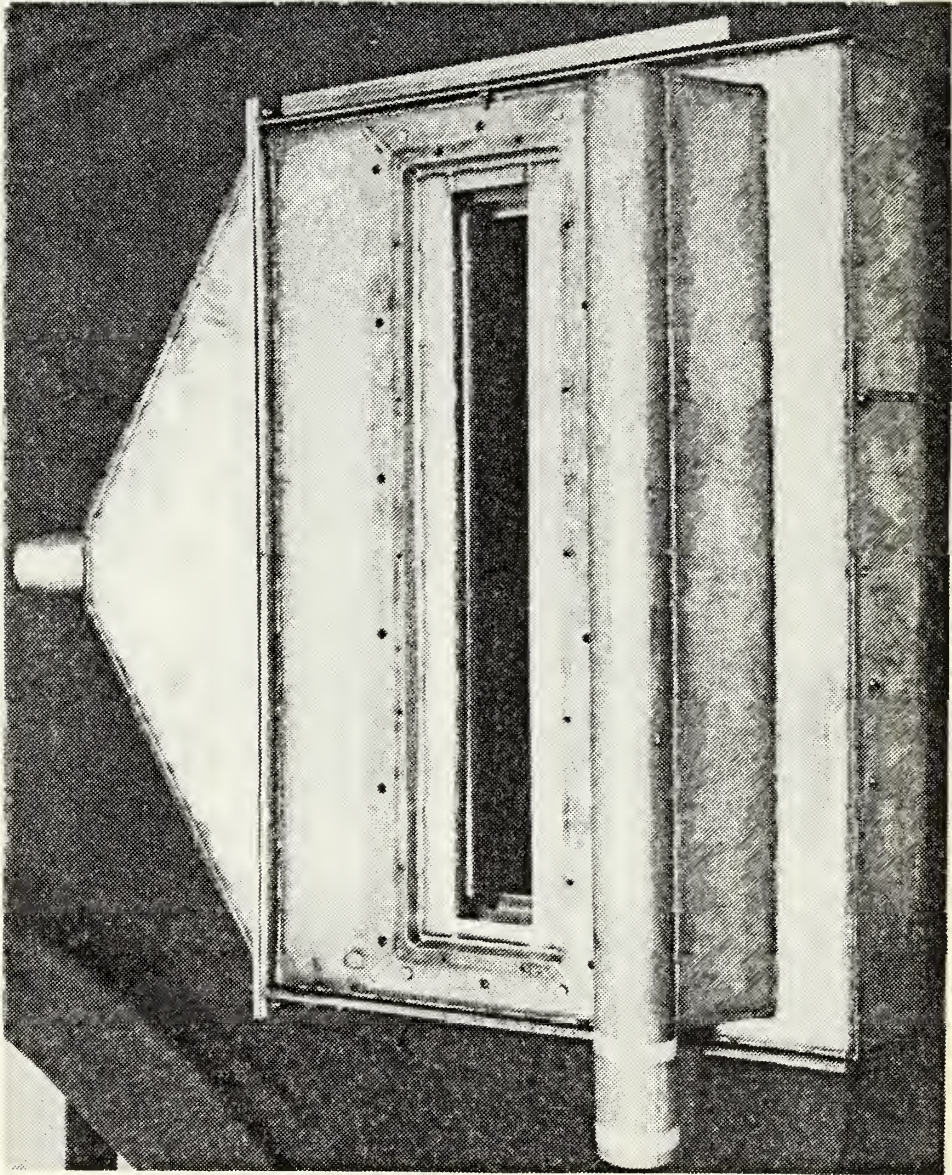


FIGURE 16. Photograph of Test Condenser.

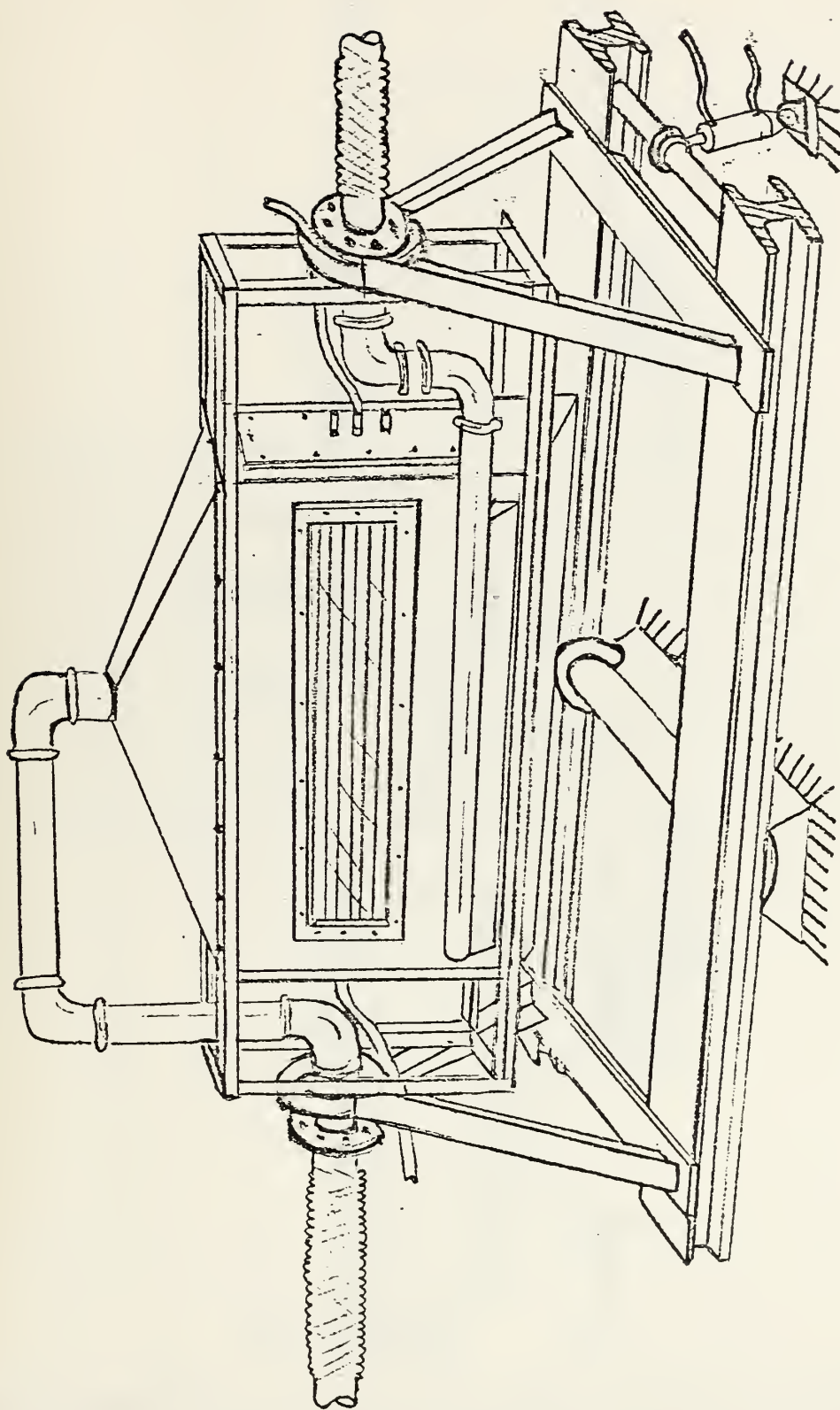


FIGURE 17. Artist's Conception of the Test Condenser and the Dynamic Test Frame.

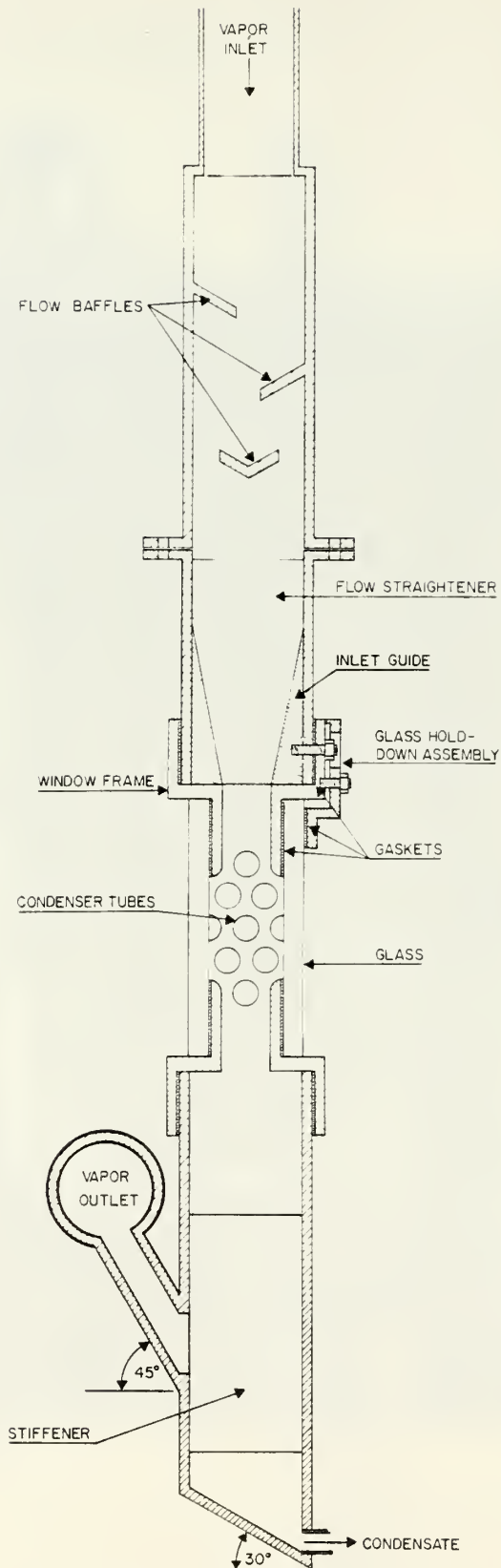


FIGURE 18. Test Condenser with Initial Tube Configuration.

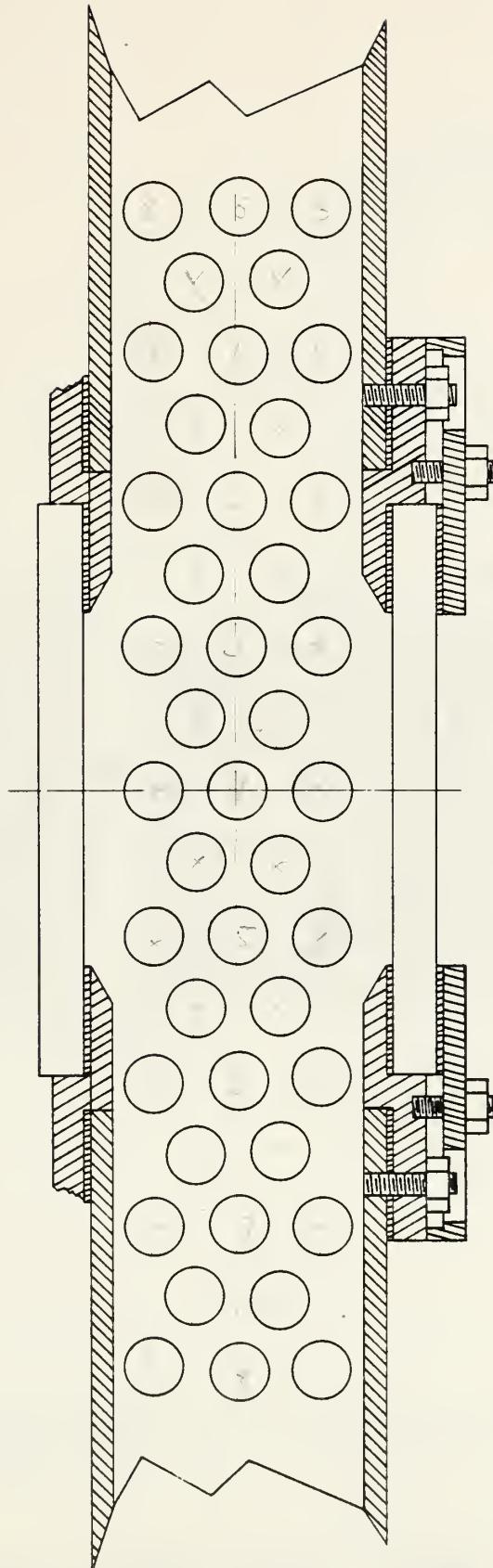


FIGURE 19. Test Condenser Maximum Tube Configuration.

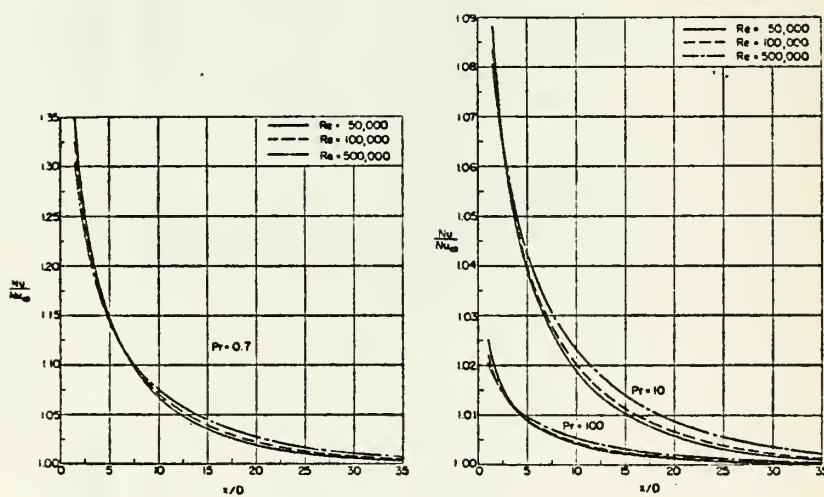


FIGURE 20. Thermal Entrance Region Nusselt Numbers for Turbulent Flow. [29]

Investigation	Type	Boundary condition *)	Pr	Entrance length, x/D $Re \times 10^{-3}$		
				50	100	500
Present	Analytical	UHF	0.7	12	13	14
Sleicher et al	Analytical	UWT	0.718	10	11	14
Beckers	Analytical	UWT	1.0	21	21	21
Latzko	Analytical	UWT	1.0	4	5	7
Deissler	Analytical	UHF	0.73	5	5	
Deissler	Analytical	UWT	0.73	5	5	
Boelter et al	Exp.	UWT	0.7	9		
Wolf and Lehman	Exp.	UHF	0.7		8	
Present	Analytical	UHF	10	4	4	4
Deissler	Analytical	UHF	10	2	1	
Hartnett	Exp.	UHF	7-8	3		
Present	Analytical	UHF	100	< 1	< 1	< 1
Deissler	Analytical	UHF	100	0.3	0.2	
Hartnett	Exp.	UHF	60	1.5		

*UHF = Uniform heat flux

*UWT = Uniform wall temperature

FIGURE 21. Thermal Entrance Lengths Based on $Nu/Nu_{\infty} = 1.05$.
[29]

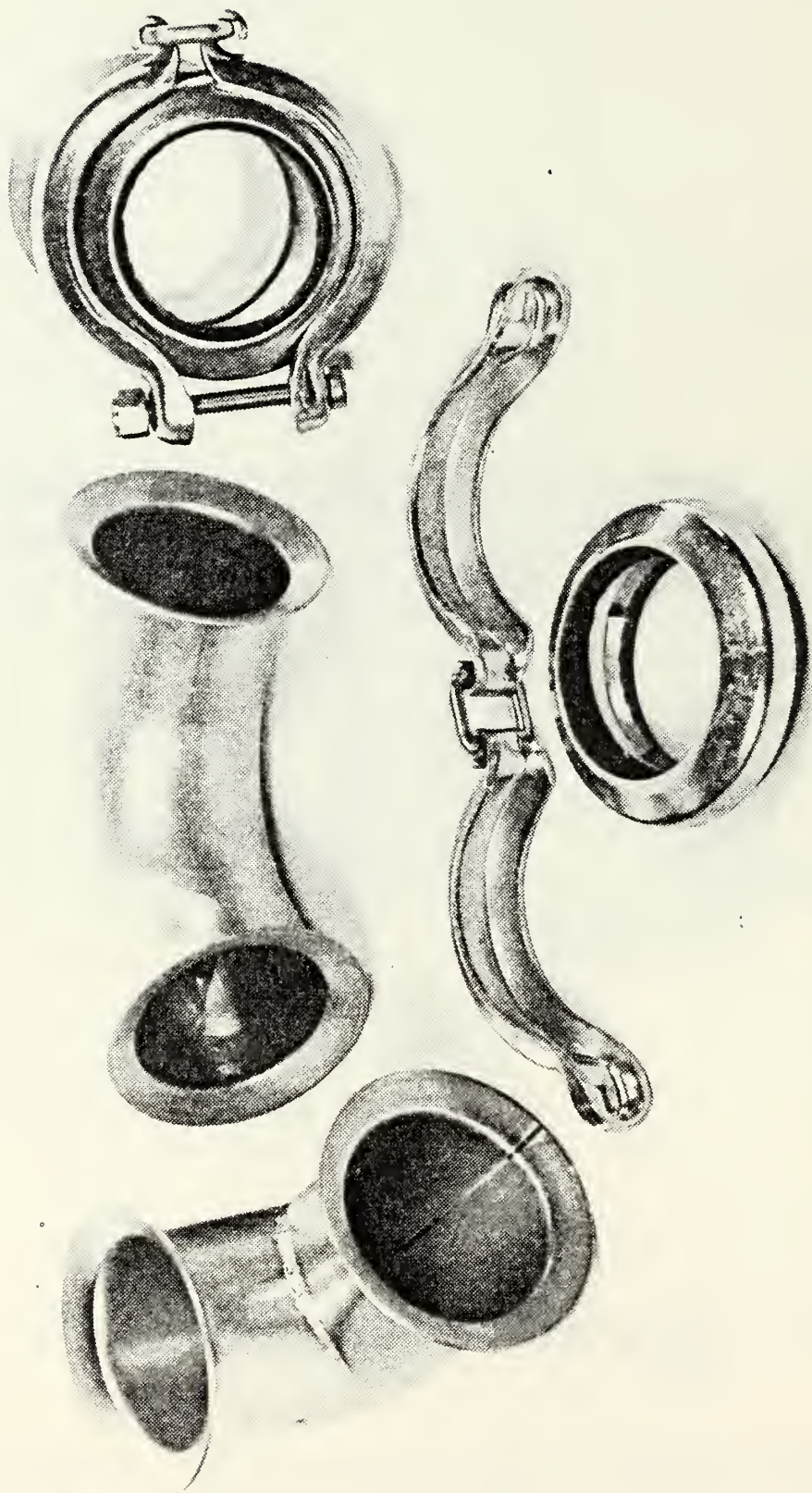


FIGURE 22. Photograph of Marman Flexmaster Couplings.

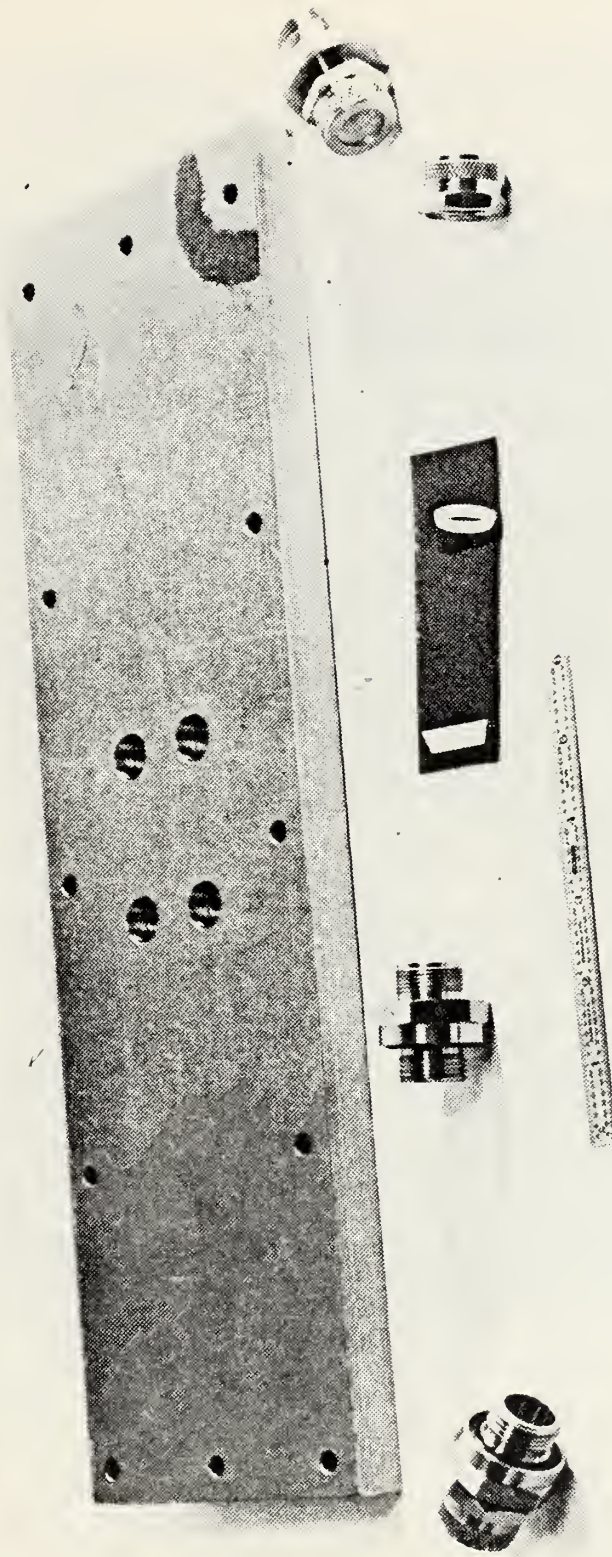


FIGURE 23. Photograph of Tube Sheet and Drilled Out Swagelok Fittings.



FIGURE 24. Photograph of Disassembled Secondary Condenser (Heliflow).

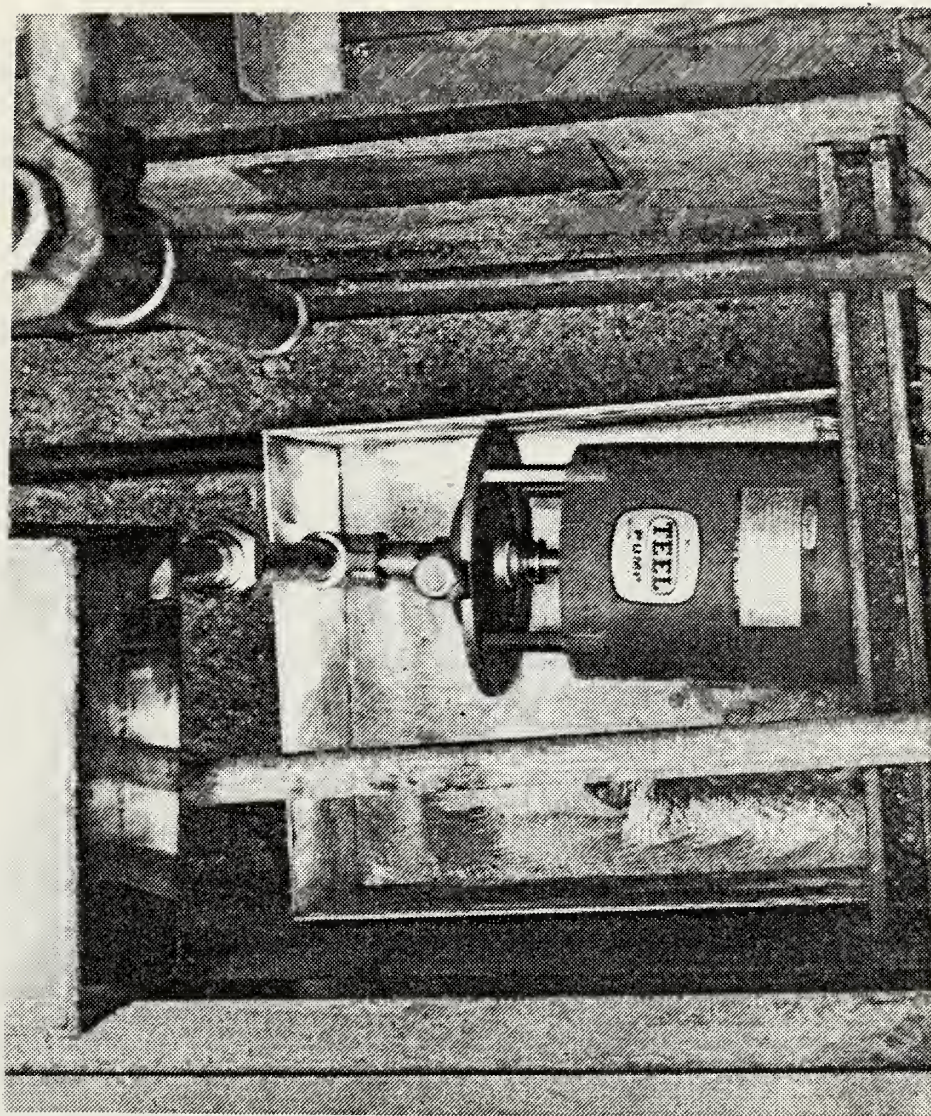


FIGURE 25. Photograph of Condensate Pump and Associated Piping.

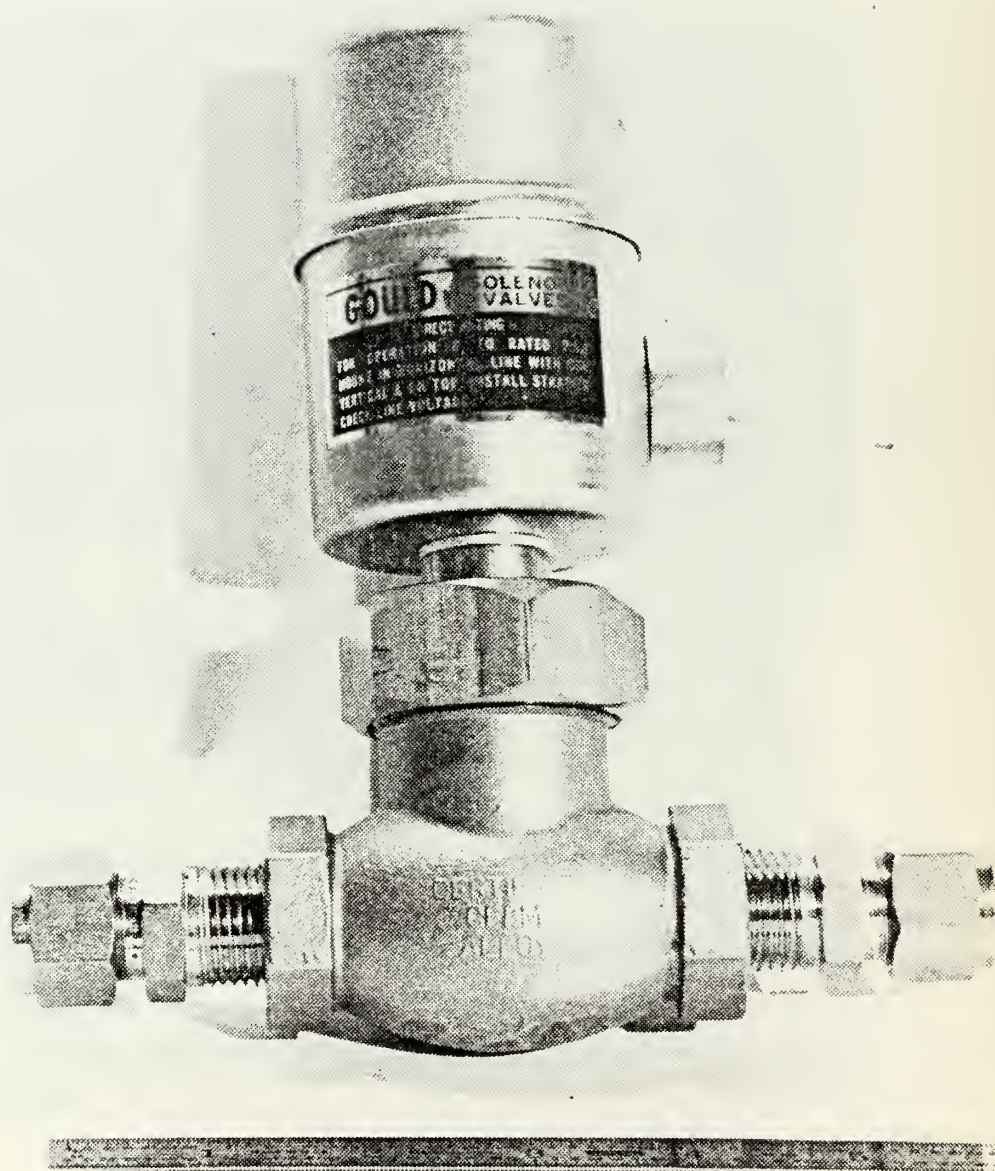


FIGURE 26. Photograph of Test Condenser Hot Well Solenoid Control Valve.

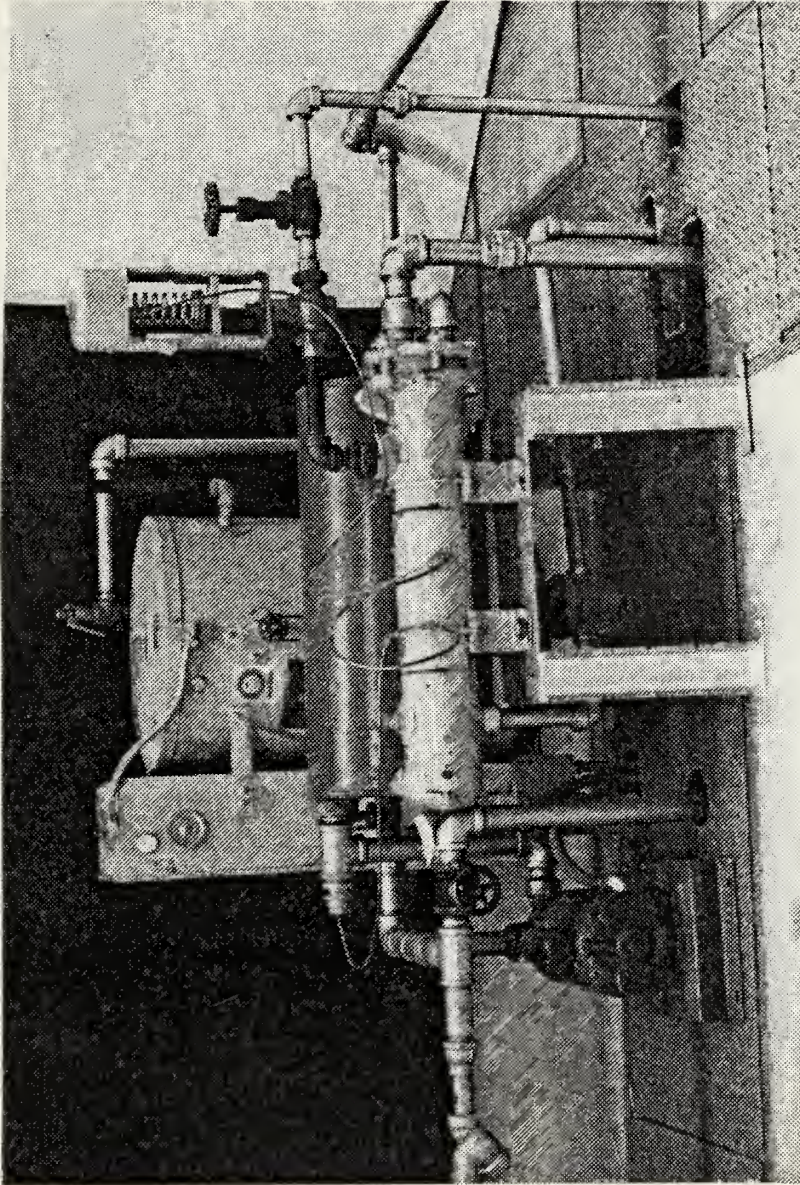


FIGURE 27. Photograph of Cooling Water Heater, Pump, and Associated Piping.

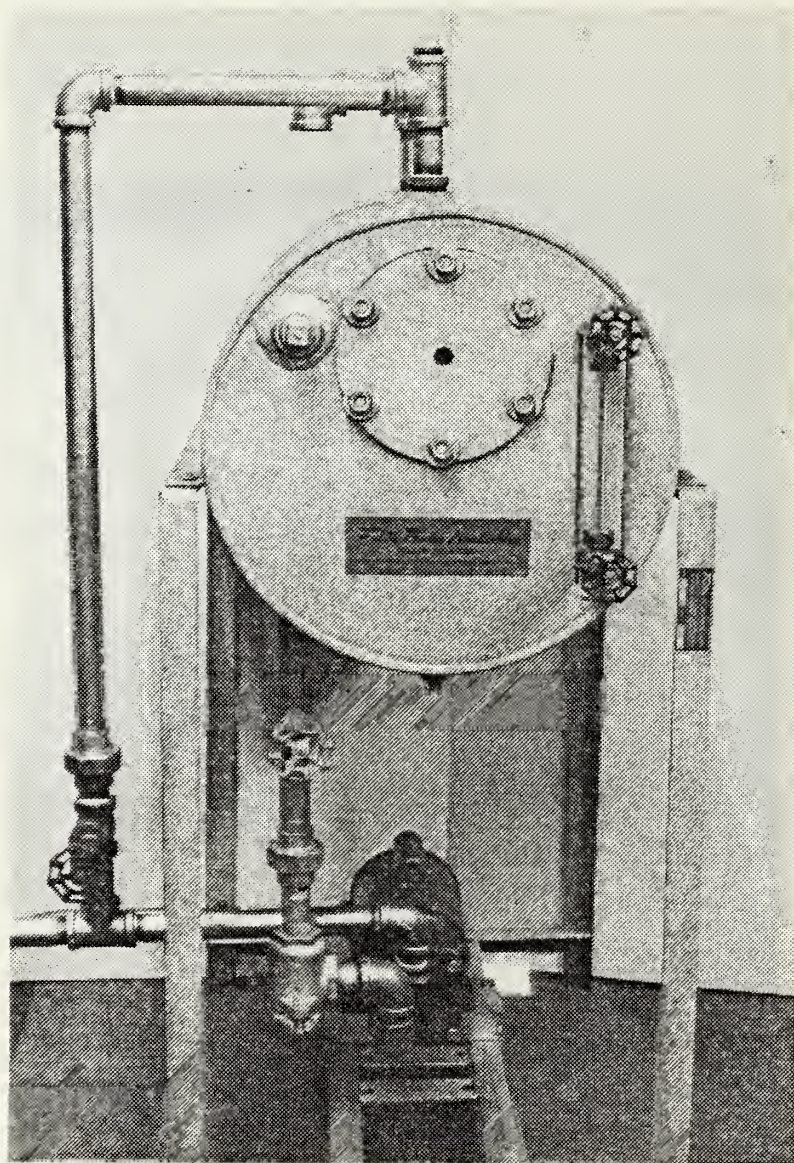


FIGURE 28. Photograph of Feed System (Fulton Return System).

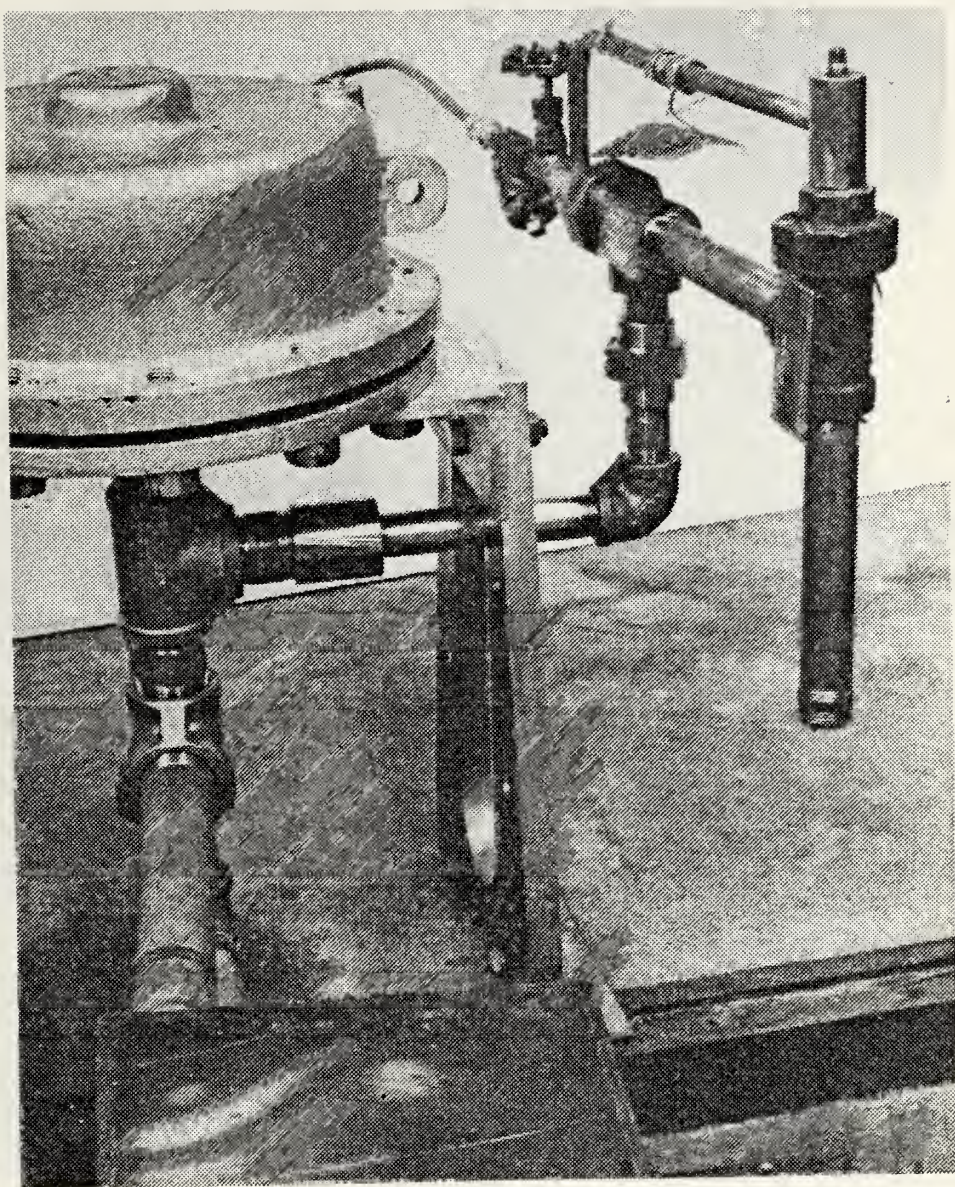


FIGURE 29. Photograph of Graham Air Operated Air Ejector.

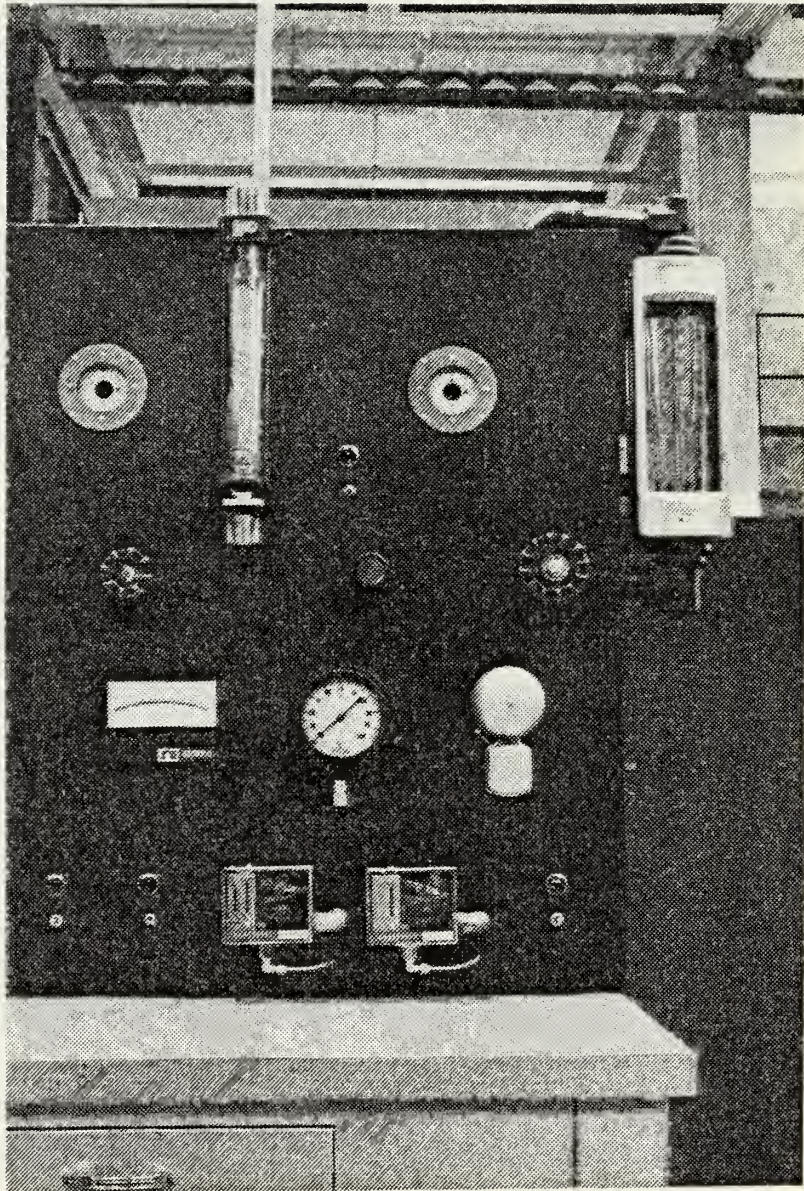


FIGURE 30. Photograph of Control and Operational Section of Instrument Panel.

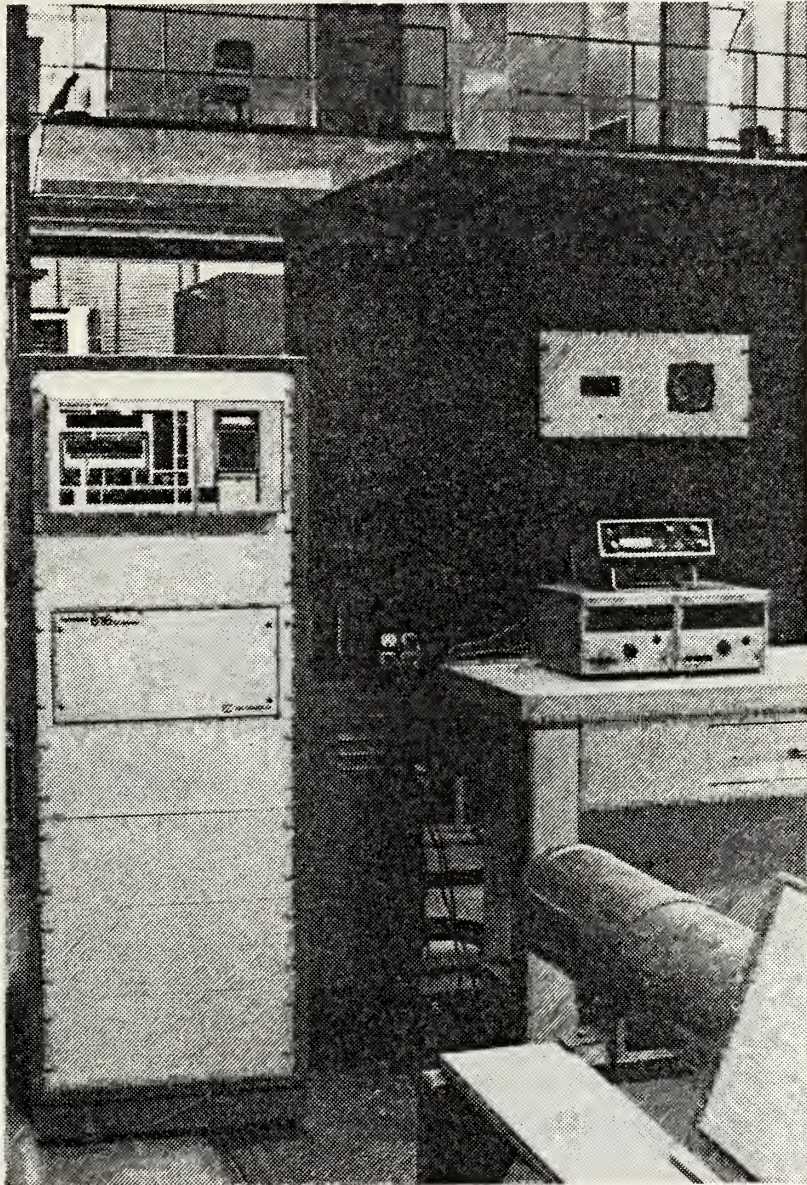


FIGURE 31. Photograph of Test Section of Instrument Panel.



FIGURE 32. Photograph of the Annubar, Primary Flow Sensor.

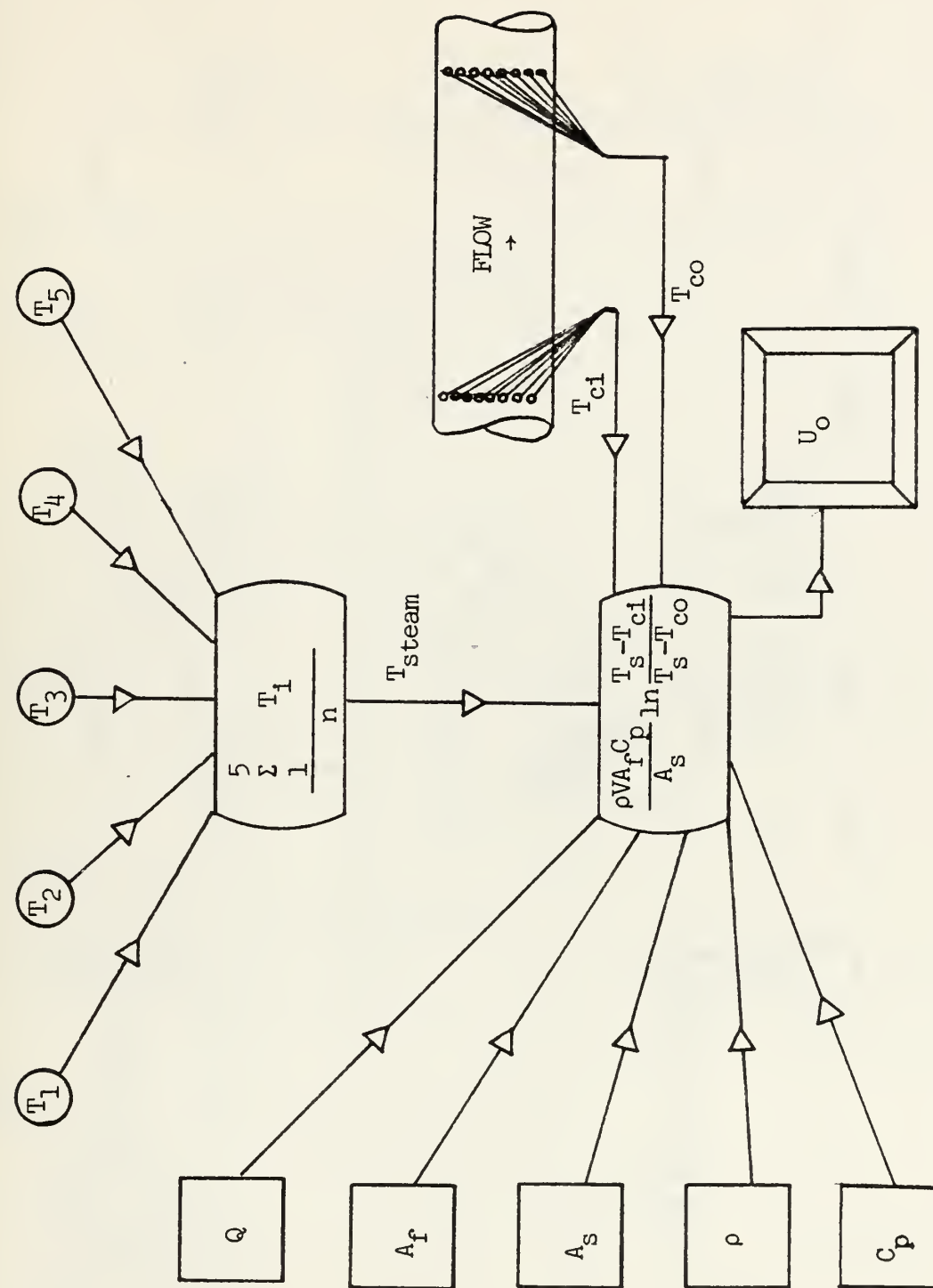


FIGURE 33. Schematic of the First Phase of Data Collection and Reduction.

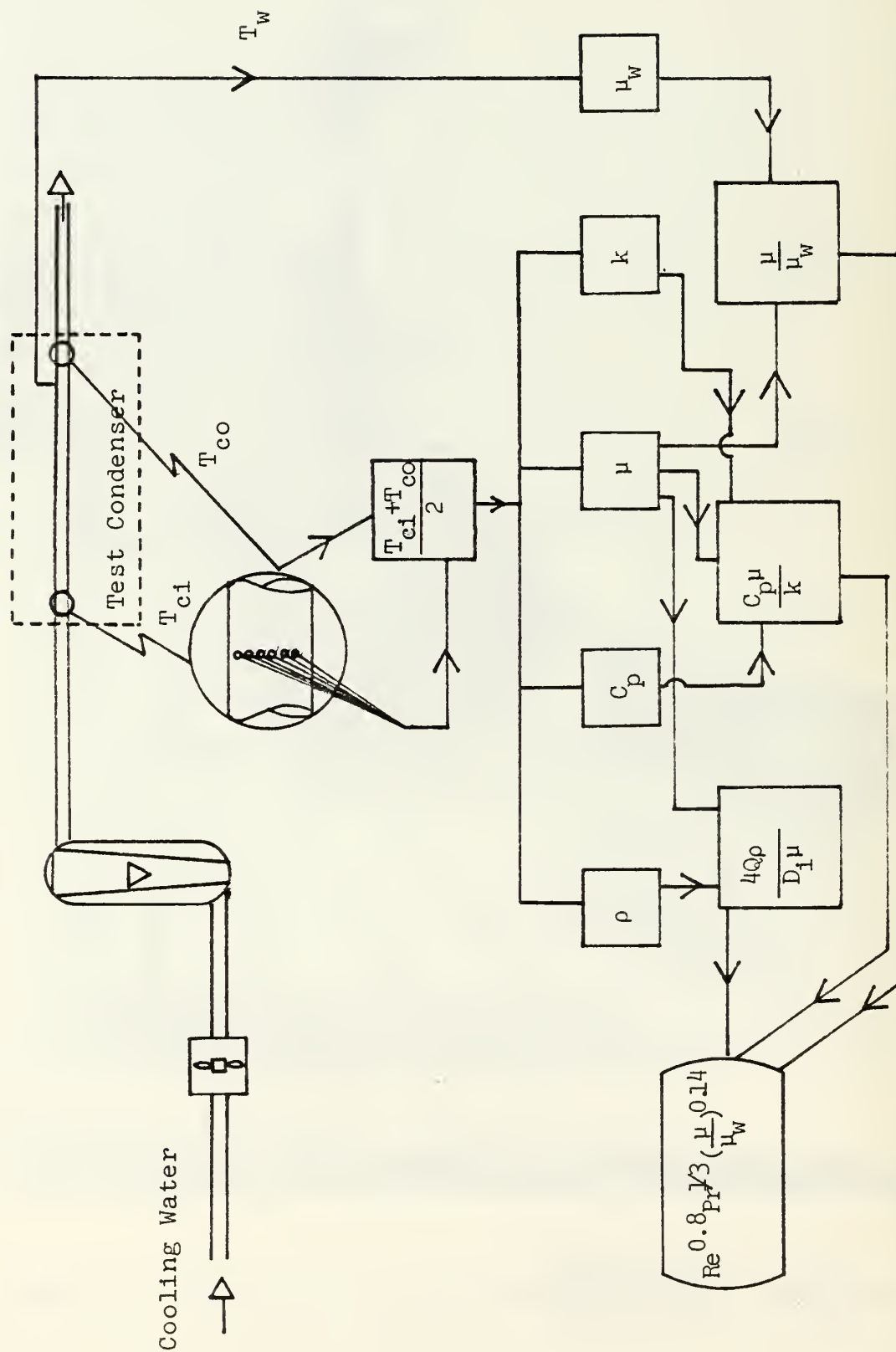


FIGURE 34. Schematic of the Second Phase of Data Collection and Reduction.

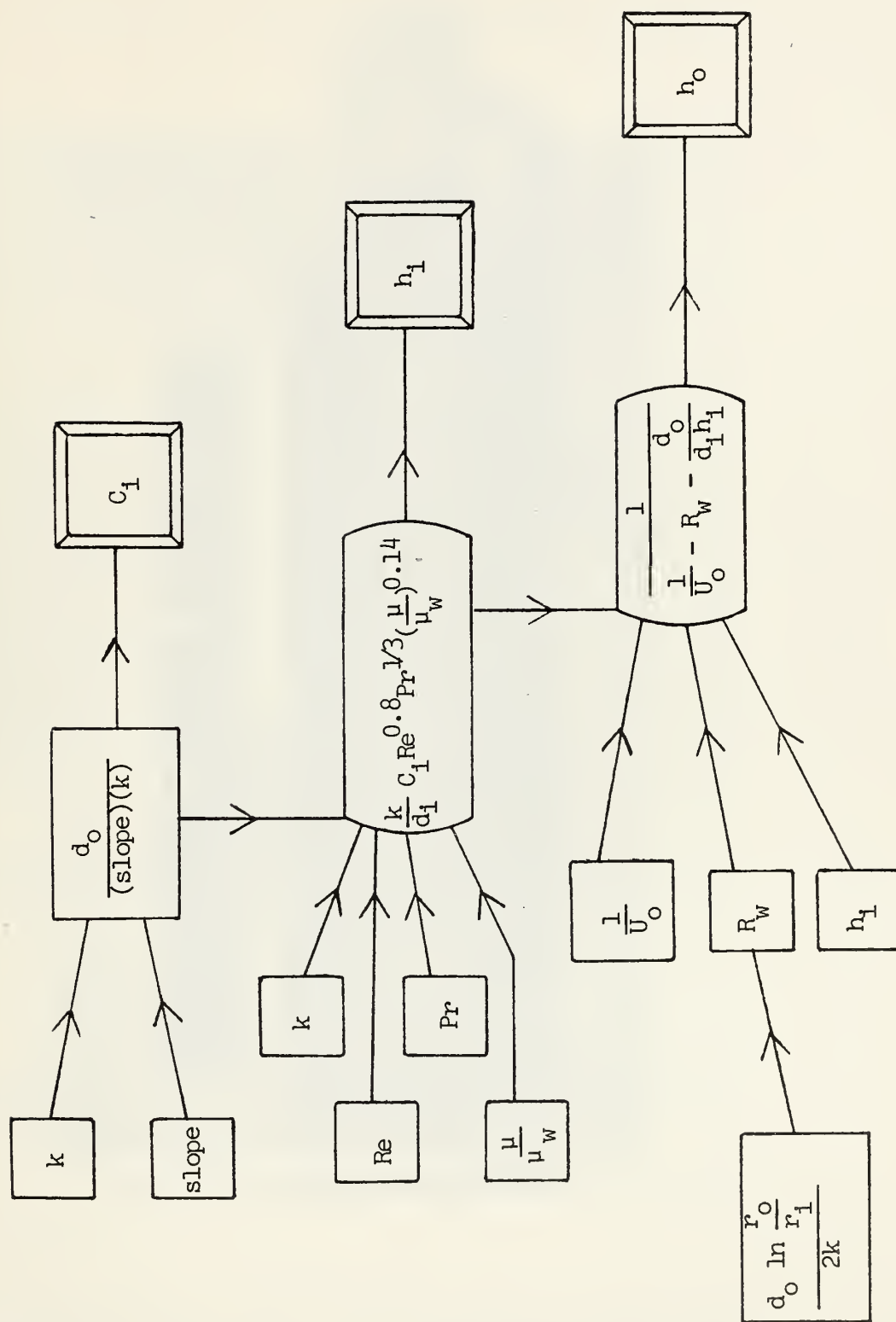


FIGURE 35. Schematic of the Third Phase of Data Collection and Reduction.

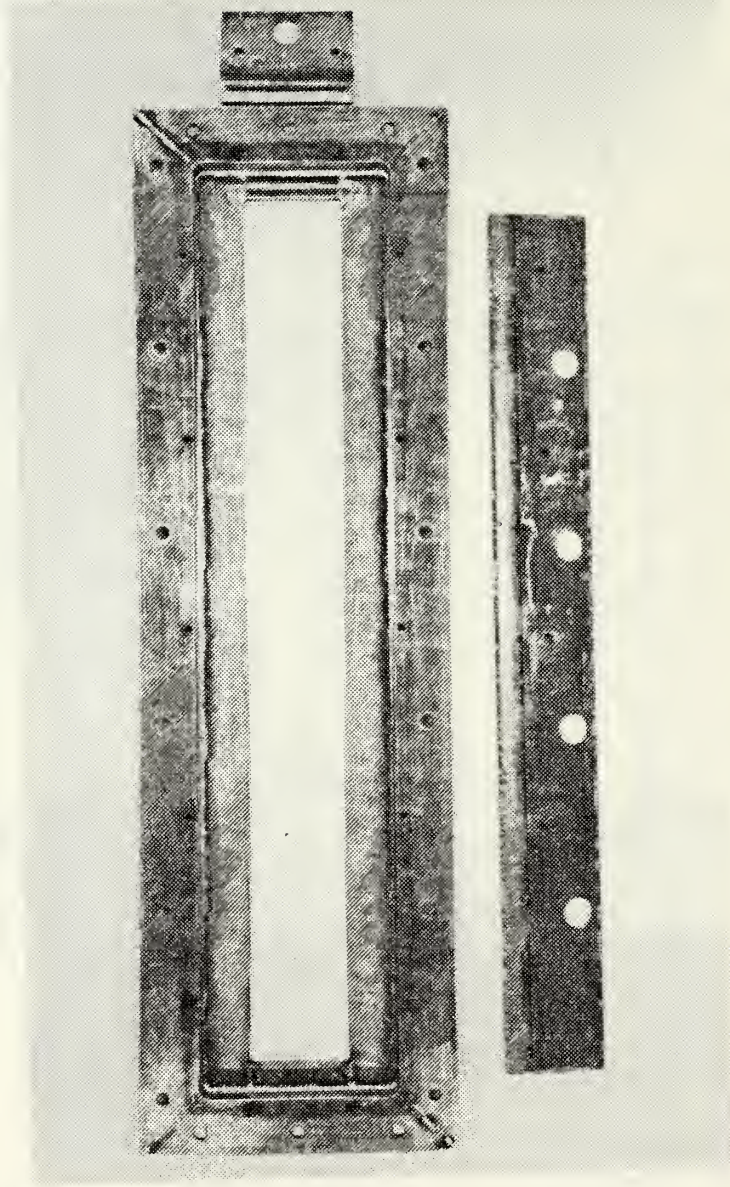


FIGURE 36. Photograph of Test Condenser Window Frame.

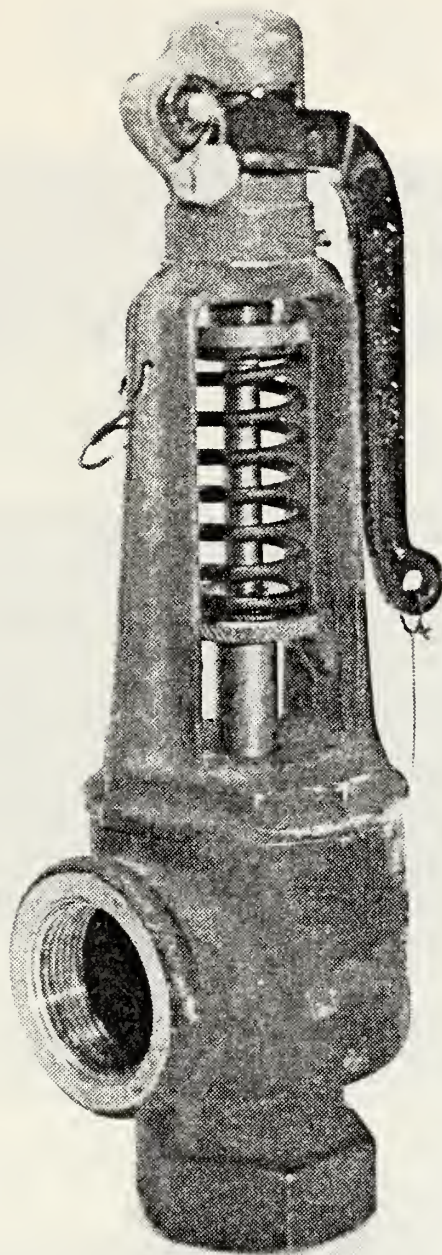


FIGURE 37. Photograph of Overpressure Relief Valve Located Between the Secondary and Test Condensers.

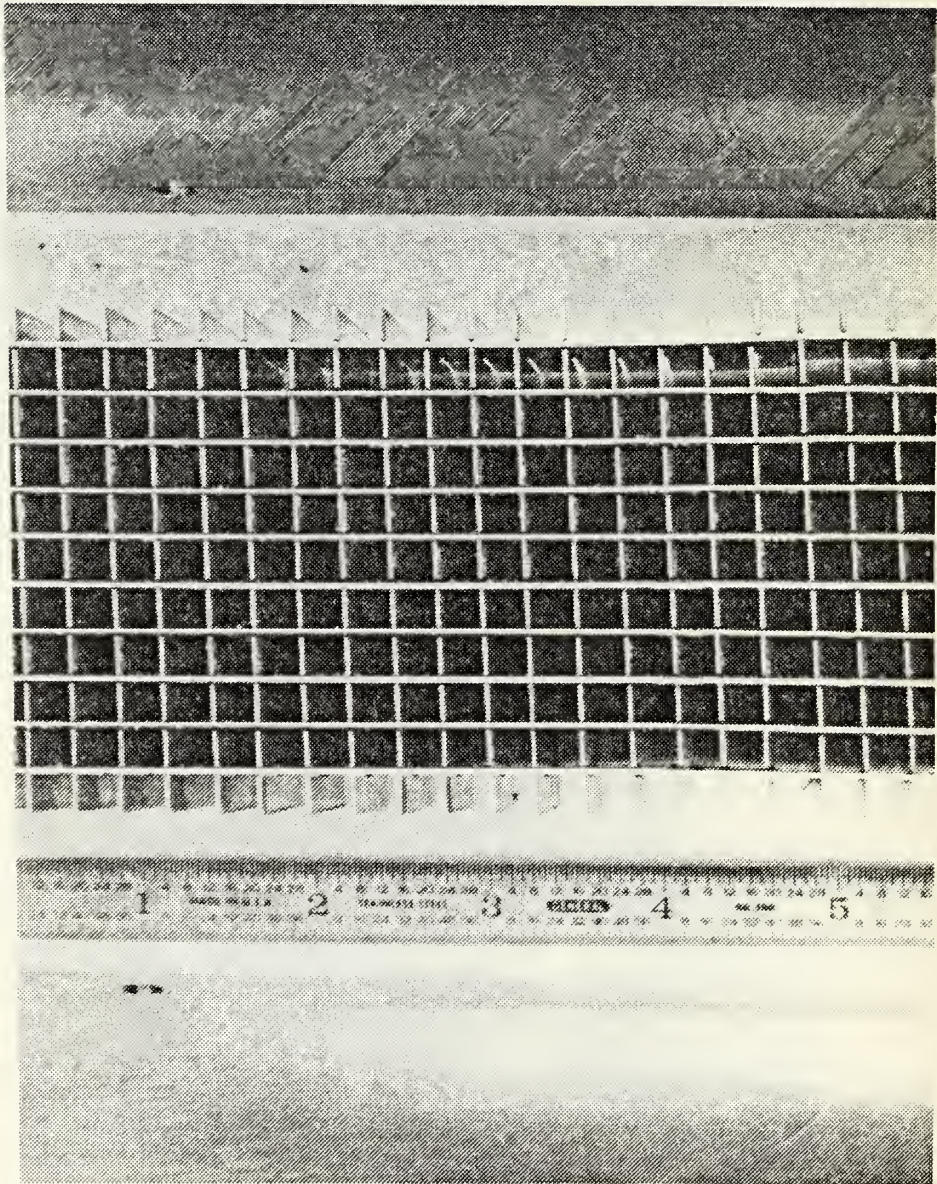


FIGURE 38. Photograph of Test Condenser Flow Straightener.

APPENDIX A: CALCULATION OF STEAM VELOCITY
IN THE TEST CONDENSER

The assumptions made are:

$$\begin{aligned}\text{Vapor Temperature} &= 126.07 \text{ }^{\circ}\text{F}, \\ \text{Vapor Pressure} &= 2.0 \text{ psia}, \\ v_g &= 173.76 \text{ ft}^3/\text{lbm}, \\ \rho &= 5.16 \times 10^{-3} \text{ lbm/ft}^3, \text{ and} \\ \dot{m} &= 140 \text{ lbm/hr.}\end{aligned}$$

To determine the velocity, the following relationship is used:

$$\dot{m} = \rho VA \quad . \quad (16)$$

Rearranging Equation (16) yields:

$$V = \frac{\dot{m}}{\rho A} \quad . \quad (17)$$

Substituting the numerical values, gives

$$V = \frac{(140 \text{ lbm/hr})(1 \text{ hr}/3600 \text{ sec})}{(5.76 \times 10^{-3} \text{ lbm/ft}^3)(0.15625 \text{ ft}^2)}$$

which results in velocity, $V = 43.25 \text{ ft/sec}$. Using Equation (16), the amount of steam required for a vapor velocity of 100 ft/sec is calculated as follows:

$$\dot{m} = \rho V A$$

Substituting numerical values, gives

$$\dot{m} = (5.76 \times 10^{-3} \text{ lbm/ft}^3)(100 \text{ ft/sec})(0.15625 \text{ ft}^2)(3600 \text{ sec/hr})$$

which yields,

$$\dot{m} = 324 \text{ lbm/hr}$$

APPENDIX B: DETAILED TEST CONDENSER DESIGN CALCULATIONS AND CONSIDERATIONS

The following topics are discussed in the order they appear:

1. Stress on the test condenser,
2. Stress on the window glass,
3. Thermal stresses,
4. Fasteners (bolt/stud) selection,
5. Tube sheet construction,
6. Pipe size,
7. Test condenser overpressurization,
8. Steam velocity in the entrance region,
9. Flexible connectors for dynamic testing, and
10. Flow straightener and backpressure screen.

1. Stress on the test condenser. To accommodate the condensate collection drains, steam entrance baffles, flow straighteners, and window frame flow shaper, an arbitrary increase in condenser depth, over that required by the tubes, was made (See Figure 18.). The largest expanse of unsupported plate was then determined to be 12.56 inches by 36 inches.

Type 304 stainless steel has the following properties:

Tensile strength = 85,000 psi [41]

Yield Strength = 35,000 psi [41]

Modulus of Elasticity = 28×10^6 psi [41], and
 Coefficient of Thermal Expansion
 = $9.6 \mu \text{ in/in-}^\circ\text{F}$ [42].

The assumptions made are:

- (a) All plate edge supports are fixed,
- (b) The load is uniform (15 psi), and
- (c) The safety factor is 0.40.

The working stress is then found as follows:

$$\begin{aligned}\sigma_{\max} &= S_m \left(\frac{1}{f_s} \right) \quad [f_s = \text{factor of safety}] \quad (18) \\ &= (35,000)(0.60) = 21,000 \text{ psi}\end{aligned}$$

Consulting Roark's "Formulas for Stress and Strain" [43], the following procedure is derived:

The length to width ratio is:

$$\frac{a}{b} = \frac{36}{12.56} = 2.87, \text{ which implies that}$$

$$\beta_1 = 0.5000,$$

$$\beta_2 = 0.2500, \text{ and}$$

$$\alpha = 0.0284.$$

The stress at the center of the long edge is given by

$$\sigma = \frac{\beta_1 q b^2}{t^2} \quad (19)$$

Therefore,

$$t = \sqrt{\frac{\beta_1 q b^2}{\sigma}}, \quad (20)$$

and upon substituting values,

$$t = \sqrt{\frac{(0.50000)(15 \text{ psi})(12.56 \text{ in})^2}{21,000 \text{ psi}}},$$

which yields the required thickness to be 0.237 inches.

The stress at the center of the plate is given by

$$\sigma = \frac{\beta_2 q b^2}{t^2} \quad (21)$$

and therefore,

$$t = \sqrt{\frac{\beta_2 q b^2}{\sigma}} \quad (22)$$

and the required thickness is 0.168 inches.

The maximum deflection at the center of the plate (for 0.25 inch thick plate) is given by:

$$\max y = \frac{\alpha q b^4}{Et^3}. \quad (23)$$

Substituting the values given yields:

$$\max y = \frac{(0.0226)(15 \text{ psi})(26 \text{ in})^4}{(28 \times 10^6 \text{ psi})(0.25 \text{ in})^3},$$

or $\max y = 0.354$ inches. Note that the values of α and b used for this calculation are for the entire side of the test condenser (worst case).

This result is obviously excessive. Recalculating, assuming that the structure is essentially stiff at the bottom of the window frame (Figure 36) yields:

$$\max y = \frac{(0.0284)(15 \text{ psi})(12.56 \text{ in})^4}{(28 \times 10^6 \text{ psi})(0.25 \text{ in})^3},$$

or

$$\max y = 0.024 \text{ inches.}$$

The upper, or steam entrance section was also investigated for strength. The section was assumed to be an isosceles triangle with simply supported sides and a uniform load. Once again Roark [43] provides the stress relationship needed. It is:

$$\max \sigma = \frac{0.262qa^2}{t^2}. \quad (25)$$

Therefore,

$$t = \sqrt{\frac{(0.262(15 \text{ psi})(10.375 \text{ in})^2)}{21,000 \text{ psi}}}, \quad (26)$$

and the required thickness is found to be 0.142 inches.

The maximum deflection is calculated as follows:

$$\max y = \frac{0.038qa^4}{Et^3} = \frac{(0.038)(15 \text{ psi})(10.375 \text{ in})^4}{(28 \times 10^6 \text{ psi})(0.25 \text{ in})^3} \quad (27)$$

so that

$$\max y = 0.015 \text{ inches.}$$

From the foregoing, it was concluded that the test condenser should be made of 0.25 inch type 304 stainless steel.

However, due to the maximum deflection calculations, three transverse stiffeners were installed in the lower condensate collection area. With these added and the width $b = 12.56$ inches, the length to width ratio is

$$\frac{a}{b} = \frac{12}{12.56} = 0.96 \text{ which implies that } \alpha = 0.0138.$$

Then using equation (23),

$$\max y = \frac{\alpha qb^4}{Et^3} = \frac{(0.0138)(15 \text{ psi})(12.56 \text{ in})^4}{(28 \times 10^6 \text{ psi})(0.25 \text{ in})^3},$$

and the value of $\max y = 0.012$ inches. With the conservative safety factor and working pressure assumptions this value is found acceptable.

2. Stress on the window glass. Previously it was decided to use glass to view the condensation process. There are two methods available to do this. The first

method is to use a double thickness of glass, with a spacer, and blow hot air between the two. The hot air would raise the temperature of the outside of the inner glass window to the temperature within the test condenser, thereby reducing the temperature gradient and the heat flux to zero. This would insure that no condensate formed on the interior of the glass to obstruct the view. The second method, to accomplish the same purpose, is to utilize a transparent, electrically conducting coating on the exterior of one glass window. The resistance of the coating would provide the heat to defog the window and minimize the heat flux. The second method, although more costly, is preferred. The possibilities of difficulty in observation due to the thickness of the framing and poor light transmission due to several layers of glass, coupled with the required use of an air heater system, make choice number one less attractive. Stress calculations to determine the required thickness of the glass are made as follows:

The strength properties of float glass are assumed to be:

Breaking strength = 15,000 to 35,000 psi,

Design strength = 1500 to 6000 psi,

Coefficient of linear expansion = $4.9 \mu\text{in/in-}^{\circ}\text{F}$, and

Modulus of Elasticity = 10×10^6 psi [42].

The glass is assumed to be a flat plate with fixed supports. The glass dimensions are chosen to be 31.125 by 6.375 inches. These actual figures are used rather than estimating the reduced dimensions when the glass is installed in the frame.

The working stress used is 1500 psi (safety factor of 10).

The glass length to width ratio is

$$\frac{a}{b} = \frac{31.125}{6.375} = 4.88.$$

This implies that

$$\beta_1 = 0.5000,$$

$$\beta_2 = 0.2500, \quad \text{and}$$

$$\alpha_3 = 0.0284.$$

The maximum stress at the center of the edge is given by Equation (19) as

$$\sigma = \frac{\beta_1 q b^2}{t^2}$$

which implies that

$$t = \sqrt{\frac{\beta_1 q b^2}{\sigma}} = \sqrt{\frac{(0.5000)(15 \text{ psi})(6.375 \text{ in.})^2}{1500 \text{ psi}}}$$

and therefore the required thickness is 0.451 inches.

Maximum stress at the center of the plate is given by Equation (21) as

$$\sigma = \frac{\beta_2 q b^2}{t^2}$$

Rearranging this formula to solve for thickness gives

$$t = \sqrt{\frac{\beta_2 q b^2}{\sigma}}$$

$$= \sqrt{\frac{(0.2500)(15 \text{ psi})(6.375 \text{ in})^2}{1500 \text{ psi}}}$$

and the required thickness is 0.319 inches.

The maximum deflection at the center of the plate using 0.50 inch thick glass is given by Equation (23):

$$y_{\max} = \frac{\alpha q b^4}{E t^3}$$

$$= \frac{(0.0284)(15 \text{ psi})(6.375 \text{ in})^4}{(10 \times 10^6 \text{ psi})(0.50 \text{ in})^3}$$

or

$$y_{\max} = 5.629 \times 10^{-4} \text{ inches.}$$

On the basis of these calculations, it is determined that 0.50 inch thick float glass is sufficiently strong for the test condenser windows.

3. Thermal stresses. Thermal stresses are substantial in a design such as this. To be certain they would not be excessive, several calculations were made. It is assumed that the window edges have fixed supports and that the electrically conducting coating of the external surface of the glass is not energized. The bending stress is then given by

$$\sigma_b = \frac{1}{2} \Delta T \alpha E / (1 - \nu), \quad (28)$$

with the hot face in compression and the cold face in tension [43]. This analysis does not account for the fact that the reduced pressure on the hot side tends to alleviate the bad effects of the bending.

Necessary constants used are :

Poisson's Ratio = ν = 0.23, and

Coefficient of thermal expansion = $4.9 \mu\text{in} / \text{in } ^\circ\text{F}$. [42]

The temperature difference is assumed to be $50 ^\circ\text{F}$. Substituting the numerical values into Equation (28) yields

$$\sigma_b = \frac{1}{2} (50 ^\circ\text{F}) (4.9 \times 10^{-6}) (10 \times 10^6 \text{ psi}) / (1 - 0.23), \text{ or}$$
$$\sigma_b = 1590.91 \text{ psi}.$$

Due to the factor of safety incorporated in the calculations, the undetermined support of the window frame,

the degree of movement possible at the window boundaries, the effect of reduced internal pressure, the conservative estimates of temperature rise and glass strength, the slightly excessive stress (above 1500 psi) is not considered sufficient to require glass thicker than 0.50 inch.

The maximum change in the length of the stainless steel frame during a 50 °F temperature rise is calculated to be:

$$(9.6 \times 10^{-6} \text{ in./in. } ^\circ\text{F})(50 ^\circ\text{F}) = 0.00048 \text{ inches}$$

The maximum change in the length of the glass due to temperature rise is calculated to be:

$$(4.9 \times 10^{-6} \text{ in./in. } ^\circ\text{F})(50 ^\circ\text{F}) = 0.00025 \text{ inches}$$

The worst case is then the sum of these two or 0.00073 inch. A clearance of 0.125 inch, overall, is allowed between the frame and the glass.

The glass chosen is a heavy duty float glass with electrically conducting coating PE-81-E made by Libby-Owens-Ford Co. The coating has a resistance of 20 ohms per square. The power required is computed using the information supplied by the manufacturer.

The glass heating requires approximately
1.25 watts/ft.²/°F (temperature rise). Therefore:

$$(1.25 \text{ W/ft.}^2/\text{°F}) (1.16 \text{ ft.}^2) (50\text{°F}) = 72.50 \text{ Watts or} \\ = 247.39 \text{ Btu/hr.}$$

4. Fasteners (bolt/stud) selection. Essentially the selection for the bolt/stud size is based upon the following calculations. It is assumed that 0.25 diameter (nominal size) is sufficient and then all calculations are made to determine the possible loading.

Assumptions:

Nominal diameter = 0.2500 inches

External minor diameter of a 1/4 - 28

2A bolt = 0.2052 inches

Plate Thickness = 0.2500 inches

Type 304 stainless steel properties:

Yield strength = 35,000 psi

Tensile strength = 85,000 psi

Safety Factor = 2 [44].

The two cases considered are:

Pure Tension,

$$\sigma = \frac{F}{A}, \text{ and} \quad (29)$$

Direct Shear,

$$\tau = \frac{F}{A} . \quad (30)$$

The working strength is found from the relationship,

$$S_w = \frac{S_m}{f_s} . \quad [44] \quad (31)$$

Substituting numerical values yields

$$S_w = 35,000/2 = 17,500 \text{ psi.}$$

For tension the relationship is,

$$F = \sigma A = (17,500 \text{ psi}) (\pi (0.2052 \text{ in})^2 / 4) .$$

Solving for Force, F, yields,

$$F = 578.74 \text{ lbf.}$$

For shear the bearing area is determined as a fraction of the major external diameter. Since the bolt hole is not a close fit, it is assumed that one half of the supporting semicircle would be applying a shearing force. Therefore the area is calculated as:

$$A = \frac{\pi D}{4} \times 0.2500 \text{ and,}$$

$$F = \tau A = (17,500 \text{ psi}) (\pi (0.2500)/4 \times 0.2500).$$

The resulting Force, F is 859.03 lbf. For comparison, one calculation of the force required to break the threaded portion of the bolt is made using the relationship,

$$P = S A_t. \quad (32)$$

Solving for A_t yields

$$A_t = 0.7854 (D - 0.9743/n)^2 \quad [44] \quad (33)$$

Note: $S = \text{UTS}$ but S_w is used. The force P then is calculated:

$$P = (17,500 \text{ psi}) (0.7854) (0.2500 \text{ in} - 0.9743/28)^2,$$

or

$$P = 636.54 \text{ lbf.}$$

The critical union in the test condenser is the flanged surface between the body and the entrance section. It is calculated that the entrance section weighs approximately 100 lbs and that the main body weighs approximately 350 lbs. Since there are 24 bolts holding these sections

together, the total force that could be supported by these bolts is;

20,617 lbf in shear, or

13,890 lbf in tension.

Therefore, 1/4-28 UNF bolts/studs are considered strong enough.

5. Tube sheet construction. The tube sheets are to be 0.750 inch thick to accommodate the Swagelok "O" ring straight thread connectors (bored out to 0.625 inch diameter). Also this thickness allows the tubes used for flow simulation only to be suspended between the sheets, which are to be partially bored through to hold them.

6. Pipe size. The pipe size used in the construction of the test condenser and other piping is designed to withstand the maximum pressure the boiler can supply (150 psi). Schedule 40 pipe was chosen also because it is readily available.

7. Test condenser overpressurization. The test condenser is not designed to withstand large overpressure, although it probably would. Consequently a relief valve (Figure 37) is installed in the line between the secondary and test condensers. It is set at approximately 5 psig.

8. Steam velocity in the entrance region. The entrance region of the test condenser contains three flow baffles/condensate collectors. They are spaced to provide nearly constant frontal area to the flow. The vapor velocity in the area of these baffles is computed to be about 50 ft/sec with the maximum output of the presently installed steam generator.

9. Flexible connectors for dynamic testing. Flexible connectors to be utilized for the condenser rocking and tilting portions of the tests are to be installed in initial construction for later use. A three foot length of 0.50 inch (tube fitting adapted) corrugated stainless steel flexible tubing, manufactured by Swagelok, was purchased for the condensate connection. The steam connections are 2.50 inches diameter by 36 inches long corrugated stainless steel tubes, fitted with 2.50 inch butt weld, schedule 40 pipe ends. Marman Flexmaster joints are used to couple the large corrugated steam tubing to the system.

10. Flow straightener and backpressure screen. A flow straightener which consists of a stainless steel grid structure, with 0.25 inch wide openings, is positioned upstream of the tubes in the test condenser (Figure 38). Above the grid, several layers of stainless steel screen are to be stacked to provide a backpressure to equalize the flow over the length of the tubes.

APPENDIX C: SECONDARY CONDENSER
DESIGN CALCULATIONS

The Design Data Sheet is used in the calculations of the size requirements for the secondary condenser.

The following information is applicable:

Heliflow Surface Area = 9.63 ft^2 [45] ,

Heliflow Cooling water required at 10 ft/sec

= 35.5 GPM [45] ,

Heliflow Tube length = 8.16 ft [45] ,

Heliflow Number of tubes = 9 [45] ,

Heliflow Tube type = 5/8 inch diameter copper/

nickel - 18 gage [45] ,

Temperature of cooling water = 70 °F (assumed),

$\Delta h = 1058 \text{ Btu/lbm}$ (subcooled to below 90 °F) [46] ,

Cooling water velocity = 9 ft/sec [4] ,

Fouling factor, $F_1 = 0.85$ [4] ,

Material conduction factor, $F_2 = 0.90$ [4] ,

Inlet cooling water factor, $F_c = 1.0$ [4] ,

Tube constant, $k = 0.2407$ [4].

The overall heat transfer coefficient from the Design Data Sheet [4] is:

$$U = 270 \sqrt{V} = 270 \sqrt{9} = 810 \text{ Btu/hr-ft.}^2\text{-}^\circ\text{F.} \quad (34)$$

The corrected overall heat transfer coefficient is,

$$U_c = UF_1F_2F_3 = 620 \text{ Btu/hr-ft}^2\text{-}^\circ\text{F}. \quad (35)$$

The equations from the DDS to calculate the cooling water outlet temperature are used as follows:

$$t_s = \text{saturated steam temperature} = 126.07 \text{ }^\circ\text{F},$$

$$a = \frac{U_c LK}{500 V} = \frac{(620)(8.16)(0.2407)}{(500)(9)} = 0.271, \quad (36)$$

and the outlet temperature

$$t_o = t_s - \frac{t_s - t_i}{e^a} = 126.07 - \frac{126.07 - 70}{1.311} = 83.29 \text{ }^\circ\text{F} \quad (37)$$

The amount of steam that the Heliflow can condense is calculated as follows:

$$W = \frac{G(500)(t_o - t_i)}{\Delta h} = \frac{(35)(500)(13.29)}{1058}, \quad (38)$$

which yields

$$W = 219.83 \text{ lbm/hr}.$$

If it were assumed that 170 lbm/hr is the desired load of the condenser then,

the cooling water flow rate would be

$$G = \frac{W (h)}{500(t_o - t_i)} = \frac{(170)(1058)}{(500)(13.29)} \quad (39)$$
$$= 27.07 \text{ GPM},$$

and the cooling surface required is

$$A = \frac{LGk}{V} = \frac{(8.16)(27.07)(0.2407)}{9}, \quad (40)$$
$$= 5.91 \text{ ft}^2 .$$

Thus using the design data sheet which is developed from the HEI information (known to be conservative), it is determined that use of the available Heliflow is feasible. This is demonstrated in the calculation of condensing area required as well as cooling water flow rate required.

APPENDIX D: TEST CONDENSER HOT WELL CALCULATIONS

The assumptions are:

$$T_{\text{film}} = 80^{\circ}\text{F} \text{ (low to be conservative),}$$

$$P = 2 \text{ psia,}$$

$$\rho_{\text{condensate}} = 62.17 \text{ lbm/ft.}^3 \text{ [8],}$$

$$\mu = 2.08 \text{ lbm/ft-hr [8],}$$

$$k = 0.355 \text{ Btu/hr/ft/}^{\circ}\text{F [8], and}$$

$$h_{fg} = 1022 \text{ Btu/lbm at } 126^{\circ}\text{F [46].}$$

The Nusselt Relationship is

$$\bar{h} = 0.725 \left\{ \frac{\rho(\rho - \rho_v) g h_{fg} k^3}{\mu d (T_{\text{sat}} - T_w)} \right\}^{1/4} \quad [8] . \quad (41)$$

Substituting in numerical values yields:

$$\bar{h} = 0.725 \left\{ \frac{(61.94 \text{ lbm/ft}^3)^2 (32.2 \text{ ft/sec}^2) (3600 \text{ sec/hr})^2}{(2.08 \text{ lbm/hr-ft}) (5/(8 \times 12) \text{ ft})} \right. \\ \left. \frac{(1022 \text{ Btu/lbm}) (0.355 \text{ Btu/hr-ft-}^{\circ}\text{F})^3}{(4^{\circ}\text{F})} \right\}^{1/4} .$$

The resultant average heat transfer coefficient is,

$$\bar{h} = 2613.77 \text{ Btu/hr-ft}^2\text{-}^{\circ}\text{F} .$$

The heat transfer is then given by

$$q = \bar{h}A(T_{\text{sat}} - T_w) = \dot{m} h_{fg} \quad (42)$$

Solving for the mass flow rate of the condensate yields:

$$\dot{m} = \frac{\bar{h}A(T_{\text{sat}} - T_w)}{h_{fg}} = \frac{(2613.77 \text{ Btu/hr-ft}^2\text{-}^\circ\text{F})}{1} \pi \frac{(5/(8 \times 12) \text{ ft})(3 \text{ ft})(4^\circ\text{F})}{1022 \text{ Btu/lbm}}$$

and the result is

$$\dot{m} = 5.02 \text{ lbm/hr} = 0.602 \text{ gal/hr} .$$

APPENDIX E: CALCULATION OF COOLING WATER REQUIREMENTS

An alternate method of calculating the cooling water required is as follows:

The assumptions are:

Cooling water velocity = 9 ft/sec., and

Diameter of cooling water entrance = 1.25 inches.

The flow rate is given by,

$$Q = VA = (9 \text{ ft/sec}) (\pi (1.25/12)^2 / 4 \text{ ft}^2) (60 \text{ sec/min}),$$

(43)

which reduces to

$$Q = 4.60 \text{ ft.}^3/\text{min}, \text{ or}$$

34.43 GPM .

It is realized that the pressure drop would be excessive with this flow rate; however, this provides an outside value for design purposes.

The test condenser, in the initial configuration, requires cooling water to only one tube.

The assumptions are:

Number of tubes = 1

Tube diameter = 5/8 inches

Tube gage = 18 (0.049 inch thickness)

Tube length = 3 feet

Cooling water velocity = 26 ft/sec (maximum).

The flow rate is given by Equation (43) as:

$$Q = VA = (26 \text{ ft/sec}) \left(\pi \left(\frac{0.527}{12} \right)^2 / 4 \text{ ft}^2 \right) (60 \text{ sec/min}),$$

which yields

$$Q = 2.36 \text{ ft}^3/\text{min} = 17.68 \text{ GPM.}$$

At $V = 9 \text{ ft/sec}$, $Q = 6.12 \text{ GPM.}$

APPENDIX F: DETAILS OF UNCERTAINTY ANALYSIS

The general form of the Kline and McClintock [32] "second order" equation is used to compute the uncertainty. If the resultant, R , is some function of primary variables x_1, x_2, \dots, x_n , then the uncertainty in R , δR , is given by:

$$\delta R = \sqrt{\left(\frac{\partial R}{\partial x_1} \delta x_1\right)^2 + \left(\frac{\partial R}{\partial x_2} \delta x_2\right)^2 + \dots + \left(\frac{\partial R}{\partial x_n} \delta x_n\right)^2} \quad (44)$$

where $\delta x_1, \delta x_2, \dots, \delta x_n$ are the uncertainties in each of the measured variables x_1, x_2, \dots, x_n .

The overall heat transfer coefficient is given by Equation (9).

$$U_o = \frac{\dot{m}_c C_p}{A_s} \ln \frac{T_s - T_{ci}}{T_s - T_{co}} \quad .$$

By applying Equation (44), Equation (9) becomes:

$$\frac{\delta U_o}{U_o} = \sqrt{\left(\frac{\delta A_s}{A_s}\right)^2 + \left(\frac{\delta C_p}{C_p}\right)^2 + \left(\frac{\delta \dot{m}_c}{\dot{m}_c}\right)^2 + \left\{ \frac{\delta T_s (T_{ci} + T_{\infty})}{(T_s - T_{ci})(T_s - T_{\infty}) \ln\left(\frac{T_s - T_{ci}}{T_s - T_{\infty}}\right)} \right\}^2} \quad (45)$$

$$+ \left\{ \frac{\delta T_{\infty}}{(T_s - T_{\infty}) \ln\left(\frac{T_s - T_{ci}}{T_s - T_{\infty}}\right)} \right\}^2 + \left\{ \frac{\delta T_{ci}}{(T_s - T_{ci}) \ln\left(\frac{T_s - T_{ci}}{T_s - T_{\infty}}\right)} \right\}^2$$

All parameters in the above expression except surface area, A_s , and cooling mass flow rate, \dot{m}_c , are functions of temperature primarily and should be found to desired accuracy with relative ease. The dimensions for computing area can be obtained without difficulty. The mass flow rate of the cooling water, because of the relatively constant properties in the temperature range under consideration, can be measured with the desired accuracy.

The Reynolds number is given by

$$Re = \frac{VD_i \rho}{\mu} \quad .$$

By applying Equation (44), the Reynolds number uncertainty becomes,

$$\frac{\delta Re}{Re} = \sqrt{\left(\frac{\delta D_i}{D_i}\right)^2 + \left(\frac{\delta V}{V}\right)^2 + \left(\frac{\delta \rho}{\rho}\right)^2 + \left(\frac{\delta \mu}{\mu}\right)^2} \quad . \quad (46)$$

D_i , the inside diameter of the tube, can be measured accurately. Cooling water density ρ and viscosity μ , at the temperatures to be considered, can be calculated from temperature which can be measured sufficiently accurately.

The Prandtl number is given by:

$$Pr = \frac{C_p \mu}{k} .$$

Applying Equation (44) to the Prandtl number yields;

$$\frac{\delta Pr}{Pr} = \sqrt{\left(\frac{\delta C_p}{C_p}\right)^2 + \left(\frac{\delta \mu}{\mu}\right)^2 + \left(\frac{\delta k}{k}\right)^2} . \quad (47)$$

The Heat Capacity C_p , viscosity μ , and thermal conductivity k can be calculated from the measured temperature.

The expression for viscosity effect is given by

$$\frac{\mu}{\mu_w} = \bar{\mu} .$$

Applying Equation (44) the uncertainty in the viscosity becomes:

$$\frac{\delta \bar{\mu}}{\bar{\mu}} = \sqrt{\left(\frac{\delta \mu}{\mu}\right)^2 + \left(\frac{\delta \mu_w}{\mu_w}\right)^2} . \quad (48)$$

Once again, viscosity can be computed from the appropriate temperature readings.

From the above information, the form of the Sieder-Tate relationship and its uncertainty, useful in the single tube evaluation phase of this test program, can be evaluated.

The Sieder-Tate relationship is:

$$Nu = \frac{h_i D_i}{k} = C_i (Re)^{0.8} (Pr)^{1/3} (\bar{\mu})^{0.14} .$$

Applying Equation (44) once again gives the uncertainty associated with the Nusselt number:

$$\frac{\delta N_u}{N_u} = \sqrt{\left(\frac{\delta C_i}{C_i}\right)^2 + \left(\frac{0.8 \delta Re}{Re}\right)^2 + \left(\frac{\frac{1}{3} \delta Pr}{Pr}\right)^2 + \left(\frac{0.14 \delta \bar{\mu}}{\bar{\mu}}\right)^2} \quad (49)$$

The uncertainty in the coefficient, $\delta C_i / C_i$, can be found as follows. From the slope of the least squares fit of the curve obtained from the Wilson Plot technique (See the Data Reduction section), the expression for C_i is:

$$C_i = \frac{d_o}{\text{slope } k} .$$

Applying Equation (44) yields:

$$\frac{\delta C_i}{C_i} = \sqrt{\left(\frac{\delta d_o}{d_o}\right)^2 + \left(\frac{\delta \text{slope}}{\text{slope}}\right)^2 + \left(\frac{\delta k}{k}\right)^2} \quad (50)$$

This uncertainty can only be evaluated by visual observation of the plotted data, the scatter of the data, and the least squares curve fit.

The desired tubeside heat transfer coefficient h_i can be obtained. The resulting equation is:

$$h_i = \left(\frac{k}{D_i}\right) (C_i) (Re^{0.8}) (Pr^{1/3}) \left(\frac{\mu}{\mu_w}\right)^{0.14} = \frac{k}{D_i} Nu \quad .$$

Applying Equation (44) results in the uncertainty in h_i , as follows:

$$\frac{\delta h_i}{h_i} = \sqrt{\left(\frac{\delta k}{k}\right)^2 + \left(\frac{\delta D_i}{D_i}\right)^2 + \left(\frac{\delta Nu}{Nu}\right)^2} \quad (51)$$

The steamside heat transfer coefficient is calculated from the following equation:

$$h_o = \frac{1}{\frac{1}{U_o} - R_w - \frac{d_o}{d_i h_i}} .$$

Applying the principle of Equation (44) yields:

$$\frac{\delta h_o}{h_o} = \sqrt{\left\{ \frac{\delta U_o}{U_o^2 \left(\frac{1}{U_o} - R_w - \frac{d_o}{d_i h_i} \right)} \right\}^2 + \left\{ \frac{\delta R_w}{\left(\frac{1}{U_o} - R_w - \frac{d_o}{d_i h_i} \right)} \right\}^2 + \left\{ \frac{\left(\frac{d_o}{d_i h_i} \right) \left(\frac{\delta h_i}{h_i} \right)}{\left(\frac{1}{U_o} - R_w - \frac{d_o}{d_i h_i} \right)} \right\}^2} .$$

From the foregoing it can be determined that:

1. The physical size measurements must be as accurate as any other measurement taken. Obtaining them should present no particular difficulty.
2. Temperature measurements need not be any more accurate than can be obtained from well-calibrated thermocouples.

3. The greatest effect on the Sieder-Tate relationship uncertainty is the Reynolds number. The most difficult measurement to be taken affecting the Reynolds number is the cooling water velocity or flowrate; for example, a one percent deviation in the cooling water velocity measurement will result in a 0.8 percent error in the results of the Sieder-Tate relationship. Therefore, great care must be exercised in the cooling water flowrate measurement.

APPENDIX G: CALCULATION OF PRESSURE HEAD OF THE
ANNUBAR, PRIMARY FLOW SENSOR [47]

The assumptions are:

Pipe size 1.25 inches (ID = 1.380 inches)

Annubar model = 711-316-SS (Figure 34)

The expression for the pressure head developed in the Annubar as given by the manufacturer [47] is:

$$h_n = \left\{ \frac{W_n}{.1266 \text{ S N D}^2 F_a F_n V_a \sqrt{\gamma_f}} \right\}^2, \quad (52)$$

$$\text{where } S = K_g F_v = 0.778 \times 0.82 = 0.638. \quad (53)$$

Substituting numerical values gives:

$$h_n = \left\{ \frac{140}{(.1266) (.638) (2835.0) (1.380)^2 (1.0) (1.0) (1.0) (0.25)} \right\}^2,$$

which yields,

$$h_n = 1.65 \text{ inches H}_2\text{O}.$$

APPENDIX H: PROPERTIES OF WATER AS A FUNCTION OF TEMPERATURE

The expressions to relate μ , k , ρ and C_p to temperature are:

$$\mu = \exp(0.004606532 T_f^* + 4759.5941/T_f^* - 10.59252566 \left[\frac{\text{lbm}}{\text{ft-hr}} \right]), \quad (54)$$

$$k = 0.32159931 + 0.000697989 T_f - 0.12506 \times 10^{-5} T_f^2 - 0.2072 \times 10^{-10} T_f^3 \left[\frac{\text{Btu}}{\text{hr-ft-}^\circ\text{F}} \right], \quad (55)$$

$$\rho = 62.707172 - 0.0043955304 T_f - 0.000046076921 T_f^2 \left[\frac{\text{lbm}}{\text{ft}^3} \right], \text{ and } (56)$$

$$C_p = 1.0121559 - 0.00024618473 T_f + 0.10282155 \times 10^{-5} T_f^2 \left[\frac{\text{Btu}}{\text{lbm-}^\circ\text{F}} \right], \quad (57)$$

where T_f = temperature in degrees F, and

T_f^* = temperature in degrees R [48] .

BIBLIOGRAPHY

1. Marine Division, Westinghouse Electric Corporation, Letter by J. W. Ward, Some Random Thoughts on the Design and Application of Condensers for Marine Application, 4 December 1973.
2. Standards for Steam Surface Condensers, 6th ed., Heat Exchange Institute, 1970.
3. Standards of Tubular Exchanger Manufacturers Association, 4th ed., Tubular Exchanger Manufacturers Association, Inc., 1959.
4. Department of the Navy, Design Data Sheet Section DOS4601-1, Steam Condensers, 15 October 1953.
5. Macnair, E. J., Introductory Remarks on Marine and Naval Condensers, Paper presented at the National Eng. Lab. Conference, East Kilbride, Glasgow, UK, 1974.
6. Search, H. T., A Feasibility Study of Compact Marine Steam Condensers, MSME Thesis, Naval Postgraduate School, March 1977.
7. Marine Division, Westinghouse Electric Corporation, Letter by J. W. Ward, Steam Condensers for Marine Application, 13 June 1974.
8. Holman, J. P., Heat Transfer, 3rd ed., McGraw-Hill, 1972.
9. Eissenberg, D. M., An Investigation of the Variables Affecting Steam Condensation on the Outside of a Horizontal Tube Bundle, Ph.D. Thesis, University of Tennessee, December 1972.
10. Heat Transfer Laboratory, Department of Mechanical Engineering, Engineering Research Institute Iowa State University, Report HTL-8, ISU-ERI-AMES-76026 ERI Project 1117, Research Workshop on Augmentation of Connective Heat Transfer, by E. E. Bergles, 22 April 1974.
11. Bergles, A. E., Survey of Augmentation of Two-Phase Heat Transfer, paper presented at ASHRAE Semi-annual Meeting, Dallas, Texas, February 1976.

12. Graham, C., The Limiting Heat Transfer Mechanisms of Dropwise Condensation, Ph.D. Thesis, Massachusetts Institute of Technology, March 1969.
13. United States Department of the Interior Research and Development Progress Report No. 184, Dropwise Condensation Characteristics of Permanent Hydrophobic Systems, by R. A. Erb and E. Thelen, April 1966.
14. Erb, R. A., "Dropwise Condensation on Gold, Improving Heat Transfer in Steam Condensers", Gold Bulletin, Vol. 6, No. 1, p. 2-6, 1973.
15. Hurst, C. J., Olson, D. R., "Conduction Through Droplets During Dropwise Condensation", Journal of Heat Transfer, ASME Paper No. 72-HT-50, p. 7, 30 November 1970.
16. Osment, B. D. J., Tudor, D., Speirs, R. M. M., and Rugman, W., "Promoters for the Dropwise Condensation of Steam", Trans, Instn, Chem. Engrs., Vol. 40, p. 9-17, 1962.
17. Watson, R. G., Brunt, J. I., and Birt, D. C., "International Developments in Heat Transfer, Part II", American Soc. Mech. Engrs., p. 296, 1961.
18. Westinghouse Electric Corp., Lester Works, Heat Transfer Department, EM-377, Investigation of the Use of Non-Wetting Agents for Promoting Dropwise Condensation on Steam Condenser Tubes, by E. F. Cox, 19 May 1959.
19. United States Naval Engineering Experiment Station Annapolis, Md., Evaluation Report 030038B, NS-643-078, Promotion of Dropwise Condensation By Teflon Coated Condenser Tubes, by G. F. Smith, 12 October 1960.
20. Young, E. H., and Briggs, D. E., "The Condensing of Low Pressure Steam on Vertical Rows of Horizontal Copper and Titanium Tubes", A.I. Ch. E. Journal, Vol. 12, No. 1, p. 31-35, 1966.
21. United States Department of the Interior, Symposium on Enhanced Tubes for Desalination Plants, by Office of Saline Water, July 1970.
22. Young, E. H., Withers, J. G., and Lampert, W. B., Heat Transfer Characteristics of Corrugated Tubes in Steam Condensing Applications, paper presented at National Heat Transfer Conference, 15th, San Francisco, California, August 1975.

23. Oak Ridge National Laboratory Report ORNL-TM-2611, Office of Saline Water, Enhanced Tubes for Seawater Plants, by R. M. Eissenberg, August 1969.
24. Oak Ridge National Laboratory Task Report No. 5, Performance of a Wolverine Korodense Tube, by D. M. Eissenberg, March 1972.
25. Oak Ridge National Laboratory Task Report No. 12, The Measurement of Heat Transfer Performance of a Korodense Tube as a Steam Condenser, by P. H. Harley, and D. M. Eissenberg, October 1973.
26. Heat Exchangers: Design and Theory Sourcebook, N. H. Afgan and E. U. Schlunder, Editors, p. 441-489, McGraw-Hill, 1974.
27. Catchpole, J. P. and Drew, B. C. H., Evaluation of Some Shaped Tubes for Steam Condensers, paper from The British Ministry of Defence. 1974.
28. Fulton Boiler Works, Electric Boiler Installation Book, p. 18, July 1969.
29. Sparrow, E. M., Hallman, T. M., and Siegal, R., "Turbulent Heat Transfer in the Thermal Entrance Region of a Pipe with Uniform Heat Flux", Applied Science Research, Section A, Vol. 7, p. 31-52, May 1957.
30. Knudsen, J. G., and Katz, D. L., Fluid Dynamics and Heat Transfer, McGraw-Hill, 1958.
31. Department of the Navy Military Spec. MIL-C-15430J (Ships), Military Specification Condensers, Steam, Naval Shipboard, 19 June 1974.
32. Kline, S. J. and McClintock, F. A., "Describing Uncertainties in Single Sample Experiments", Mech. Engin., Vol. 74, p. 3-8, Jan. 1953.
33. Process Instruments and Controls Handbook, 2nd ed., D. M. Considine editor-in-chief, McGraw-Hill, 1974.
34. American Society of Mech. Eng., ASME Power Test Codes PTC 19.11-1959 Part II, Quality and Purity of Steam, Jan. 1959.
35. O'Connor, K., The Design and Operation of an Experimental Steam Condensing System, MSME Thesis, Naval Postgraduate School, Monterey, California, June 1972.

36. E. E. Wilson, A Basis for Rational Design of Heat Transfer Apparatus, paper presented at the Spring Meeting of The Society of Mechanical Engineers, Buffalo, N.Y., June 1965.
37. Briggs, D. E., and Young, E. H., "Modified Wilson Plot Techniques for Obtaining Heat Transfer Correlations for Shell and Tube Heat Exchangers", Heat Transfer - Philadelphia, Vol. 65, No. 92, p. 35-45, 1969.
38. Wolverine Korodense Tube General Information and Heat Transfer, Design Notes, Bulletin No. 402D, Wolverine Tube Division, Universal Oil Products Co., 10 Jan 1973.
39. U.S. Naval Engineering Experiment Station Evaluation Report 720038D, Heat Transfer Rates of Teflon-Coated Condenser Tubes, by J. T. Duck and C. W. Brown, 7 November 1960.
40. Deutschman, A. D., Michels, W. J., and Wilson, C. E., Machine Design, MacMillan, 1975.
41. Standard Handbook For Mechanical Engineers, 7th ed., T. Baumeister, Ed.-in-Chief, McGraw-Hill, 1967.
42. Handbook of Tables for Applied Engineering Science, 2nd ed., Bolz, R. E., and Tuve, G. L., Editors, CRC Press, 1973.
43. Roark, R. J. and Young, W. C., Formulas For Stress and Strain, 5th ed., McGraw-Hill, 1975.
44. Oberg, E., and Jones, F. D., Machinery's Handbook, 18th ed., Industrial Press, 1970.
45. Heliflow Coders and Heaters, Bulletin 6127, Graham Manufacturing Co., Inc.
46. 1967 ASME Steam Tables, 2nd ed., American Society of Mechanical Engineers, New York, 1967.
47. Ellison Instrument Division Dictrich Standard Corp., Calculation Report E-78, Section D. Annubar Flow Calculation Report, 1968.
48. AEC - Department of the Interior, Report ORNL-TM-4248, ORCON1: A Fortran Code for the Calculation of a Steam Condenser of Circular Cross Section, by J. A. Hafford, July 1973.

INITIAL DISTRIBUTION LIST

	<u>No. Pages</u>
1. Defense Documentation Center Cameron Station Alexandria, Virginia 22314	2
2. Library Naval Postgraduate School Monterey, California 93940	2
3. Chairman, Department of Mechanical Engineering Naval Postgraduate School Monterey, California 93940	1
4. Professor P.J. Marto Department of Mechanical Engineering Naval Postgraduate School Monterey, California 93940	5
5. LCDR A.C. Beck II, USN Box 72 Marlborough, New Hampshire 03455	1
6. CDR N.P. Nielsen Naval Sea Systems Command (033) 2221 Jefferson Davis Hwy, CP#6 Arlington, Virginia 20360	1
7. Mr. Charles Miller Naval Sea Systems Command (0331) 2221 Jefferson Davis Hwy, CP#6 Arlington, Virginia 20360	1
8. Mr. Walter Aerni Naval Ship Engineering Center (6145) Washington, D.C. 20362	1
9. Mr. Frank Ventriglio Naval Sea Systems Command (0331) 2221 Jefferson Davis Hwy, CP#6 Arlington, Virginia 20360	1
10. Mr. Wayne L. Adamson, Code 2761 Naval Ship Research and Development Center Annapolis, Maryland 21402	1
11. Dean of Research Naval Postgraduate School Monterey, CA 93940	1

